2011

Conductive tough hydrogels

Sina Naficy
University of Wollongong

Conductive Tough Hydrogels

A thesis submitted in fulfilment of the

requirements for the award of the degree

Doctor of Philosophy

From

University of Wollongong

By

Sina Naficy

B.Sc. (Chem. Eng.), M.Sc. (Polym. Eng. Sci.)

School of Mechanical, Materials and Mechatronic Engineering

2011

Declaration

I, Sina Naficy, declare that this thesis, submitted in fulfilment of the requirements for the award of Doctor of Philosophy, in the Faculty of Engineering, University of Wollongong, is wholly my own work unless otherwise referenced or acknowledged. The document has not been submitted for qualifications at any other academic institution.

Sina Naficy

December, 2010

Acknowledgement

Most of all, I would like to thank my supervisors Professor Geoffrey Spinks and Professor Gordon Wallace for providing both general and technical advice, persistent support and kind encouragement throughout my study.

I would like to thank Dr Joselito Razal and Dr Philip Whitten for their precious contribution to this study. It was not possible to finish this thesis without their help. Also, I acknowledge Professor Hugh Brown, Dr Surreya Saricilar and Mrs Shideh Nasrallah for all the discussions we had on hydrogels.

I greatly appreciate the help and support offered by all of my colleagues and friends at the Intelligent Polymer Research Institute (IPRI). In particular, I would like to acknowledge the technical assistance provided to me by Mr Tony Romeo for SEM pictures, and the administrative assistance given to me by Mr Phil Smugreski. Much appreciation also goes to Dr Damia Mawad, Dr Byung Chul Kim, Dr Javad Foroughi, Mr Adrian Gestos, Mr Ali Jalili, and Mr Wen Zheng for their assistance in the laboratories.

I would like to thank my parents (Nasrin and Taghi) and my brother Babak for their kind and endless supports during my study. And last but not least, I would like to thank my lovely wife Sahar Okhovat for her love and never-ending supports. I will never forget her kind words and having so much faith in me that I would complete this stage. This thesis is dedicated to them.

Abstract

The aim of this thesis was to develop a hydrogel system with enhanced mechanical performance. This hydrogel system has to be preferentially electrically conductive to facilitate possible controlled drug release. To fabricate a tough hydrogel system, a double network (DN) approach was employed by forming two polymer networks interpenetrated in each other with considerably different crosslinking ratios.

The new developments in tough hydrogel materials are highlighted in Chapter 1, and their enhanced mechanical performance and corresponding toughening mechanisms are discussed. These tough hydrogels have been mainly developed over the past ten years with many now showing mechanical properties comparable with those of natural tissues. The possibility of employing a conductive hydrogel system for controlled drug release purposes was investigated by studying chitosan hydrogel films containing carbon nanotubes in Chapter 2. A modulated release behaviour was demonstrated by tuning the strength and polarity of the applied voltage, ranging from -0.8 to +0.15 V. Attempts to make stronger hydrogels based on chitosan and other synthetic hydrogel networks resulted in fabricating chitosan-poly(acrylamide) fibres in Chapter 3, with up to, respectively, 11 and 8 times enhancement in modulus and tensile strength compared to PAAm hydrogel. Furthermore, to combine the strengthening mechanisms of hydrogen-bonding and double network hydrogels in forming a toughened hydrogel system, a double network system based on poly(acrylic acid) and a bottlebrush network made of poly(ethylene glycol) methyl ether methacrylates oligomers was made and characterized in Chapter 4. Mechanical properties (tensile, compression) and swelling behaviour of

this system at various pHs were studied systematically, along with other physical properties such as transparency and surface contact angle. The results indicated that this system is strongly pH sensitive, with all of the mechanical and physical properties affected by the pH.

Finally, a conducting polymer (PEDOT) and carbon nanotubes were employed to introduce conductivity to the aforementioned hydrogel network, and the results are presented in, respectively, Chapter 5 and Chapter 6. Conductivity of hydrogels at various pHs was studied in Chapter 5, showing the DN-PEDOT hydrogels have remained pH sensitive with a conductivity up to 4.3 S/cm at acidic pH. In Chapter 6 the formation of a carbon nanotube-rich sheath around a tough double network hydrogel core via a phase segregation process is described. This phenomenon was observed in various double network hydrogel structures, regardless of the nature and composition of the networks. The obtained hydrogels are potentially applicable in the field of controlled drug release. The conclusion chapter (Chapter 7) summarises the thesis, with a few suggestions for future studies in this field.

Table of Contents

List of Figures

Chapter One

Chapter Two

Chapter Three

Chapter Four

Chapter Five

Chapter Six

Chapter Seven

List of Tables

List of Symbols and Abbreviations

ε	Strain
η	Viscosity
λ	Extension
ρ	Density
σ	Stress
AA	Acrylic acid
AAm	Acrylamide
AMPS	2-acrylamido-2-methyl-1-propanesulfonic acid
APS	Ammonium persulphate
BC	Bacterial cellulose
BIS, MBAA	N,N'-methylenebisacrylamide
CD	Cyclodextrin
CNT	Carbon nanotube
C-PS	Cationic Poly(styrene)
CS, CHIT	Chitosan
D	Diameter; Diffusion coefficient
DEX	Dexamethasone sodium phosphate
DLS	Dynamic light scattering
DN	Double network hydrogel
E	Young's modulus
EDOT	3,4-ethylenedioxythiophene
EG	Ethylene glycol
G	Fracture energy; Shear modulus
HA	Hydrophobic association hydrogels
HEMA	Poly(hydroxyethyl methacrylate)
IPN	Interpenetrating polymer network
K_c	Critical stress factor
KPS	Potassium persulphate
LCST	Lower critical solution temperature
M_c	Molecular weight between crosslinks
MD	Molecular dynamic simulation
MMS	Macromolecular microspheres
N, n	Number of network chains/clays per unit volume
N_A	Avogadro's number
NC	Nanocomposite hydrogel
PAA	Poly(acrylic acid)
PAAm	Poly(acrylamide)
PAMPS	Poly(2-acrylamido-2-methyl-1-propanesulfonic acid)
PANi	Poly(aniline)
PBDT	124
PDMAAm	Poly(N,N-dimethyl acrylamide)
PDMAPS	Poly(N-(3-sulfopropyl)-N-methacroyloxyethyl-N,N-

	dimethylammonium betain)
PDMS	Poly(dimethylsiloxane)
PEDOT	Poly(3,4-ethylenedioxythiophene)
PEG	Poly(ethylene glycol)
PEGMA	Poly(ethylene glycol)methyl ether methacrylate
PEO	Poly(ethylene oxide)
PHA	Haluronan
PNIPAM	Poly(N-isopropylacrylamide)
PNVA	Poly(N-vinylacetamide)
PPy	Poly(pyrrole)
PSBMA	Poly(sulfobetaine methacrylates)
PSS	Poly(styrenesulfonate)
PVA	Poly(vinyl alcohol)
Q	Swelling ratio
q	Swelling ratio
r	Radius; distance between junction in polymer chains
SANS	Small angle neutron scattering
SAXS	Small angle X-ray scattering
SLS	Static light scattering
SN	Single network
SPANi	Sulfonated polyaniline
SWNT	Single walled carbon nanotubes
T_g	Glass transition temperature
T_p	Polymerization temperature
TN	Triple network
TP	Topological hydrogel
TFEA	2,2,2-trifluoroethyl acrylate
W_{ex}	Work of extension

Preface

The aim of this thesis was to develop a hydrogel system with enhanced mechanical performance. This hydrogel system has to be preferentially electrically conductive to facilitate the possible controlled drug release. This thesis consists of seven chapters, including a literature review chapter (Chapter 1) and the conclusions (Chapter 7). The framework of each chapter constitutes of an introduction section, followed by the experimental section, results and then discussion sections. Each chapter has a separate reference section which lists the references cited in that particular chapter.

In the literature review chapter (Chapter 1), the new developments in tough hydrogel materials are highlighted, regarding their enhanced mechanical performance and their corresponding toughening mechanisms. These tough hydrogels have been mainly developed over the past ten years with many now showing mechanical properties comparable with those of natural tissues. This review focuses on recently developed tough hydrogels, including topological hydrogels, nanocomposite hydrogels, double networks, hydrogels with hydrogen bonding, nano and micro sphere-based hydrogels,

hydrophobic association hydrogels, and hydrogels that are fabricated by click chemistry or made from tetrahedron-like macromonomers.

The possibility of employing a conductive hydrogel system for controlled drug release purposes was investigated by studying chitosan hydrogel films containing carbon nanotubes in Chapter 2. Attempts to make stronger hydrogels based on chitosan and other synthetic hydrogel networks resulted in fabricating chitosan-poly(acrylamide) fibres (Chapter 3) and a pH sensitive and mechanically strong double network system based on poly(acrylic acid) and a bottlebrush network made of poly(ethylene glycol) methyl ether methacrylates oligomers (Chapter 4). Mechanical properties (tensile, compression) and swelling behaviour of hydrogel systems at various pHs were studied systematically, along with other physical properties such as transparency and surface contact angle. Conducting polymers and carbon nanotubes were also employed to introduce conductivity to the hydrogel networks, and the results are presented in, respectively, Chapter 5 and Chapter 6. Conductivity of hydrogels at various pHs was also studied in Chapter 5. In Chapter 6 the formation of a carbon nanotube (CNT)-rich sheath around a tough double network hydrogel core via a phase segregation process is described. This phenomenon was observed in various double network hydrogel structures, regardless of the nature and composition of the networks. The obtained hydrogels are potentially applicable in the field of controlled drug release. The conclusion chapter (Chapter 7) summarises the thesis, with a few suggestions for future studies in this field.

CHAPTER ONE

Introduction

1. Introduction

1.1. Introduction

Hydrogels [1] are three dimensional networks made from hydrophilic polymer chains with chemical or physical crosslinking. Because of their hydrophilicity, hydrogels readily swell when brought in contact with aqueous solutions, but do not dissolve due to their crosslinks. Moreover, most of the hydrogels can respond to environmental signals such as temperature [2-7], pH [8-11], certain chemicals [12, 13], solution ionic strength [11], light [11, 14], and external electric fields [15]. The response is in the form of a volume change resulting from a change in the water content of the hydrogel and results in a change in shape or generation of a stress.

The dynamic responses of hydrogels is useful for many applications including artificial muscles [16, 17] and stimulated-release systems [18]. Since the pioneering work of Wichterle and Lim in 1950's [19], hydrogels have been the subject of extensive studies in various fields ranging from food industry [20], delivery systems [18, 21, 22], tissue engineering [23-27], sensors and bio-sensors [13, 28-30] to flow control [31-33], supercapacitors [34], and actuators [35-40]. Because of the similarity in appearance and

properties to many soft, natural tissues, hydrogels have always been of interest for use in biological related applications [41-43]. Since then, the swelling [44], diffusion [45], and physical and mechanical behaviour [46-48] of hydrogels have been well documented, especially for drug delivery systems.

In this chapter, new advances that have been made over the last ten years to enhance the mechanical properties of hydrogels will be described. Emphasises will be on the structure of tough hydrogels, their mechanical properties and the mechanism of toughening. The next section describes the methods that have been used to characterise the toughness of a hydrogel, followed by the definition of toughness in section 1.3. In section 1.4 the mechanical performance of various hydrogels is compared with each other and other materials. Various new categories of tough hydrogels including TP hydrogels, NC hydrogels, DN hydrogels, hydrogels toughened by hydrogen-bonding (H-bonding hydrogel), nano – micro sphere composite hydrogels, hydrogels prepared by click chemistry, tetrahedron-like PEG hydrogels, and hydrophobic association hydrogels are introduced in more details in section 1.5. The toughness mechanisms of some of these novel hydrogels are discussed in section 1.6. In section 1.7 conductive hydrogels are discussed with an emphesis on their electrical conductivity and mechanical properties. A brief introduction on the modulated drug release from hydrogels is presented in section 1.8. Finally, section 1.9 covers a brief summary and thesis outline.

1.2. Mechanical Properties of Hydrogels

Despite the extensive previous research, many applications of hydrogels are limited by their weak mechanical performance. Some applications proposed for hydrogels do not require any considerable mechanical strength. For instance, in food industry, drug delivery systems, cell culturing (where hydrogels are used as scaffolds), supercapacitors, and sensors and bio-sensors, there is no significant force involved in the process and mechanical failure is unlikely. In most of these applications the hydrogel does not even require sufficient strength to resist its own weight, as the hydrogel itself is supported by another element. However, there are many other applications for hydrogels such as actuators, flow control systems, and tissue engineering applications, where the mechanical properties of hydrogels have become an important factor. In many of these examples, hydrogels are not only required to sustain their own weight, but also should tolerate an external force as well. Thus, an optimal material for these applications is a *tough* hydrogel which can resist the applied force without failure. Many biological gel materials combine a high swelling degree and low modulus with high extensibility and high toughness. This combination of properties has been difficult to achieve with synthetic hydrogels, as they typically become brittle when highly swollen.

A further confounding factor in the application of hydrogels is the need to make thin gels to reduce their reaction time. Brittle gels made as thin films or fibres are very fragile and difficult to handle. These materials need to have reasonable toughness to be practically useful. The benefits of smaller dimensions giving faster response times can be illustrated by using hydrogel actuators as an example. Here, the volume change in the hydrogel is derived from a diffusion process making the actuation intrinsically slow unless the operational dimension reduces to microns. Figure 1.1 depicts the size

dependence of the corresponding characteristic time of volume change for a spherical hydrogel with a radius of r in a simple diffusion process with diffusion coefficient of $D \sim 10^{-7}$ cm^2/s. To get a response (due to the swelling of the hydrogel) in around 1 second, which is similar to the response of skeletal muscle, the gel diameter should be about ~ 6 μm. If the tensile strength of this hydrogel is ~ 30 kPa, the force it can support before rupturing is only ~ 1 μN.

In recent years several new hydrogel categories have emerged with significantly improved mechanical properties that might make them suitable for advanced applications mentioned above. These new systems include topological (TP) hydrogels [49], nano-composite (NC) hydrogels [50], and double network (DN) hydrogels [51].

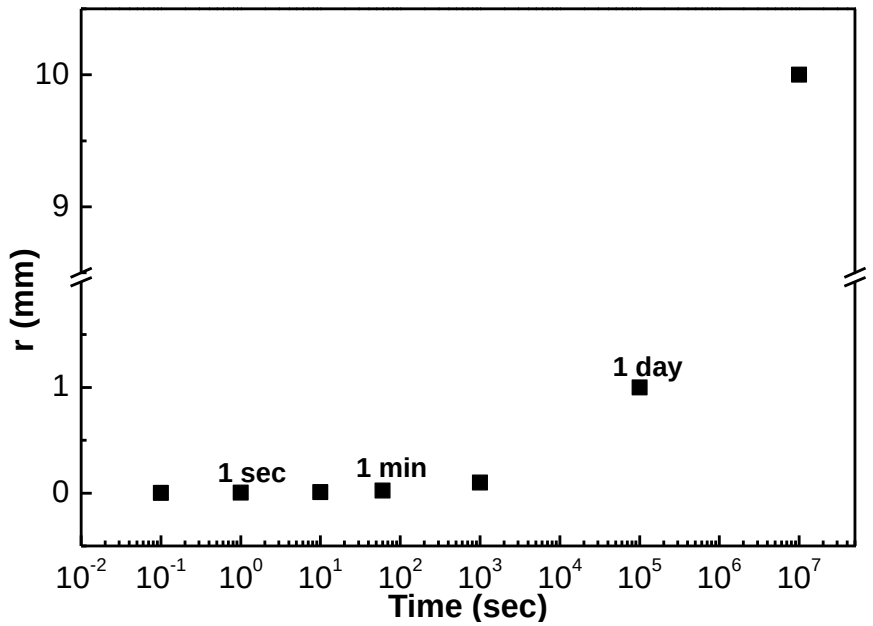

Figure 1.1. A spherical hydrogel's radius r against time to achieve equilibrium swelling t. The swelling is because of a diffusive process where $D \sim 10^{-7}$ cm^2/s.

These materials all exhibit interesting mechanical properties, and several recent review articles have described the properties of particular types of tough hydrogels [52-54]. Also, new polymerisation methods such as click chemistry [55] along with new monomer structures such as tetrahedron macromonomers [56] have been employed to produce hydrogels with a more homogeneous network and improved mechanical properties. Other tough hydrogels such as micro and nano sphere-based hydrogels [57] and hydrogels with hydrophobic associations [58] have also been produced and characterized.

1.3. Definition of Toughness

Measuring the toughness of materials is an old subject in material science. Standard fracture tests determine the fracture threshold stress by increasing the load until the sample breaks. The fracture stress is sensitive to the size of stress-concentrating defects that inevitably occur in all materials so that the fracture process in brittle materials is described by equation 1.1:

$$\sigma = \frac{K_c}{Y\sqrt{\pi a}} \qquad (1.1)$$

where σ is the fracture stress, K_c is the critical stress intensity factor, Y is a geometry constant and a is the length of the largest sharp crack within the material. Since the size of natural cracks varies from sample to sample, so does the breaking stress. To overcome this problem, fracture testing involves inserting a sharp crack of known size prior to testing. The fracture stress then allows the determination of K_c. The latter is a

material constant that describes the material's resistance to brittle fracture. It is well recognized that the fracture energy (or "toughness" G_c) is a more informative parameter for understanding a material's fracture behavior, as the toughness can be directly related to the molecular mechanisms of fracture occurring within the material. G_c and K_c are related by:

$$G_c = \frac{K_c^2}{2E} \qquad (1.2)$$

where E is the material's elastic modulus and G_c has units of J/m^2 representing the energy absorbed in creating unit area of crack surface. Although the fracture properties of various polymeric systems including rubbers, composites, thermoplastics and thermosets have been extensively explored, little fracture testing has been done on polymer gels. Indeed, only the recent advent of tough gels has made it possible to conduct such fracture tests.

While fracture testing provides direct information regarding a material's resistance to crack growth and insight into toughening mechanisms, simple tensile testing is more commonly employed. It is possible to estimate the toughness of a material from the area under the stress-strain curve. This area represents the actual energy stored and absorbed by the sample during a tensile test until the failure of the sample. This energy includes the fracture energy but also the elastically stored energy and any energy dissipated through plastic deformation. In the absence of true fracture energy values, the area under the stress-strain curve has been taken to be indicative of the material's toughness as tougher materials will sustain higher loads and higher extensions before failure. To distinguish the area-under-the-curve method from the true toughness the term work of

extension, W_{ex}, is used for the former. To measure W_{ex} in this review, wherever the actual tensile curve was available the area under the curve was measured. In some cases that the tensile curve was not available W_{ex} was estimated from tensile strength, σ_b, Young's modulus, E, and elongation at break, ε_b, assuming $W_{ex} = ½\ \sigma_b\ \varepsilon_b = ½\ E\ \varepsilon_b^2$. This can give valid values for W_{ex} when the material is brittle and the stress-strain curve is an almost straight line. Since most of the conventional hydrogels are very brittle the above estimation can predict acceptable values for W_{ex}. The work of extension is given in units of kJ/m^3 or energy per unit volume.

1.4. Mechanical Behaviour of Hydrogels

Reported fracture energy values for typical hydrogels normally range from 0.1 to 10 J/m^2 [59, 60]. Considering that rubbers usually have much higher toughness (typically 10^3 –10^5 J/m^2) [61]. it is a challenging problem to enhance the mechanical properties of hydrogels. Yet hydrogels are simply solvent-swollen rubbers, so the deterioration in strength of gels compared to rubbers can be attributed to the action of the solvent. The degree of swelling of gels can be controlled through the strength of the polymer-solvent interaction and the crosslink density of the network. Figure 1.2 illustrates the relationship between measured toughness values (expressed as work of extension) and the swelling ratio (mass of swollen gel / mass of dry gel) for various types of hydrogel and gel could be found in the literature [62-70]. In the case of conventional hydrogels, it is clear that as swelling ratio increases the work of extension tends to decline sharply (approximately to the inverse square power). However, even within these chemically

simple single network gels, the toughness can vary greatly at the same swelling ratio. For example, conventional gels with a swelling ratio ~ 20 show W_{ex} that vary over 3 orders of magnitude. Clearly, factors other than simple swelling ratio also have a strong bearing on the gel's toughness.

Modification of the gel structure to improve the toughness usually also affects the swellability. Inclusion of hydrophobic monomers in copolymer single network gels, for example, reduces their swellability and consequently improves the toughness. Of more practical interest are those newer gel systems that maintain a high swellability (>10) with a high toughness. Tough hydrogel systems possess work of extension more than 10^3 kJ/m^3 with swelling ratio values around or higher than 10. In general, it seems that most of the recently introduced tough hydrogel systems can exhibit a work of extension of at least two orders of magnitude larger than a conventional hydrogel with the same swelling ratio. For instance, for a NC hydrogel with a swelling ratio of ~ 50 the work of extension is ~ 10^3 kJ/m^3 while for a conventional hydrogel with a similar swelling ratio the work of extension can range from 10 to less than 0.1 kJ/m^3. DN gels tend to have lower swelling ratios (5 – 30) than NC hydrogels (25 – 70) and W_{ex} that ranges from 10-10^4 kJ/m^3 with no strong link apparent between swellability and toughness. The W_{ex} of NC gels is consistent around 10^3 kJ/m^3 regardless of the swellability. PEG hydrogels made by click chemistry can reach a work of extension as high as 10^4 kJ/m^3 with a swelling ratio of ~ 10. These systems have similar performance to the best DN hydrogels.

The wide variation in W_{ex} values for the various materials shown in Figure 1.2 reflect the differences in stress-strain behavior of these materials. The tensile strength of

various hydrogels is plotted against their corresponding elongation at break in Figure 1.3 and the hydrogel modulus is shown in Figure 1.4 [62-69, 71-86]. The Young's modulus is a key property of gels with many applications exploiting the exceptionally low modulus values of these materials. For use as implant biomaterials, it is important that the implant matches the modulus of the surrounding tissue so as to avoid inflammation. The moduli of softest tissue like heart muscle is in the range of 20 – 500 kPa [87], which is similar to highly swollen hydrogels. Modulus is directly related to the swelling degree, initially decreasing due to chain dilution as the swelling increases but then increasing again at higher swelling due to full extension of the network chains.

As shown in Figures 1.3 and 1.4 conventional hydrogels such as PAA, PAAm, PNIPAM, etc. show brittle mechanical properties with elongation at break (ε_b < 50 %) and low strength (σ_b ~ 10 kPa). There are not many examples in the literature of tensile data for these conventional hydrogels, simply because they are too brittle for tensile testing. I have not included here the data from compression testing as the interpretation of such data is less straightforward (especially at high strains) than tensile tests. The moduli of these conventional gels are usually quite low (< 100 kPa) since they are normally formulated to give high swelling ratios and modulus tends to decrease with higher swelling.

For comparison, hydrogels based on biopolymers with no reinforcement structure, such as gelatin, alginate, and *l*-carrageenan usually have higher Young's modulus (~ 300 kPa), low to medium elongation at break (10 – 90 %) and low to medium strength (10 – 500 kPa) giving similar work of extension (10 – 250 kJ/m^3). Bio-gels with internal ordered structure, such as BC, collagen, or cell derived matrices (e.g. elastin reinforced

collagen), have higher modulus and strength (up to 2000 kPa), and low elongation at break (~ 20 %) giving medium work of extension (up to 300 kJ/m^3).

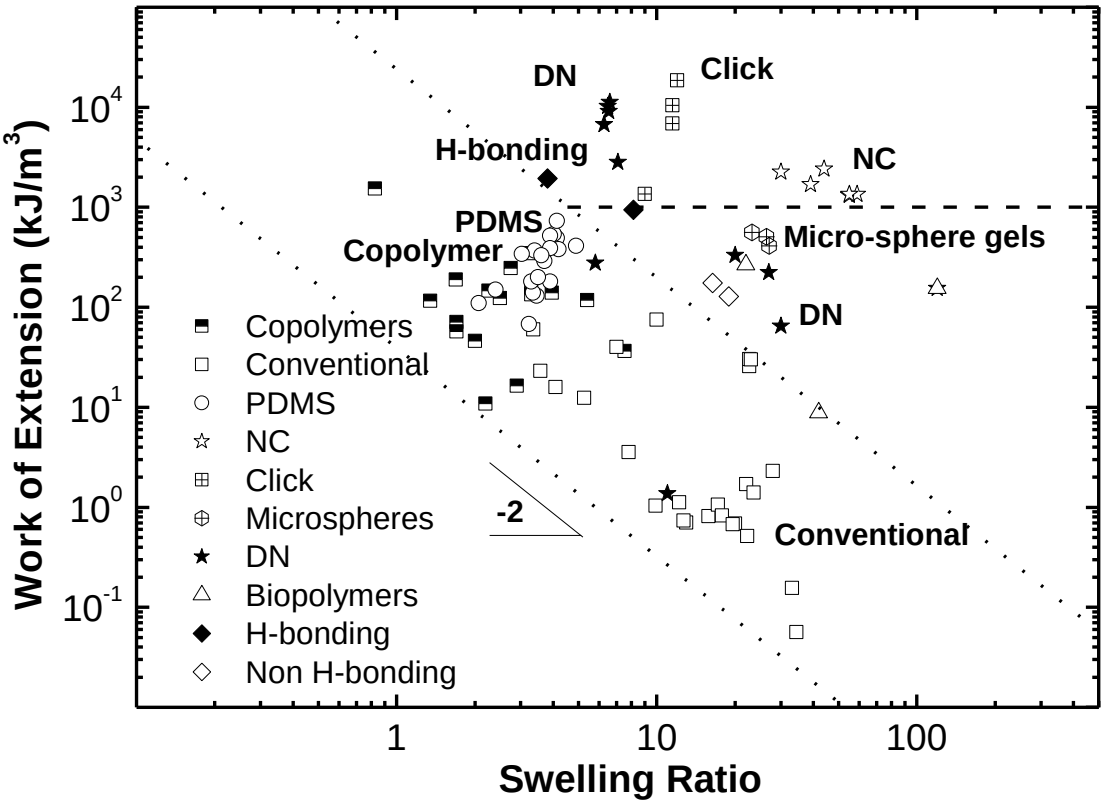

Figure 1.2. Work of extension of various hydrogels and gels vs. their swelling ratio. The non H-bonding hydrogels are the same as H-bonding hydrogels with no hydrogen bonding due to pH. The dashed line indicates the work of extension of 10^3 kJ/m^3. The dotted lines highlight the region with slope -2.

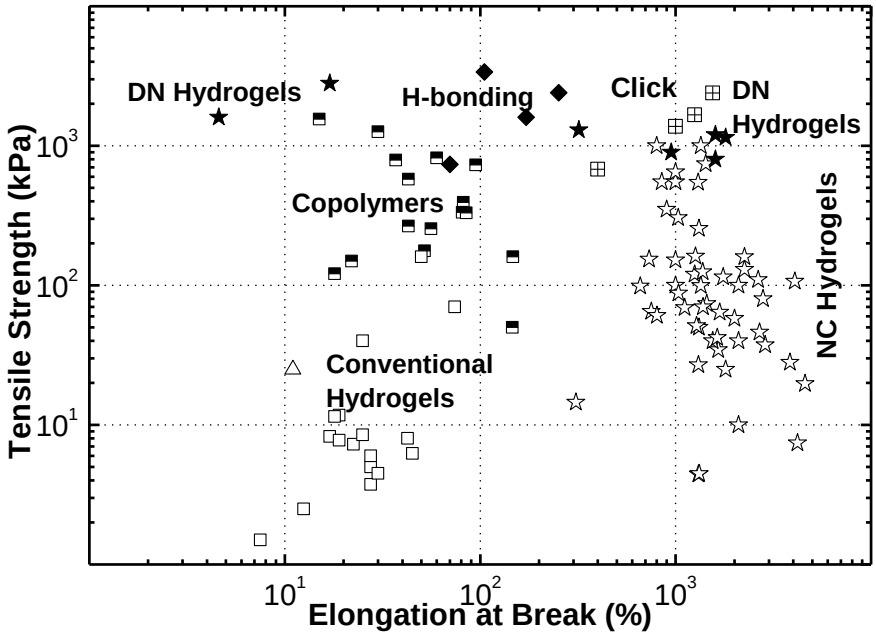

Figure 1.3. Tensile strength of various hydrogels and gels vs. their corresponding elongation at break.

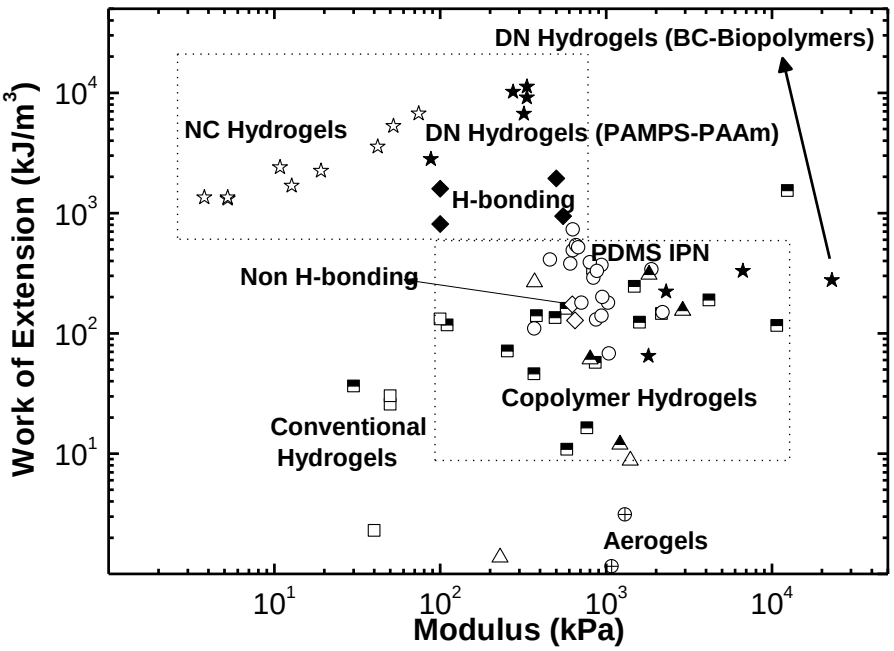

Figure 1.4. Work of extension of various hydrogels and gels vs. their corresponding Young's modulus.

Synthetic copolymer hydrogels with both hydrophobic and hydrophilic segments have higher tensile strength ($50 < \sigma_b < 10^4$ kPa) than conventional, synthetic hydrogels but have similarly low elongation at break ($\varepsilon_b < 100$ %). Their reduced hydrophilicity limits the swelling ratio thereby increasing modulus (10^2 -10^4 kPa) compared to the more highly swollen conventional gels. The hydrogels with hydrogen bonding, e.g. PEG-PAA gels, have high tensile strength (~ 1 MPa), with an elongation at break of about 100 %.[64] Similarly, poly(dimethylsiloxane) (PDMS) IPN gels swollen in toluene exhibit similar Young's modulus (370 – 1800 kPa) and work of extension (70 – 730 kJ/m^3).

The toughness of high swelling NC and DN hydrogels is derived from quite different mechanical properties in each case. NC hydrogels are characterised by their extremely high elongation at break (up to 4500 %) and low moduli (<100 kPa). NC hydrogels show a wide range of tensile strengths from quite low (10 kPa) to high (up to ~ 1 MPa). The very high elongations of the strongest NC hydrogels give these materials a very high toughness with area under the tensile curve of up to ~ 6700 kJ/m^3 [71]. For DN hydrogels, the tensile behavior depends on the constituent components, ranging from very brittle with ε_b ~ 5 % in PAMPS-TFEA DN [51] to very tough with ε_b up to 1700 % in some of the PAMPS-PAAm DN gels. These latter gels even demonstrate necking behavior associated with plastic deformation in tough plastics [65]. The tensile strength of all the DN gels is mainly around 1 MPa. Modulus values for DN hydrogels (10^2 – 10^4 kPa) are significantly higher than single network synthetic hydrogels (< 10^2 kPa). DN hydrogels based on BC exhibit the highest modulus due to BC's ordered

internal structure (up to 23 MPa) with medium work of extension (65 – 330 kJ/m^3), when samples were stretched along the stratified direction of BC [69].

An interesting hydrogel system here is PEG-PAA IPN hydrogels with hydrogen bonding [64]. The IPNs were produced from a crosslinked PAA network within an end-crosslinked PEG network. Because of strong *inter*polymer hydrogen bonding, considerably high tensile strength (σ_{true} ~ 2 – 12 MPa) and initial Young's modulus (1 – 19 MPa) could be achieved, with W_{ex} of up to 2000 kJ/m^3 [64]. Interestingly, the intermolecular hydrogen bonding can be turned on and off by immersing the gel in a solution of controlled pH. At high pH the acrylic acid moieties are deprotonated thereby disrupting the hydrogen bonding with PEG units. The deprotonation of the acid groups also causes a large increase in swelling. The result is a decrease work of extension due to the drop in strength and elongation at break while modulus remains almost unaffected.

To summarize the mechanical performance of hydrogels in relation to the other materials the fracture energy of different categories of materials including conventional hydrogels [60, 88-90], organo-glasses [91] and glasses, silica sonogels [59], polymers [92-96], rubbers [61, 97], metals and DN hydrogels [98-101] is plotted against their modulus in Figure 1.5. All the fracture energy data presented in this graph has been originally obtained from a proper fracture test. As a result, there is no data included for other types of new hydrogel systems since true fracture data is not yet available. Interestingly, the PAMPS-PAAm DN hydrogels occupy the gap between rubbers and conventional hydrogels, with the modulus ranging from 0.1 to less than 0.5 MPa and fracture energy between 100 and 4000 J/m^2.

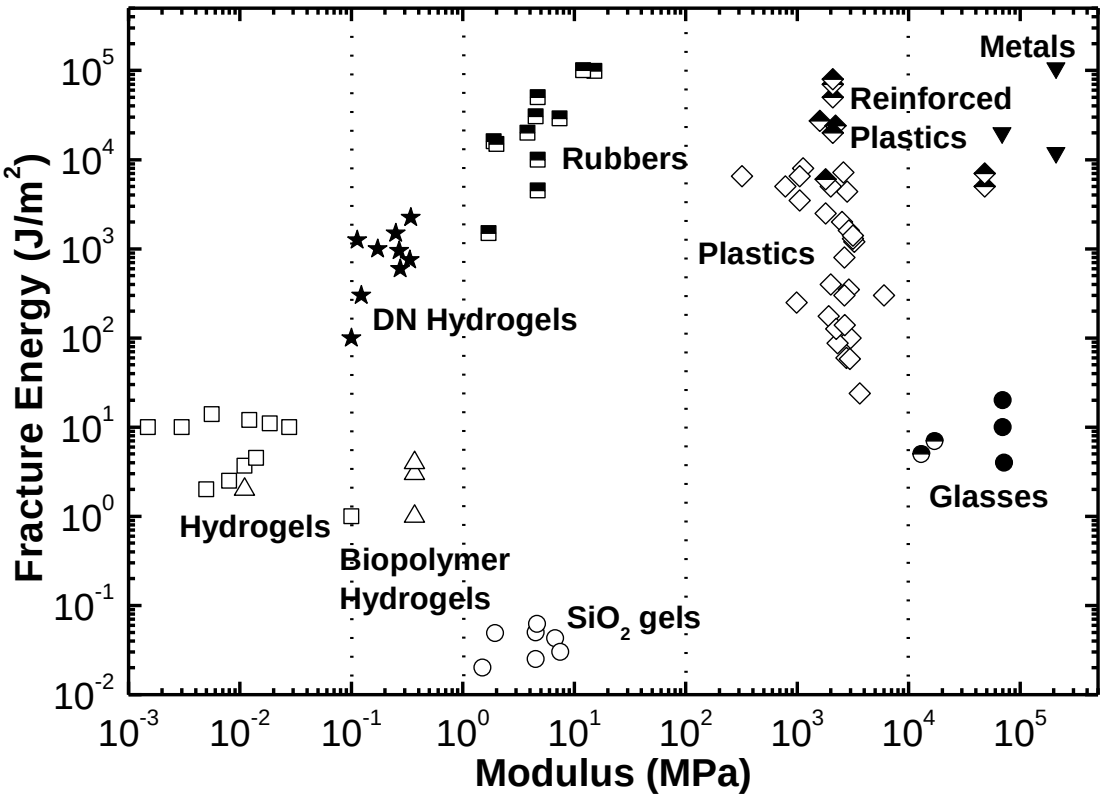

Figure 1.5. Fracture energy of various materials vs. their modulus.

Conventional hydrogels have the lowest modulus in Figure 1.5 (< 0.1 MPa), followed by DN hydrogels which have modulus in the same order as some of biopolymers but with the former showing much higher fracture energy. The modulus of rubbers mainly fall between 10 and 100 MPa, followed by plastics ($10^2 < E < 10^4$ MPa), glasses (~ 10^5 MPa) and metals (10^4 MPa <). Although the fracture energy of PAMPS-PAAm DN hydrogels can not reach that of rubbers (>10^3 J/m^2), it is in the same order as that of unreinforced conventional plastics (~ 10^3 J/m^2).

1.5. Tough Hydrogels

1.5.1. Topological Hydrogels

In 2001, Okumura and Ito [49] reported a new type of hydrogels based on PEG chains and α-cyclodextrin (α-CD) cyclic molecules. In their system, α-CD cyclic molecules were threaded by long chains of PEG capped with bulky end groups. To obtain the gel, α-CD molecules were chemically crosslinked by cyanuric chloride to achieve a structure similar to the illustration in Figures 1.6a and 1.6b. The structural model in Figure 1.6c suggests a slide-ring gel, in which the crosslinkers are able to slide along the polymer chians (pulley effect), providing high extensibility and swelling ratio (~ 400) [49]. It was shown that in contrast to elongated conventional crosslinked networks in which an abnormal butterfly-pattern [102-104] appears in scattering measurements representing increased spatial inhomogeneities due to stretching [105], a normal butterfly pattern forms for TP gels under uniaxial elongation [106].

Furthermore, SAXS results revealed that in poor solvent when the sliding crosslinks aggregate the pulley effect suppresses and an abnormal butterfly-pattern appears in SAXS measurements of these gels [107]. Based on these experimental evidences it is clear that when the crosslinks are not aggregated and are able to move freely, the polymer chains will orient under a uniaxial elongation in a similar way as the polymer chains would align in a flow field (Figure 1.6c).

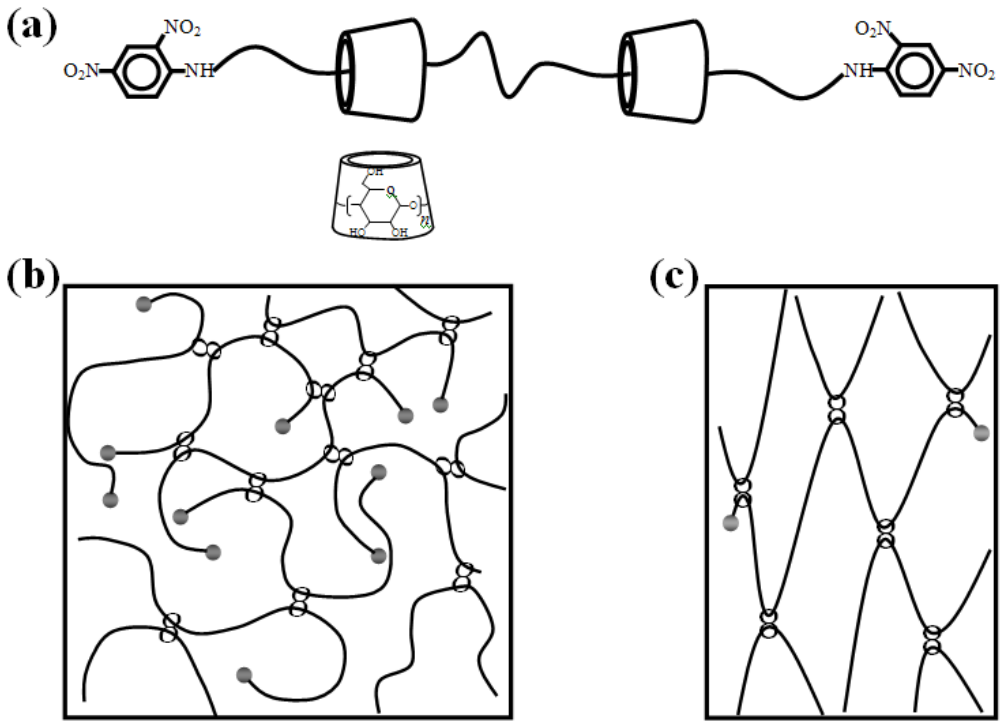

Figure 1.6. Schematic drawing of a polyrotaxane with a) a polymer chain (PEG) threading the cyclic molecules (CD) and end capped with bulky end groups; b) after crosslinking of CD cyclic molecules to form the TP gels; c) pulley effect of cyclic molecules and polymer chains under tension.

To explain the elasticity of TP hydrogels a simple model was proposed by Koga and Tanaka [108]. They treated the TP hydrogels as a network with tri-functional sliding junctions. A simulation technique based on Brownian dynamics was used, adopting bead-spring model chains. The elastic force between two adjacent beads along a chain was described with a nonlinear elastic potential. To model the sliding crosslinks a slip-link connection was assumed between chains. This slip-link could move along the chain and interact with beads of that chain. Similar elastic filed was used for the interaction of

slip-links and beads. The simulation could successfully present a qualitative stress – strain curve for non-slip model (chemically crosslinked chains) and slip model (TP gels), where higher elongation at break was predicted for TP gels (Figure 1.7). Interestingly, the simulation showed that the slip-links aggregate during the elongation and the distribution of these aggregated clusters would change as the extension ratio increases, while larger clusters would obtain at higher extension ratio [108].

1.5.2. Organic – Inorganic Nanocomposite Hydrogels

The organic – inorganic nanocomposites consisting of an organic polymeric matrix and inorganic nanoparticles were introduced in 1985 as the first nylon6-clay hybrid.[109] In 2002, Haraguchi and Takehisa[50] introduced a nanocomposite hydrogel by supposedly initiating the polymerisation of NIPAM monomers from the surface of exfoliated hectorite clays without using any chemical crosslinking agent (Figure 1.8).

The exfoliated clay platelets were regarded as crosslinking linkages and the resulting hydrogels exhibited very high elongation at break. Higher mechanical properties were achieved by optimizing the clay content [71], and monomer composition [73, 110]. In general, NC hydrogels exhibit very high elongation at break in tensile test (ε_b > 1000 %), with tensile strength of 10 – 1000 kPa and modulus of 1 – 50 kPa. Compression strengths are typically higher than tensile strengths at about ~ 1 – 5 MPa [74], and the addition of a small amount of a chemical crosslinking agent was shown to further enhance the compression strength of PNIPAM NC hydrogels to more than 5 MPa [111].

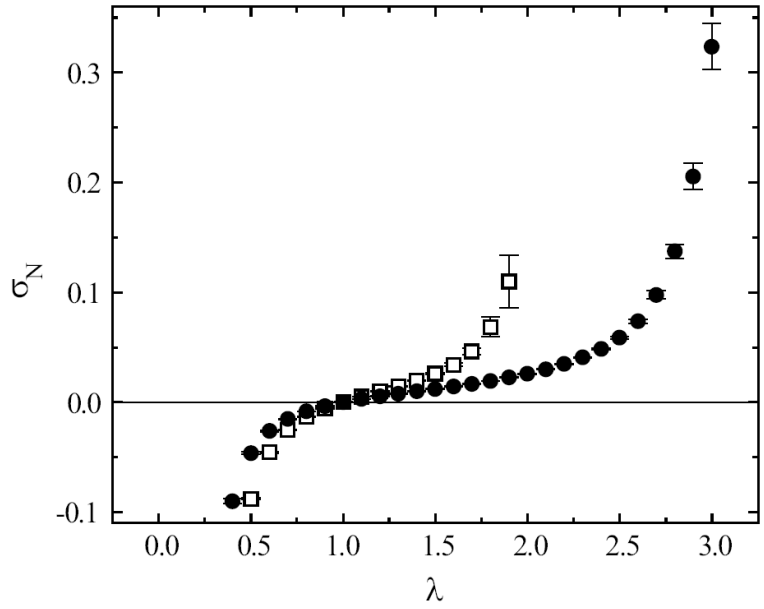

Figure 1.7. Uniaxial stress-extension curve for a) topological gel (slip-link) and b) chemically crosslinked gel (fixed-link) [108].

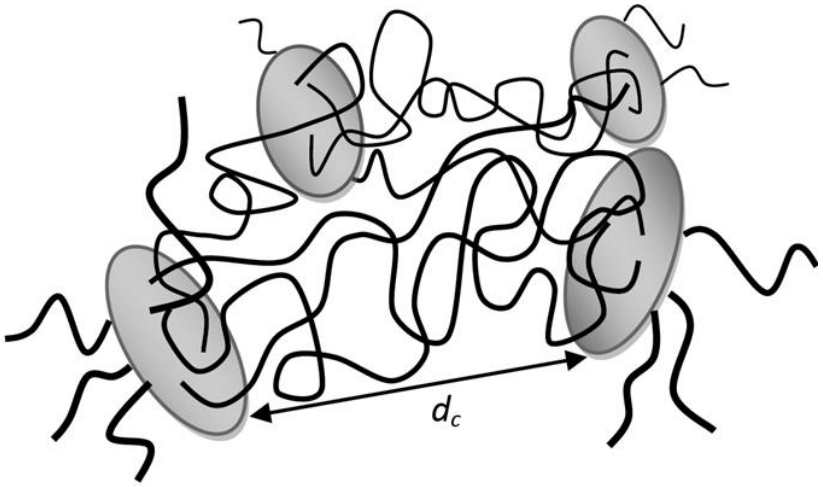

Figure 1.8. Schematic illustration of a NC hydrogel's structure. Polymer chains connect the neighboring clay platelets separated with an average distance of d_c.

Based on experimental evidences, it is believed that the crosslinking structure within these NC hydrogels is more homogeneous than their chemically crosslinked analogues [50, 72, 74]. As a results, the hydrogels can experience very high elongation at break in a tensile test. Evidence of the homogeneous structure include: (1) minimal changes in transparency of NC hydrogels prepared at a polymerisation temperature T_p above the LCST of PNIPAM (in contrast to opaque chemically crosslinked PNIPAM hydrogels when T_p > LCST); (2) very high elongation at break with almost complete recovery of largely deformed samples; (3) no significant change in glass transition temperature T_g of PNIPAM in NC hydrogels when clay content varies (in contrast to considerable changes in chemically crosslinked samples when crosslinking ratio changes); and (4) remarkable enhanced deswelling rate of PNIPAM NC hydrogels when temperature increases above LCST in comparison to similar-sized chemically polymerized PNIPAM.

The initial model suggested to explain the mechanical behavior of NC hydrogels was based on the classic rubber elasticity [50], where the chains between the clays were assumed to be in their rubbery state. Using the classic rubber elasticity theory equation [112], the tensile stress σ is related to the extension of the sample λ by:

$$\sigma = \Phi N^{*} kT \left[\lambda - \left(1/\lambda\right)^{2}\right] \qquad (1.3)$$

where Φ is a front factor ($\Phi = (r_j)^2/(r_f)^2$, r_j and r_f are the distance between the network junctions in swollen state and end-to-end distance of the network chains, respectively), and N^* is the number of network chains per unit volume in swollen state. N^* is approximately related to the molecular weight between crosslinks M_c by [72]:

$$N^* \sim \rho^* \frac{N_A}{M_c} \qquad (1.4)$$

here ρ^* is the density of polymer in swollen state and N_A is Avogadro's number. By using equations 1.3 and 1.4 and tensile data of NC hydrogels, M_c and N^* can be calculated. If the clay is completely exfoliated then the number of separated clay platelets per unit volume n can then be estimated as well. Consequently, the number of crosslinked chains per each clay platelet can be calculated as: N^*/n. This number is reported to increase with clay concentration, ranging from ~ 50 to ~ 120 [72]. This analysis provides evidences for the clay particles acting as multiple crosslinking sites for the polymer network.

Although the rubber elasticity model is very successful in explaining some of the tensile properties of NC hydrogels, it does not consider the possible effects of clays on the mechanical properties. For instance, a considerable tensile hysteresis was observed for PNIPAM NC hydrogels [67, 113] and NIPAM-co-sodium acrylate copolymer NC hydrogels,[76] when the gels were stretched up to 800 % (well below their failure elongation). On the other hand, PAAm NC hydrogels exhibited smaller tensile hysteresis with elastic recovery of ~ 95 % [67]. The differences in behavior was related to the molecular structure of polymer chains, where PNIPAM has bulky hydrophobic side groups which do not exist in PAAm case [67]. However, it was shown that a full recovery is possible even for PNIPAM NC hydrogels after a certain time, depending on the clay content [74]. A fast recovery (< 1 min) was observed for PNIPAM NC hydrogels with initial elongation of 900 % when clay content was small, while a slower time-dependent recovery was experienced when clay content was medium, with full

recovery after less than 24 h [74]. For higher clay contents a "pseudo-permanent" strain remained even after 14 days. Based on these experimental observations, a four-element mechanical model comprising of two springs (E_1 and E_2), and two dashpots (η_2 and η_3) was adopted (Figure 1.9). In this model, the dashpot η_2 and spring E_2 provide the viscoelasticity feature of the hydrogels, while the spring E_1 models the elastic behavior of polymer chains and dashpot η_3 models the permanent strain that occurs in some samples.

A three-element model with two springs and one dashpot was also presented elsewhere [114]. A simple structural model has been proposed to explain the recovery behaviour of NC hydrogels after elongation [74]. It was assumed that when clay content is more than a certain value, the clay platelets would be aligned parallel to the direction of elongation. Then, after the release of stress and as a result of high clay content, the clay platelets will partially retain their orientation as well as their residual strain. In lower clay content case, however, the orientation of clay platelets under the tension is not significant and it does not last for long after the force was removed. Figure 1.10 illustrates a schematic picture for this mechanism [74]. To support this model, the SANS experiments showed an abnormal butterfly-pattern in the low q regions ($q < 0.02$ Å^{-1}) originated from the orientation of clay platelets during the deformation, which is different to the abnormal butterfly-pattern assigned to crosslinking inhomogeneities [114, 115].

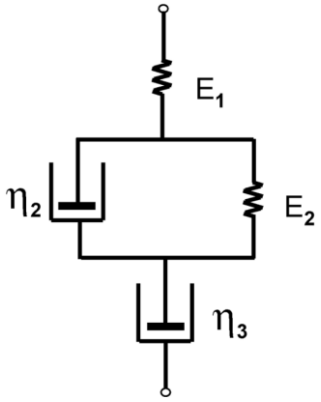

Figure 1.9. Four-element mechanical model.

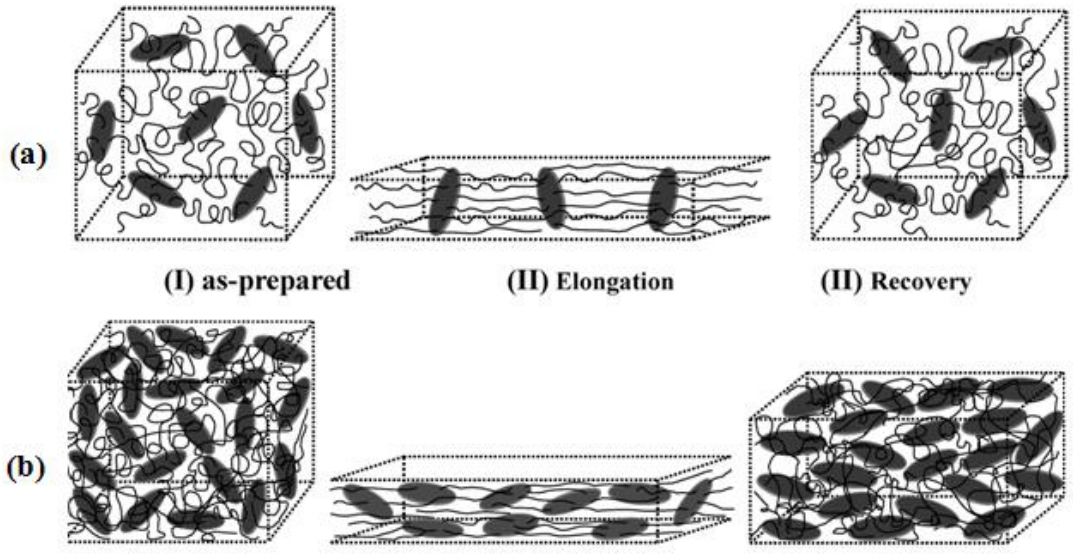

Figure 1.10. Schematic illustration of the structural model for a NC hydrogel with a) low clay content and b) high clay content. The model shows (I) an as-prepared NC hydrogel, (II) the elongation process and (III) the recovery of NC hydrogel after the test [74].

1.5.3. Double Network Hydrogels

Double network hydrogels were introduced by Gong *et al*. [51] in 2003, with considerably high compression strength while the hydrogels could maintain high swelling ratio (60 – 90 wt%). In general, DN hydrogels consist of two interpenetrating networks independently prepared and crosslinked. The "first network" hydrogel is usually more highly crosslinked than the "second network" which is loosely crosslinked or sometimes not crosslinked at all [116]. For substantial improvement in the toughness, the molar ratio of the second network to the first network has to be in the range of several to a few tens [51].

Although the most impressive enhancement in the compression strength of hydrogels was obtained when the first network was a rigid polyelectrolyte and the second network was a flexible neutral polymer, there have been several different interpenetrating polymer network (IPN) systems, reported in the literature as DN gels. Table 1.1 lists various IPN hydrogels with structures similar to the first series of DN hydrogels. In Table 1.1, the classic DN hydrogels made from a charged first network and a neutral second network show the highest improvement in their compression strength [51]. For example, in PAMPS and PAAm case a significant improvement in compression strength was obtained ($\sigma_{b,\mathrm{DN}}$ ~ 17.2 MPa, $\sigma_{b,\mathrm{PAMPS}}$ ~ 400 kPa).

Table 1.1. Various IPN hydrogels inspired by the first double network (DN) systems.

Material	Q	Tensile			Compression			Ref.
		σ_b (MPa)	ε_b	E (MPa)	σ_b (MPa)	ε_b	E (MPa)	
PVA[a]-PAMPS-PAAm *DN*	12.5	0.6	10	-	-	-	-	[117]
PAMPS-PAAm *DN*	10	1.2	14	-	-	-	-	
PAAm-PEDOT-PSS *DN*	7.7	-	-	-	0.275	0.65	-	[118]
PAAm *SN*[b]	14	-	-	-	0.1	0.50	-	
BC-PAAm *DN*	4	2.5	1.0	2.5	4	0.35	1	[119]
PAMPS-PAAm *ultra thin DN*	10	2.25	12	-	-	-	-	[120]
Silica gel-PAAm *DN*	5.9	-	-	-	0.392	-	-	[121]
Silica gel	4.2	-	-	-	0.2	-	-	
Chitosan-PVA[c]	-	-	-	-	-	-	-	[122]
PVA-PEG[d1]	-	-	-	-	0.718	-	7.156	[84]
PVA[d1]	-	-	-	-	0.213	-	1.194	
PVA-PEG[d2]	-	6.10	3.07	0.16	25.15	0.95	29.71	
PVA[d2]	-	1.51	4.34	0.03	3.03	0.90	1.49	
PAA-PAA-PEDOT *TN*[e]	12.5	0.042	0.90	-	1.8	0.8	-	[123]
PAA-PAA *DN*	7.7	0.0225	0.65	-	0.6	0.6		
PAA *SN*	10	-	-	-	0.1	0.35	-	
PBDT-PAAm *DN*	33	0.450 axial	20	-	-	-	-	[124]
		0.150 verti.	20	-	-	-	-	
PBDT *SN*	33		0.70	-	-	-	-	
PAAm *SN*	-	0.055 -	-	-	-	-	-	
PHA-PDMAAm *DN*	14	-	-	-	5.5	0.85	0.508	[125]
PHA *SN*	50	-	-	-	0.3		0.045	

Material	Q	Tensile			Compression			Ref.
		σ_b (MPa)	ε_b	E (MPa)	σ_b (MPa)	ε_b	E (MPa)	
PNVA-PNVA *DN*	9.9	-	-	-	1.6	-	-	[126]
PNVA *SN*	14.4	-	-	-	0.51	-	-	
PNVA-PAAm *DN*	9.0	-	-	-	-	-	-	
PAAm *SN*	9.1	-	-	-	-	-	-	
PSBMA-PSBMA[f1]	1.4	-	-	-	0.595	0.57	0.198	[127]
PSBMA[f2]	2.5	-	-	-	0.350	0.42	0.269	
PEG-PAA DN	5	3.4	1.05	-	-	-	-	[64]
PEG SN	10	0.250	0.6	-	-	-	-	
PAA SN	10	0.111	1	-	-	-	-	
PDMAPS-PAAm *DN*	3.8	-	-	-	-	-	15.8	[128]
PDMAPS *SN*	2.2	-	-	-	-	-	11.2	
PAAm *SN*	22.2	-	-	-	-	-	1.6	
PAMPS-PAAm *DN*	10	-	-	-	17.2	0.92	0.33	[129, 130]
PAMPS-PDMAAm *DN*	16.7	-	-	-	3.1	0.73	0.20	
BC-PDMAAm *DN*	6.7	-	-	-	2.9	0.50	1.6	
BC-Gelatin *DN*	4.5	-	-	-	3.7	0.37	1.7	
PAMPS-PAAm *DN*	6.6	-	-	-	4.6	0.65	0.84	[131]
PAMPS-PAAm *TN*[g1]	5.7	-	-	-	4.8	0.57	2.0	
PAMPS-PAAm *DN-L*[g2]	6.6	-	-	-	9.2	0.70	2.1	
BC-Gelatin 50 wt% *DN*	3.1	3.8	0.28	21	5.3	0.44	3.9	[69]
Gelatin 50 wt% *SN*	3.8	0.18	0.10	1.8	1.2	0.37	1.2	
BC *SN*	120	2.2	0.21	2.9	-	-	0.007	
BC-Gellan gum *DN*	27	1.2	0.30	2.3	-	-	0.38	
Gellan gum *SN*	42	0.16	0.11	1.4	0.47	0.60	0.62	
BC-Sodium Alginate *DN*	20	2.2	0.30	6.7	-	-	0.61	
Sodium Alginate *SN*	22	0.6	0.89	0.37	-	-	0.14	
BC-*l*-Carrageenan *DN*	30	0.5	0.26	1.8	-	-	0.12	
l-Carrageenan *SN*	158	-	-	-	-	-	0.009	

Material	Q	Tensile			Compression			Ref.
		σ_b (MPa)	ε_b	E (MPa)	σ_b (MPa)	ε_b	E (MPa)	
PAMPS-PAAm *DN*	10	-	-	-	17.2	0.92	-	[51]
PAMPS-PAMPS *DN*	14	-	-	-	3.0	0.80	-	
PAMPS-PAA *DN*	12.5	-	-	-	2.3	0.75	-	
PAMPS-TFEA *DN*	2.1	1.6	0.05	-	-	-	-	
PAMPS *SN*	12.5	0.006	0.001	-	0.4	0.41	-	
PAA-PAA *DN*	20	-	-	-	0.7	0.77	-	
PAA-PAAm *DN*	9.1	-	-	-	2.1	0.95	-	
PAA *SN*	100	-	-	-	0.1	0.65	-	
PAAm-PAAm *DN*	12.5	-	-	-	5.4	0.92	-	
PAAm *SN*	14	-	-	-	0.7	0.98	-	
AMPS-co-TFEA-PAA *DN*	14	-	-	-	21.0	0.97	-	
AMPS-co-TFEA *SN*	20	-	-	-	0.03	0.73	-	
Collagen-PDMAAm *DN*	7.7	-	-	-	2.9	0.53	-	
Collagen *SN*	14	-	-	-	0.26	0.52	-	
Agarose-HEMA *DN*	2.3	-	-	-	2.4	0.87	-	
Agarose *SN*	25	-	-	-	0.02	0.20	-	
BC-Gelatin *DN*	4.5	-	-	-	3.7	0.37	-	
BC *SN*	-	-	-	-	-	-	-	

[a] PVA is used as an internal mold; [b] SN: single network; [c] physical crosslinking, mechanical properties reported for semi-dry samples; [d1] freeze-thawing cycle: 5, [d2] freeze-thawing cycle: 3; [e] TN: triple network; [f1] first network is chemically crosslinked, second network is physically crosslinked, [f2] chemically crosslinked; [g1] third network: crosslinked PAMPS, [g2] DN-L: DN with a third linear PAMPS structure.

Amongst various DN hydrogels in Table 1.1, one category belongs to DN gels based on bacteria cellulose (BC) as the first network, and a second network made from a

natural or synthetic polymer [51, 69, 119, 129, 130]. The zwitterionic DN hydrogels made from a chemically crosslinked poly(sulfobetaine methacrylates) (PSBMA) as the first network and a physically crosslinked second network of a similar polymer was also reported showing some improvement in their compression strength [127]. Thin DN hydrogels were developed from PAMPS and PAAm with thickness ranges from ~ 30 to ~ 110 μm when fully swollen in water [120]. These thin DN hydrogels offer high tensile elongation (ε_b > 1000 %), high tensile strength (σ_b > 2 MPa), and high tearing energy (G > 600 J/m^2).

The important structural factors that control the enhancement of PAMPS-PAAm DN hydrogels as the most studied system in this category were described to be the molar ratio of second network to the first network, and the crosslinking ratio of each networks [51]. The former parameter was shown has to be more than 10 to achieve high compression strength in mechanical tests [51]. Also, viscosity measurements of the aqueous PAMPS/PAAm solution showed a maximum in zero-shear viscosity when the molar ratio of PAMPS to PAAm was between 1:15 and 1:3 [132, 133]. This maximum was independent of the total concentration, and the range of two networks molar ratio within which the viscosity peaks is approximately similar to the range where the mechanical properties begin to enhance considerably. In terms of crosslinking content, in an early report it was shown that the toughest PAMPS-PAAm DN hydrogel is obtained when there is no crosslinking agent added to the second network [116]. However, in a succeeding report on *truly* independent PAMPS-PAAm DN gels, where no covalent bond exists between two networks, the fracture strength of samples with linear PAAm chains as the second network was shown to be much lower than those with

a critical amount of crosslinking density (~ 0.01 mol%) [99]. To explain this finding, it was suggested that even when there is no crosslinking agent in the second network monomer solution there are some active double bonds remaining in the first network from half-reacted bi-functional crosslinking agents that could participate in the second network polymerisation. In general, to obtain an optimum toughness a minimum amount of crosslinking is essential to exist in the second network just to form a substantial network inside the first network [99].

To explain the toughness of IPN systems consisting of two "energetically independent" networks made from a stiff first network and a soft second network, Okumura [134] proposed a model based on the properties of each individual network (modulus, mesh size, maximum stress) as well as the IPN composition. Although the predicted fracture energies for DN hydrogels predicted by this model fall in the range of experimental values, some of the assumptions in this model such as the two networks being energetically independent seem to be incorrect for most of DN gels, as explained in the literature [99, 135]. Moreover, the necking phenomenon has been reported for some of the DN hydrogels [65, 66, 136]. Also, large hysteresis was exhibited by PAMPS-PAAm DN gels in the first loading cycle of uniaxial tension and compression tests [137]. In another series of experiments, the tearing test suggested that G in DN gels hardly depends on crack velocity V, which indicates that the anomalously high fracture energy of DN gels cannot be explained by the well-known toughening mechanisms of soft-polymer systems [101]. Based on these experimental observations, Brown [138] and Tanaka [139] independently proposed a similar phenomenological model to explain the toughness of DN gels. In both models, the crack propagation was considered to occur in

two stages. First, the cracks initiate within the brittle first network, which has higher degree of crosslinking and is already fully stretched due to the swelling stage of the gel preparation process. As a result of this failure in the brittle network, the cracks would be bridged by the second network (Brown's model) or by the second network polymer chains attached to the fractured fragments of the first network (Tanaka's model). In both models the damaged zone is very soft and elastic. In Tanaka's model, the fragments of the first network in the damaged zone play a role similar to crosslinkers in the second network [139, 140]. However, it is hard to quantify to what extent the fragments will affect the model. Supporting Tanaka's and Brown's model that are based on the occurrence of a damaged zone around the crack, microscopic images from the crack tip in a PAMPS-PAAm DN gel clearly showed a damaged area developed around the crack tip as presented in Figure 11.1a [141]. It was shown that the size of this damaged zone (h ~ 100 – 800 μm) has a linear relation with the recorded fracture energy in the tearing test (Figure 1.11b). Moreover, AFM measurements conducted on PAMPS-PAAm DN gels determined that the local Young's modulus right below the fracture surface is very close to the bulk modulus measured after the yielding deformation [142], proving the formation of a damaged zone with physical properties similar to the soft network.

Mont Carlo simulation [143] and full atomistic molecular dynamic (MD) simulation [144] were used to investigate the DN hydrogels structure. The MD simulations of a PEO-PAA DN hydrogel with 76 wt% water content showed that the effective mesh size of the DN gel is smaller than the corresponding SN components with the same water content. The stress-strain curve obtained by MD simulations also

suggested a sudden increase in stress above 100 % strain, where the PEO first network in the DN is fully stretched due to its smaller M_c [144].

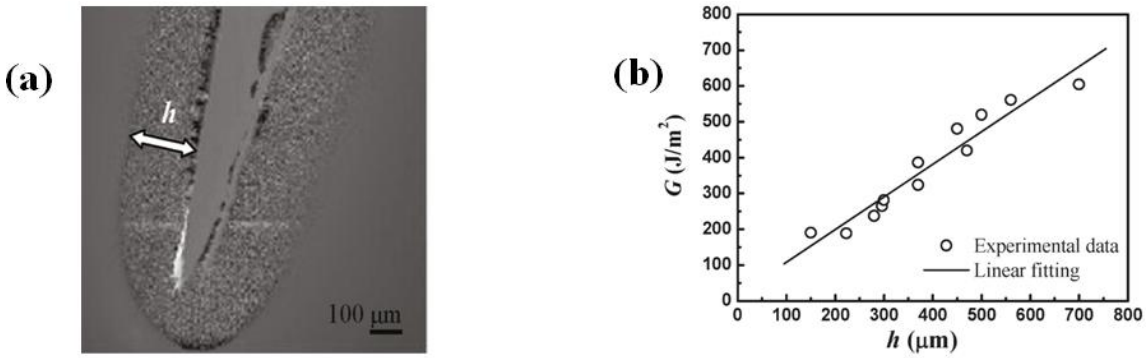

Figure 1.11. The role of damaged zone in toughness of the DN gels: a) an image taken with a 3D violet laser scanning microscope, showing the thickness of damaged zone *h*; b) the fracture energy of DN gels as a function of *h* [141].

1.5.4. Hydrogels with Hydrogen Bonding

As mentioned previously, most of the DN hydrogels with enhanced compression strength and necking in tensile test are made from a polyelectrolyte first network and a neutral second network. Indeed, a fully stretched rigid polyelectrolyte first network was suggested to be one of the main conditions to achieve an optimal DN gel [116]. Also SANS data showed that there might be favourable interactions between the PAMPS first network (polyelectrolyte) and the PAAm second network (neutral polymer) in a PAMPS-PAAm DN hydrogel [135]. This interaction was suggested to be due to the polarisable neutral polymer chains in a polar solvent such as water which makes them

liable for weak electrostatic interactions with polyelectrolyte chains. However, none of these interactions are as strong as the hydrogen bonding between two polymer chains. The IPNs formed by crosslinked PAA within an end-linked PEG network performed considerable enhancement in their tensile properties with strain-hardening [64]. The interaction between these two networks is due to the hydrogen bonding [145] that is also pH sensitive. In this example, the first network was a neutral polymer end-linked via acrylate end groups. Here, the chain length of the starting PEG chains determines the mesh size of the first network. Unlike traditional DN hydrogels with tightly crosslinked first network, the PEG network was less crosslinked with an equivalent crosslinking degree of less than 2.6 mol%, compared to ~ 4 mol% in usual PAMPS-PAAm gels. Similarly, the second network PAA was more crosslinked (1 mol%) than its PAAm counterpart in a PAMPS-PAAm gel (0.1 mol%). Again, unlike PAMPS-PAAm gels, the water content varied significantly with pH from ~ 60 wt% at acidic pHs to ~ 90 wt% at more neutral pHs [64]. No necking was observed in PEG-PAA IPN gels while the tensile mechanical properties were sensitive to pH. Although considerably high true stress (2.0 – 12.0 MPa) and initial Young's modulus (1.0 – 19.0 MPa) was reported for these hydrogels [64], it is not clear if the molar ratio of the two networks satisfies the high molar ratio condition of traditional DN gels. In fact, since the hydrogen bonding carboxylic groups of PAA and repeating units of PEG ([AA]:[EG]) takes place in an equimolar fashion [146] up to a 1:3 ratio [147], and because of this fact that the PEG network does not swell in AA monomer as much as a polyelectrolyte might do in a neutral monomer solution, the final molar ratio of PEG and PAA could be close to 1:1. The drop in tensile mechanical properties as pH increases also suggests a weaker IPN system at high pHs when there is no hydrogen bonding between the two networks. On

the other hand, by replacing the PAA network with a neutral polymer such as PAAm the resulting IPN hydrogel exhibits much lower mechanical properties (σ_b ~ 0.2 – 1.2 MPa) [85], which is similar to that of a PEG-PAA IPN hydrogel at high pHs (σ_b ~ 0.8 MPa at pH ~ 6). A similar strain-hardening was observed in PEG-PAAm case, with an increasing tensile strength with PAAm concentration. The strain-hardening phenomena is expected when chains are fully stretched, similar to rubbers, but the higher mechanical properties of PEG-PAA gels (compared to PEG-PAAm), along with pH sensitivity suggest that hydrogen bonding plays a central role in such systems.

1.5.5. Click Chemistry Hydrogels

Click chemistry [148, 149] is one of the new synthesis techniques that has been used to fabricate hydrogels [55, 150-156]. Click chemistry is known to be one of the strategies to produce uniform polymers and polymer networks [157]. Uniform PEG-based hydrogels with improved mechanical properties were synthesized using azide/acetylene coupling click reaction [55]. The well-defined networks of PEG hydrogels obtained by this method had very high elongation at break (400 < ε_b <1600 %) with high true tensile strength (680 < σ_b < 2390 kPa). It was shown that both tensile properties and swelling ratio of these hydrogels depend on the length of PEG chains, where ε_b, σ_b and swelling ratio increase with PEG chain length. The swelling ratio for a hydrogel with ε_b ~ 1550 % and σ_b ~ 2.4 MPa was measured ~ 12 [55]. The PEG hydrogels that were produces by click chemistry exhibited much higher tensile mechanical properties than those prepared by photopolymerisation (σ_b ~ 70 – 160 kPa, ε_b ~ 50 – 150 %) [55].

1.5.6. Macromolecular Nano/Microsphere Composite Hydrogels

Another type of hydrogels with enhanced mechanical properties is those made from nano – micro-sized spheres acting as crosslinking. Macromolecular microspheres (MMS) with active surfaces were used to form surprisingly tough hydrogels [57, 70, 158]. Microspheres made from styrene, butyl acrylate and AA were prepared in an emulsion polymerisation, followed by γ-irradiation in the presence of oxygen to introduce peroxides onto the surface of microspheres (Figure 1.12) [57]. These active microspheres then were used as both initiator and crosslinking agent to polymerize AA monomers. Very high compression stresses ranging from 1 to 20 MPa was reported with full strain recovery in many cases, while the maximum compression strength measured was ~ 78 MPa for a hydrogel with 70 % water content [57]. Depending on the composition of hydrogels, the water content changed between 70 and 90 wt%, affecting the mechanical properties accordingly [57].

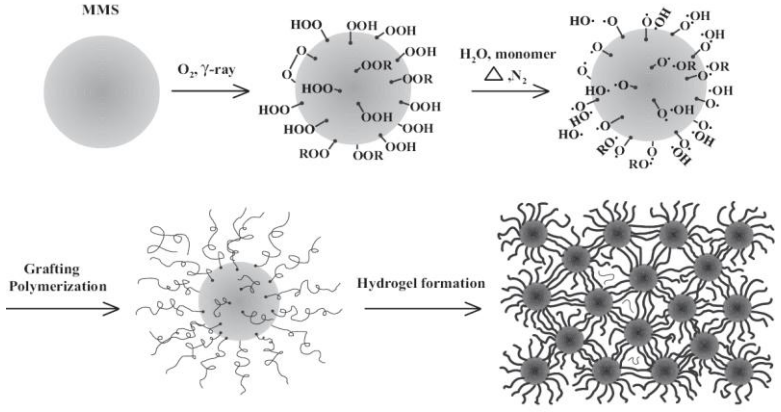

Figure 1.12. A schematic illustration of the formation of a macromolecular microsphere gel [57].

Cationic PS (C-PS) nanosphers (~ 100 nm) were used to fabricate a PAAm-based hydrogel, where C-PS nanospheres were acting as the crosslinkers [70]. High swelling ratio (up to 75) and compression strength (~ 40 MPa) was achieved. These hydrogels had tensile behavior similar to that of NC hydrogels with high elongation at break (up to 5000 %) and maximum reported tensile strength of around 1 MPa [70]. In another example, nano-sized spheres (~ 300 nm) were prepared from AAm and AMPS monomers crosslinked with MBAA, followed by substituting some of the amide groups of the surface with double bonds [158]. These nanospheres with double bonds on the surface were used as the crosslinking agent to form the final hydrogels. Depending on the nanospheres level in the final hydrogels composition, the compression strength of 2 to 4.60 MPa was reported, with tensile strength of 190 – 270 kPa and elongation at break of 420 – 550 %. A similar concept was used to make a two network hydrogel consisting of a microgel network with grafted copolymer chains of AA and acryloyloxyethyl trimethyl ammonium chloride and AAm onto the PNIPAM-poly(vinyl amine) spheres while the other network was ungrafted copolymer chains [159]. Again, high compression strength was reported (5 – 30 MPa) depending on the composition of hydrogels. Similarly, poly(NIPAM-co-AA) microgels were prepared and used to crosslink poly(NIPAM-co-AA) hydrogels [160]. These hydrogels were demonstrated to be pH and temperature sensitive. Biodegradable and biocompatible starch-based nanospheres were also prepared from the self-assembly of acetylated allylic starch macromolecules [161]. The AAm hydrogels were prepared using these starch-based spheres as the crosslinking agent. Compression strength as high as ~ 30 MPa with fracture strain of ~ 90 % was reported in some cases for this hydrogel.

1.5.7. Tetrahedral PEG Hydrogels

Another method to form a uniform hydrogel network with enhanced mechanical properties is to combine two star-shaped polymers with symmetrical arms of the same size, where the tetrahedron macromonomers can react with each other via the functional groups on the end of their arms [56]. Maximum compression strength of 2.5 MPa was obtained for a gel made from two PEG-based tetrahedral-like macromonomers with amine and succinimidyl ester functional groups when the stoichiometric ratio of the two macromonomers was 1. The SANS measurements confirmed that the network structure is uniform, and the structural defects start to increase as the ratio of two macromonomers deviates from stoichiometric condition [162]. It was found that the formation of topological defects, e.g. entanglements and loops, are negligible in these networks [163], and regardless of the initial concentration of macromonomers the characteristic length of the final swollen state remains constant and is related to the length of arms [164]. It is worth to mention that although SANS, DLS and SLS measurements provided evidences of an extremely uniform network, there were some examples of defects due to the imperfect formation of networks in tetrahedron PEG stars with shorter arms [164].

1.5.8. Hydrophobic Association Hydrogels

Hydrophobic association hydrogels (HA) are mainly prepared by micellar copolymerisation of conventional hydrophilic monomers with small amount of hydrophobic comonomers, where the latter will form the hydrophobic micelles. These micelles, resulting from self-assembly of hydrophobic groups attached to the hydrophilic

backbone, will then act as the crosslinking points to form the hydrogel network. The backbone of these hydrogels can be made from any hydrophilic monomer, such as acrylamide [165-168] or acrylic acid [169, 170], and the network can be formed without any chemical crosslinking agent or with the aid of an additional crosslinking comonomer [167]. The molecular structure of some of the hydrophobic monomers is illustrated in Figure 1.13.

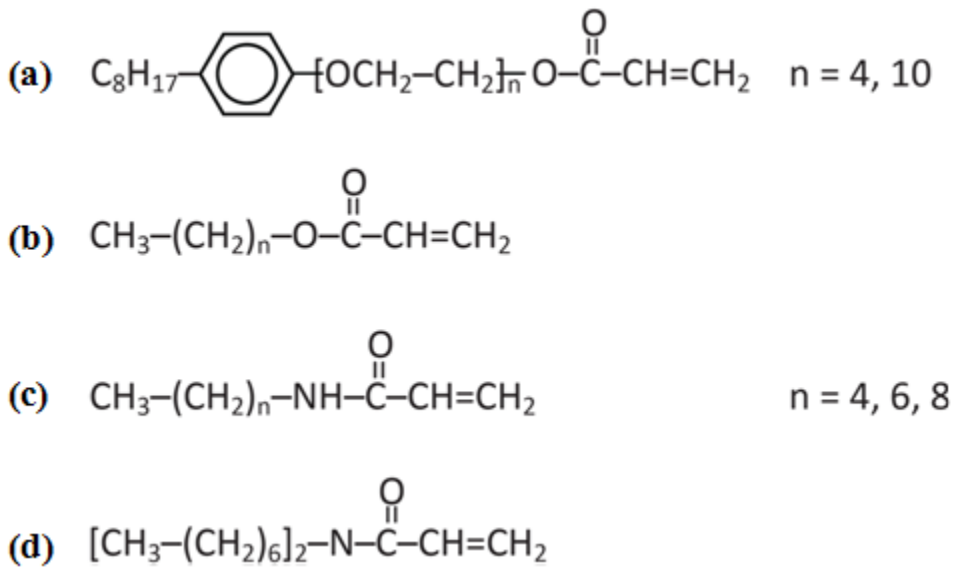

Figure 1.13. Molecular structure of some of the hydrophobic comonomers used in HA hydrogels: a) octylphenol polyoxyethylene acrylate, b) *n*-alkyl acrylate, c) *N*-alkyl acrylamide, and d) *N*,*N*-dihexyl acrylamide.

In general, the HA hydrogels are not as strong as other previously mentioned hydrogels showing a tensile strength of 50 – 200 kPa, elongation at break of 1000 – 2500 % and modulus of 2 – 10 kPa [58, 166]. The HA hydrogels obtained without using any chemical crosslinking agent could exhibit an interesting self-healing feature [58,

166]. The self-healed specimen could retain its high elongation at break but performed slightly poorer than the uncut sample. Moreover, the HA hydrogels were shown to have the capability of being re-molded and forming the shape of their new mold [58, 168]. The self-healing and re-molding characteristics of these hydrogel indicate that the micelles can rearrange themselves and form new micellar structure during the molding or self-healing.

1.6. Toughening Mechanisms

An understanding of the enhanced toughness of DN gels, NC gels, topological gels and homogenous networks can be approached by first considering the reasons for the low toughness of conventional hydrogels. The Lake-Thomas description of fracture in rubbers [171] predicts the minimum fracture energy and involves a process where the network strands that span the crack plane are fully extended and subsequently fractured as the crack propagates. The toughness is determined by the energy dissipated during crack growth and involves the energy stored during the full extension of each strand. Rubber toughness increases with increasingly long network strands or as the crosslink density of the network decreases. In real rubbers the actual toughness is further increased by other energy-dissipating mechanisms such as visco-elastic interactions and melting/crystallisation [138]. The toughness of hydrogels is small compared with rubbers since the solvent swelling already stretches the network strands considerably and there are fewer network strands per crack area. The solvent in the gel also limits the

energy dissipation due to viscoelasticity [172]. Consequently, little external energy is needed to cause bond fracture, microcrack formation and crack propagation.

Network inhomogeneity further reduces the strength of gels [137], but also allows for the improvement in gel strength through the careful preparation of homogeneous networks, as described above. The principal problem with heterogeneously crosslinked gels is that cracks will form in the more highly crosslinked parts of the network where network strands are fully extended first. Figure 1.14a shows a simple 2-D picture of a homogeneously crosslinked network whereby a crack can continuously propagate through the hydrogel. Real heterogeneous networks will be more complicated than shown in Figure 1.14a and it is possible that crack initiation could occur in many isolated, more densely crosslinked regions, therefore, lower toughness (Figure 1.14b). Whether such microcracks coalesce into a propagating macro-crack ultimately determines the toughness of the material. Certainly, it is readily appreciated that in a homogeneously crosslinked network there will be no favoured sites for micro-crack formation and no "paths of least resistance" for crack propagation. At least qualitatively it can be appreciated that such homogeneous networks should be more resistant to fracture than equivalent heterogeneous network of same *average* crosslink density. Further, the "slip-knot" type crosslinks that occur in topological gels allow the crosslinks to move so that the loaded network is evenly stressed. The topological networks act like homogeneously crosslinked systems.

The toughness imparted by DN gels appears to be related to the stabilising ability of the second network to prevent propagation of microcracks in the first network [137, 138]. The more tightly crosslinked first network inevitably fails first and likely forms

micro-cracks in a similar manner to a single network gel. Unlike the latter, however, micro-cracks can be stabilised by the unfractured second network strands that span the microcrack. The micro-cracks do not immediately coalesce and propagate as a macro-crack. Instead, new micro-cracks open up within other regions of the first network. These, too, are stabilised by the second network and the continued loading of the gel results in a "damage zone" around stress concentrators, like crack tips. The larger the damage zone and the more stable microcracks that form, the greater is the energy absorbed prior to failure and so the toughness is enhanced.

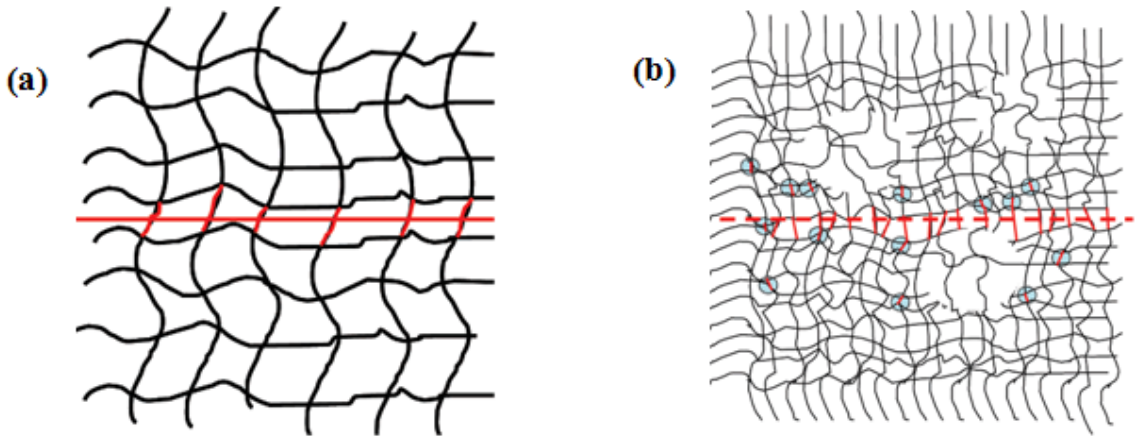

Figure 1.14. Fracture of a a) homogeneous and b) heterogeneous network. The dashed line shows the plane of fracture with circles representing the higher crosslinked areas [137].

NC gels and similar systems may provide a similar toughening mechanism to that seen in DN gels. These systems are characterised by crosslinking sites that involve

multiple network strands and the proabability that multiple strands span neighbouring crosslink sites. Upon loading it is likely to be the shorter strands between crosslinks that fail first. As with DN gels, microcrack propagation may be prevented by unfractured network strands that link the same crosslink points. Thus, micro-cracks are stabilised and damage zones may form in which considerable energy dissipation can occur.

The toughness of any system must be related to molecular (or atomic) processes that cause dissipation of elastically stored energy during crack propagation. The more energy dissipated, the greater the toughness. Presented above are plausible explanations for the enhanced toughness of homogeneous networks, DN gels and NC gels. It should also be noted that visco-plastic energy dissipation mechanisms may also contribute to gel toughness. Indeed, it is shown that the toughness of gelatin, a common physically crosslinked gel, is likely influenced by frictional sliding processes between polymer chains and the solvent [173]. Such behaviour is evident by increasing fracture energy with increasing crack velocities and is demonstrated by gelatin gels. Interestingly, little dependence of fracture energy on crack velocity has been noted for some DN gels [100] indicating that visco-plastic deformation is not prominent in such systems. It remains to be determined whether further toughness enhancement of gels is possible through the introduction of multiple toughening mechanisms in a single gel system.

1.7. Tough Conductive Hydrogels

Conductive hydrogels hold significant promises in drug release, bioactive electrode coating, and actuators [174-176]. Combining the physical and mechanical properties of

hydrogels with the electrical activity of an electroactive component can create unique opportunities for the next generation of materials. However, in many cases, conductivity is not part of the inherent characteristics of the hydrogel and is provided by other elements which are incorporated within the network of the hydrogel (e.g. conductive particles, conducting polymer, etc.). In general, electrically conductive gels can be fabricated via several methods such as: (1) adding conductive particles to the gel matrix [177]; (2) producing the gel directly from the conjugated polymers [178-181]; or (3) incorporating conducting polymers into the network structure of the gels [182, 183]. Except for conducting polymer gels, the electrical conductivity is given by the conductive network formed from the conductive elements within an insulating gel, and the gel structure simply constrains this conductive network to provide the required mechanical resistance against the external forces. However, most conventional hydrogels lack the adequate toughness required in many applications. Moreover, the swelling of the hydrogel can also suppress the electrical conductivity of the system due to the percolation phenomenon. Since the conductivity is mainly provided by the conductive network within the hydrogel, the hydrogel network is essentially diluting the conductive network. As the swelling ratio increases, this effect becomes more and more significant and the system loses its conductivity. Therefore, it is important to develop a conductive hydrogel system that retains its conductivity at different gel swelling ratios and also displays enhanced mechanical performances.

The fully swollen hydrogels with conducting particles, such as graphite [177, 184-186], carbon nanotubes [187, 188], or metallic particles [189], incorporated in their structure typically have conductivity lower than 10^{-3} S/cm, with the mechanical

properties similar to the constituent hydrogel matrix. In all of these examples, the conductivity is inversely affected by the swelling ratio, and hydrogels exhibit brittle mechanical behaviour [177, 188]. To obtain suitable mechanical performance for bioapplications, poly(vinyl alcohol) (PVA) has been widely used (alone or with other polymers) as the hydrogel matrix. For example, PVA-graphite hydrogels were used as an artificial cornea with tensile strength dropping constantly as graphite content increases [186].

Conjugated gels made directly from conjugated polymers have also been reported previously as conductive hydrogel/gel systems. Examples include ionically crosslinked poly(3,4-ethylenedioxythiophene) (PEDOT)-poly(styrenesulfonate) (PSS) [190], PEDOT-PSS-polypyrrole (PPy) [34], PPy-PSS, PEDOT-sulfonated polyaniline (SPANi), and PPy-SPANi [191, 192]. The swelling ratio of these conjugated gels was reported to range typically between 10 – 80. The conductivity of these hydrogels was reported to be in the order of 10^{-2} S/cm, and the mechanical properties were demonstrated to vary significantly with the composition of the hydrogel. The highest compression strength in this category was reported for an ionically crosslinked PEDOT-PSS hydrogel with an optimum amount of excess PSS, which was 3.3 MPa with a fracture strain of 90 % [192]. The same hydrogel showed a tensile strength of about 180 kPa and elongation at break of 64 % [192].

An alternative approach to introduce conductivity to a hydrogel is by incorporating a conjugated polymer into a pre-formed gel network to form an interpenetrating network (IPN) where one network is a conjugated polymer. Various conducting polymers such as polyaniline (PANi) [193-198] were chemically polymerised within a pre-formed

hydrogel network (or directly added to the network) to make the hydrogel conductive. The measured conductivity for most of these hydrogels in their swollen state was in the order of 10^{-3} S/cm. In one study, PEDOT-PSS was chemically polymerised within a PAAm network to produce a conductive hydrogel [118]. The hydrogels were tough with compression strength as high as 1.3 MPa, fracture strain of 60 – 90 %, and electrical conductivity in the order of 10^{-3} S/cm. The maximum conductivity that could be achieved in these studies was limited by the solubility of EDOT in the aqueous solution of PSS. Interfacial polymerisation has also been employed to form PANi within PAAm hydrogels where aniline monomers were chemically polymerised at the organic/water interface between the reaction media (organic phase) and PAAm hydrogel (water phase). As the polymerisation reaction proceeded the PANi becomes hydrophilic and migrated into the aqueous phase confined within the PAAm hydrogel [199]. The achieved hydrogels were reported to be tough with compression strength of up to 1.1 MPa, fracture strains from 80 to 90 % (90 % water content), and electrical conductivity of up to 3.4× 10^{-2} S/cm (PANi content ~ 28 wt%).

Electropolymerisation has also been employed to introduce the conducting polymers into the network. For example, PPy and PANi were electrochemically polymerised within a PAAm hydrogel [200, 201], or copolymer hydrogels based on poly(hydroxyethyl methacrylate) (HEMA) [202, 203]. The measured electrical conductivity for these hydrogel films was reported to be in the order of ~ 10^{-2} S/cm [204]. Again, the mechanical performance of these hydrogels was similar to the constituent hydrogel with low tensile elongation at break and low strength [205].

In order to enhance the mechanical performance of these conductive hydrogels, the “double network” toughening approach has also been used. Hydrogels made from a tightly crosslinked polyelectrolyte and a loosely crosslinked neutral polymer have been shown to have significantly improved mechanical strength and toughness [206]. The hydrogels obtained by this approached are called double networks (DN). In one example, a PAA-based tough hydrogel was formed followed by chemical polymerisation of 3,4-ethylenedioxythiophene (EDOT)-PSS within the hydrogel [123]. The tough PAA hydrogel was built from two PAA interpenetrated networks with different crosslinking ratio. The PEDOT incorporated PAA-PAA DN hydrogels were reported to be electroactive and the final gel having a compression strength as high as 1.8 MPa and fracture strain of 80 %. It was shown that this fracture strength was three times larger than that of the initial PAA-PAA DN hydrogel, and more than 20 times larger than that of PAA single network. The conductivity of these hydrogels were measured to be less than 10^{-3} S/cm.

1.8. Modulated Drug Release from Hydrogels

Precise release from drug delivery devices is highly desirable to overcome the disadvantages of oral and injection dosage methods [207]. The conventional methods of introducing medicines into the body initially supply a maximum dose of the drug but this dosage dramatically decreases over a short period of time. The design of a drug delivery system would be ideal if it responds to the physiological conditions like patterns of hormonal concentration, body temperature, blood glucose level, changes in pH

conditions, and electrical signals [11, 18, 208-210]. The use of electrical signals to stimulate drug release is attractive because electronics are readily available and versatile for *in vitro* investigation. Parameters such as pulse type, amplitude, polarity and duration can be easily adapted to a drug delivery system to control the release. Several studies have demonstrated that electrical stimulation is a viable route to enhance drug release [208, 211-219]. Typically, these drug release systems are fabricated from hydrogels that utilize an electric field as a means to activate the release.

Hydrogels have been extensively studied for various potential *in vivo* applications. The high water content and flexibility of hydrogels make them suitable for implants without irritating surrounding tissues [220]. Their application as biomaterials is extensive, including contact lenses [221], denture adhesives [222], dermatological patches [223], and drug delivery carriers [11, 208, 224-226]. In the latter, drug release is enabled either passively (normal diffusion) or through some stimulus, in particular pH or temperature which triggers a gel collapse and release of trapped chemical species [208]. Electrically stimulated release has also been demonstrated from hydrogels [227-229]. Different release mechanisms have been proposed, including the diffusion of drug into the surrounding media; electrophoresis of charged drugs resulting from the electrostatic repulsion between a charged drug and applied charges; and release of drug due to erosion of hydrogels due to pH change [211, 230, 231].

1.9. Summary

This review of the mechanical properties of hydrogels illustrates the tremendous advances made in recent years in improving the strength and toughness of synthetic hydrogels. This improvement in mechanical properties allows the development of hydrogels for new, demanding applications. Of particular interest in this thesis is the development of electrically conducting hydrogels that can be fashioned into thin fibres and films. These materials are believed to be useful for controlled release of drugs (eg. for cell growth stimulation) and as artificial muscles. Because thin films and fibres are required, it is imperative that the gels be tough. The main objective of this thesis, then, is to combine methods to produce tough gels with methods to render the gels conducting. In addition, it is important to establish that such gels can be produced as fibres and can be used for controlled release. Progress towards these aims are described in the following chapters as follows:

Chapter 2: Illustration of the ability to stimulate the release of a drug from an electronically conducting hydrogel;

Chapter 3: Demonstration of the possibility of producing tough gel fibres using the double network approach;

Chapter 4: Evaluation of enhanced toughening and pH switching in a double network gel using inter-network hydrogen bonding;

Chapter 5: Introduction of electronic conductivity to a tough gel using a polythiophene conducting polymer;

Chapter 6: Introduction of electronic conductivity to a tough gel using carbon nanotubes.

Each chapter contains a short introduction, followed by an experimental section, results, discussion and conclusions.

1.10. References

1. Kopecek J. Journal of Polymer Science Part A: Polymer Chemistry 2009;47(22):5929-5946.
2. Tanaka T. Physical Review Letters 1978;40(12):820.
3. Hirokawa Y and Tanaka T. The Journal of Chemical Physics 1984;81(12):6379-6380.
4. Chen G and Hoffman AS. Nature 1995;373(6509):49-52.
5. Yoshida R, Uchida K, Kaneko Y, Sakai K, Kikuchi A, Sakurai Y, and Okano T. Nature 1995;374(6519):240-242.
6. Jeong B, Kim SW, and Bae YH. Advanced Drug Delivery Reviews 2002;54(1):37-51.
7. Ruel-Gariépy E and Leroux J-C. European Journal of Pharmaceutics and Biopharmaceutics 2004;58(2):409-426.
8. Brannon-Peppas L and Peppas NA. Chemical Engineering Science 1991;46(3):715-722.
9. Dong L-c and Hoffman AS. Journal of Controlled Release 1991;15(2):141-152.
10. Torres-Lugo M and Peppas NA. Macromolecules 1999;32(20):6646-6651.
11. Qiu Y and Park K. Advanced Drug Delivery Reviews 2001;53(3):321-339.
12. Holtz JH and Asher SA. Nature 1997;389(6653):829-832.
13. Miyata T, Uragami T, and Nakamae K. Advanced Drug Delivery Reviews 2002;54(1):79-98.
14. Suzuki A and Tanaka T. Nature 1990;346(6282):345-347.
15. Kim SJ, Kim HI, Park SJ, Kim IY, Lee SH, Lee TS, and Kim SI. Smart Materials and Structures 2005;14(4):511.

16. Osada Y, Okuzaki H, and Hori H. Nature 1992;355:242-244.

17. Osada Y and Gong JP. Advanced Materials 1998;10(11):827-837.

18. Kikuchi A and Okano T. Advanced Drug Delivery Reviews 2002;54(1):53-77.

19. Wichterle O and Lim D. Nature 1960;185(4706):117.

20. Chen X, Martin BD, Neubauer TK, Linhardt RJ, Dordick JS, and Rethwisch DG. Carbohydrate Polymers 1995;28(1):15-21.

21. Byrne ME, Park K, and Peppas NA. Advanced Drug Delivery Reviews 2002;54(1):149-161.

22. Lin C-C and Metters AT. Advanced Drug Delivery Reviews 2006;58(12-13):1379-1408.

23. Lee KY and Mooney DJ. Chemical Reviews 2001;101(7):1869-1880.

24. Nguyen KT and West JL. Biomaterials 2002;23(22):4307-4314.

25. Landers R, Hübner U, Schmelzeisen R, and Mülhaupt R. Biomaterials 2002;23(23):4437-4447.

26. Drury JL and Mooney DJ. Biomaterials 2003;24(24):4337-4351.

27. Lutolf M, Raeber G, Zisch A, Tirelli N, and Hubbell J. Advanced Materials 2003;15(11):888-892.

28. Strong ZA, Wang AW, and McConaghy CF. Biomedical Microdevices 2002;4(2):97-103.

29. Richter A, Paschew G, Klatt S, Lienig J, Arndt K-F, and Adler H-JP. Sensors 2008;8(1):561-581.

30. Ma B, Wu S, and Zeng F. Sensors and Actuators B: Chemical 2010;145(1):451-456.

31. Beebe DJ, Moore JS, Bauer JM, Yu Q, Liu RH, Devadoss C, and Jo B-H. Nature 2000;404(6778):588-590.

32. Arndt KF, Kuckling D, and Richter A. Polymers for Advanced Technologies 2000;11(8-12):496-505.

33. Satarkar NS, Zhang W, Eitel RE, and Hilt JZ. Lab on a Chip 2009;9(12):1773-1779.

34. Ghosh S and Inganäs O. Advanced Materials 1999;11(14):1214-1218.

35. Westbrook KK and Qi HJ. Journal of Intelligent Material Systems and Structures 2008;19(5):597-607.

36. Swann JM and Ryan AJ. Polymer International 2009;58(3):285-289.

37. Shin MK, Spinks GM, Shin SR, Kim SI, and Kim SJ. Advanced Materials 2009;21(17):1712-1715.

38. O'Grady ML, Kuo P-l, and Parker KK. ACS Applied Materials & Interfaces 2010;2(2):343-346.

39. Zhu D, Li C, Zeng X, and Jiang H. Applied Physics Letters 2010;96(8):081111-081113.

40. Kwon GH, Choi YY, Park JY, Woo DH, Lee KB, Kim JH, and Lee S-H. Lab on a Chip 2010;10(12):1604-1610.

41. Peppas NA, Bures P, Leobandung W, and Ichikawa H. European Journal of Pharmaceutics and Biopharmaceutics 2000;50(1):27-46.

42. Peppas N, Hilt J, Khademhosseini A, and Langer R. Advanced Materials 2006;18(11):1345-1360.

43. Deligkaris K, Tadele TS, Olthuis W, and van den Berg A. Sensors and Actuators B: Chemical 2010;147(2):765-774.

44. Li Y and Tanaka T. The Journal of Chemical Physics 1990;92(2):1365-1371.

45. Amsden B. Macromolecules 1998;31(23):8382-8395.

46. Pines E and Prins W. Macromolecules 1973;6(6):888-895.

47. Peppas NA and Merrill EW. Journal of Applied Polymer Science 1977;21(7):1763-1770.

48. Anseth KS, Bowman CN, and Brannon-Peppas L. Biomaterials 1996;17(17):1647-1657.

49. Okumura Y and Ito K. Advanced Materials 2001;13(7):485-487.

50. Haraguchi K and Takehisa T. Advanced Materials 2002;14(16):1120-1124.

51. Gong JP, Katsuyama Y, Kurokawa T, and Osada Y. Advanced Materials 2003;15(14):1155-1158.

52. Mayumi K and Ito K. Polymer 2010;51:959-967.

53. Haraguchi K. Current Opinion in Solid State and Materials Science 2007;11(3-4):47-54.

54. Gong JP. Soft Matter 2010;6:2583-2590.

55. Malkoch M, Vestberg R, Gupta N, Mespouille L, Dubois P, Mason AF, Hedrick JL, Liao Q, Frank CW, Kingsbury K, and Hawker CJ. Chemical Communications 2006(26):2774-2776.

56. Sakai T, Matsunaga T, Yamamoto Y, Ito C, Yoshida R, Suzuki S, Sasaki N, Shibayama M, and Chung U-i. Macromolecules 2008;41(14):5379-5384.

57. Huang T, Xu H, Jiao K, Zhu L, Brown H, and Wang H. Advanced Materials 2007;19(12):1622-1626.

58. Jiang G, Liu C, Liu X, Zhang G, Yang M, and Liu F. Macromolecular Materials and Engineering 2009;294(12):815-820.

59. Zarzycki J. Journal of Non-Crystalline Solids 1988;100(1-3):359-363.

60. Tanaka Y, Fukao K, and Miyamoto Y. Eur. Phys. J. E 2000;3(4):395-401.

61. Morton M. Rubber Technology. New York: Van Nostrand Reinhold Co., 1987.

62. Tranoudis I and Efron N. Contact Lens and Anterior Eye 2004;27(4):177-191.

63. Johnson BD, Beebe DJ, and Crone WC. Materials Science and Engineering: C 2004;24(4):575-581.

64. Myung D, Koh W, Ko J, Hu Y, Carrasco M, Noolandi J, Ta CN, and Frank CW. Polymer 2007;48(18):5376-5387.

65. Kawauchi Y, Tanaka Y, Furukawa H, Kurokawa T, Nakajima T, Osada Y, and Gong JP. Journal of Physics: Conference Series 2009;184(1):012016.

66. Na Y-H, Tanaka Y, Kawauchi Y, Furukawa H, Sumiyoshi T, Gong JP, and Osada Y. Macromolecules 2006;39(14):4641-4645.

67. Zhu M, Liu Y, Sun B, Zhang W, Liu X, Yu H, Zhang Y, Kuckling D, and Adler HJP. Macromolecular Rapid Communications 2006;27(13):1023-1028.

68. Yoo SH, Cohen C, and Hui C-Y. Polymer 2006;47(17):6226-6235.

69. Nakayama A, Kakugo A, Gong JP, Osada Y, Takai M, Erata T, and Kawano S. Advanced Functional Materials 2004;14(11):1124-1128.

70. Wu Y, Zhou Z, Fan Q, Chen L, and Zhu M. Journal of Materials Chemistry 2009;19(39):7340-7346.

71. Liu Y, Zhu M, Liu X, Zhang W, Sun B, Chen Y, and Adler H-JP. Polymer 2006;47(1):1-5.

72. Haraguchi K, Takehisa T, and Fan S. Macromolecules 2002;35(27):10162-10171.

73. Haraguchi K, Farnworth R, Ohbayashi A, and Takehisa T. Macromolecules 2003;36(15):5732-5741.

74. Haraguchi K and Li H-J. Macromolecules 2006;39(5):1898-1905.

75. Xiong L, Zhu M, Hu X, Liu X, and Tong Z. Macromolecules 2009;42(11):3811-3817.

76. Hu X, Xiong L, Wang T, Lin Z, Liu X, and Tong Z. Polymer 2009;50(8):1933-1938.

77. Zhu M, Xiong L, Wang T, Liu X, Wang C, and Tong Z. Reactive and Functional Polymers 2010;70(5):267-271.

78. Ma J, Zhang L, Fan B, Xu Y, and Liang B. Journal of Polymer Science Part B: Polymer Physics 2008;46(15):1546-1555.

79. Hu X, Wang T, Xiong L, Wang C, Liu X, and Tong Z. Langmuir 2010;26(6):4233-4238.

80. Song L, Zhu M, Chen Y, and Haraguchi K. Macromolecular Chemistry and Physics 2008;209(15):1564-1575.

81. Fukasawa M, Sakai T, Chung U-i, and Haraguchi K. Macromolecules 2010;43(9):4370-4378.

82. Xiong L, Hu X, Liu X, and Tong Z. Polymer 2008;49(23):5064-5071.

83. Djonlagić J and Petrović ZS. Journal of Polymer Science Part B: Polymer Physics 2004;42(21):3987-3999.

84. Zhang X, Guo X, Yang S, Tan S, Li X, Dai H, Yu X, Weng N, Jian B, and Xu J. Journal of Applied Polymer Science 2009;112(5):3063-3070.

85. Lee Y, Kim DN, Choi D, Lee W, Park J, and Koh W-G. Polymers for Advanced Technologies 2008;19(7):852-858.

86. Myung D, Waters D, Wiseman M, Duhamel PE, Noolandi J, Ta CN, and Frank CW. Polymers for Advanced Technologies 2008;19(6):647-657.

87. Chen Q-Z, Bismarck A, Hansen U, Junaid S, Tran MQ, Harding SE, Ali NN, and Boccaccini AR. Biomaterials 2008;29(1):47-57.

88. Baumberger T and Ronsin O. Biomacromolecules 2010;11(6):1571-1578.

89. Baumberger T, Caroli C, and Martina D. Eur. Phys. J. E 2006;21(1):81-89.

90. Zhang J, Daubert CR, and Foegeding EA. Rheologica Acta 2005;44(6):622-630.

91. Dubois G, Volksen W, Magbitang T, Miller R, Gage D, and Dauskardt R. Advanced Materials 2007;19(22):3989-3994.

92. Crawford RJ. Plastics Engineering, 3rd ed. Oxford: Elsevier, 2004.

93. Friedrich K and Karsch UA. Fibre Science and Technology 1983;18(1):37-52.

94. Meeks AC. Polymer 1974;15(10):675-681.

95. Borggreve RJM, Gaymans RJ, Schuijer J, and Housz JFI. Polymer 1987;28(9):1489-1496.

96. Parker DS, Sue HJ, Huang J, and Yee AF. Polymer 1990;31(12):2267-2277.

97. Hofman W. Rubber Technology Handbook. New York: Hanser, 1988.

98. Huang M, Furukawa H, Tanaka Y, Nakajima T, Osada Y, and Gong JP. Macromolecules 2007;40(18):6658-6664.

99. Nakajima T, Furukawa H, Tanaka Y, Kurokawa T, Osada Y, and Gong JP. Macromolecules 2009;42(6):2184-2189.

100. Tsukeshiba H, Huang M, Na Y-H, Kurokawa T, Kuwabara R, Tanaka Y, Furukawa H, Osada Y, and Gong JP. The Journal of Physical Chemistry B 2005;109(34):16304-16309.

101. Tanaka Y, Kuwabara R, Na Y-H, Kurokawa T, Gong JP, and Osada Y. The Journal of Physical Chemistry B 2005;109(23):11559-11562.

102. Mendes E, Lindner P, Buzier M, Bou, eacute, F., and Bastide J. Physical Review Letters 1991;66(12):1595-1598.

103. Rouf C, Bastide J, Pujol JM, Schosseler F, and Munch JP. Physical Review Letters 1994;73(6):830-833.

104. Ramzi A, Zielinski F, Bastide J, and Boue F. Macromolecules 1995;28(10):3570-3587.

105. Moses E, Kume T, and Hashimoto T. Physical Review Letters 1994;72(13):2037-2040.

106. Karino T, Okumura Y, Zhao C, Kataoka T, Ito K, and Shibayama M. Macromolecules 2005;38(14):6161-6167.

107. Shinohara Y, Kayashima K, Okumura Y, Zhao C, Ito K, and Amemiya Y. Macromolecules 2006;39(21):7386-7391.

108. Koga T and Tanaka F. Eur. Phys. J. E 2005;17(2):225-229.

109. Okada A and Usuki A. Macromolecular Materials and Engineering 2006;291(12):1449-1476.

110. Nie J, Du B, and Oppermann W. Macromolecules 2005;38(13):5729-5736.

111. Haraguchi K and Song L. Macromolecules 2007;40(15):5526-5536.

112. Tobolsky AV, Carlson DW, and Indictor N. Journal of Polymer Science 1961;54(159):175-192.

113. Liu Y, Zhu M, Liu X, Jiang Y, Ma Y, Qin Z, Kuckling D, and Adler HJP. Macromolecular Symposia 2007;254(1):353-360.

114. Shibayama M, Karino T, Miyazaki S, Okabe S, Takehisa T, and Haraguchi K. Macromolecules 2005;38(26):10772-10781.

115. Miyazaki S, Karino T, Endo H, Haraguchi K, and Shibayama M. Macromolecules 2006;39(23):8112-8120.

116. Na Y-H, Kurokawa T, Katsuyama Y, Tsukeshiba H, Gong JP, Osada Y, Okabe S, Karino T, and Shibayama M. Macromolecules 2004;37(14):5370-5374.

117. Nakajima T, Takedomi N, Kurokawa T, Furukawa H, and Gong JP. Polymer Chemistry 2010;1(5):693-697.

118. Dai T, Qing X, Zhou H, Shen C, Wang J, and Lu Y. Synthetic Metals 2010;160(7-8):791-796.

119. Hagiwara Y, Putra A, Kakugo A, Furukawa H, and Gong JP. Cellulose 2010;17(1):93-101.

120. Liang S, Yu QM, Yin H, Wu ZL, Kurokawa T, and Gong JP. Chemical Communications 2009(48):7518-7520.

121. Kato M, Shoda N, Yamamoto T, Shiratori R, and Toyooka T. Analyst 2009;134(3):577-581.

122. Liang S, Liu L, Huang Q, and Yam KL. Carbohydrate Polymers 2009;77(4):718-724.

123. Dai T, Qing X, Lu Y, and Xia Y. Polymer 2009;50(22):5236-5241.

124. Yang W, Furukawa H, and Gong JP. Advanced Materials 2008;20(23):4499-4503.

125. Weng L, Gouldstone A, Wu Y, and Chen W. Biomaterials 2008;29(14):2153-2163.

126. Ajiro H, Watanabe J, and Akashi M. Biomacromolecules 2008;9(2):426-430.

127. Zhang Z, Chao T, and Jiang S. The Journal of Physical Chemistry B 2008;112(17):5327-5332.

128. Georgiev G, Dyankova K, Vassileva E, and Friedrich K. e-Polymers 2006:054.

129. Yasuda K, Gong JP, Katsuyama Y, Nakayama A, Tanabe Y, Kondo E, Ueno M, and Osada Y. Biomaterials 2005;26(21):4468-4475.

130. Azuma C, Yasuda K, Tanabe Y, Taniguro H, Kanaya F, Nakayama A, Chen YM, Gong JP, and Osada Y. Journal of Biomedical Materials Research Part A 2007;81A(2):373-380.

131. Kaneko D, Tada T, Kurokawa T, Gong JP, and Osada Y. Advanced Materials 2005;17(5):535-538.

132. Tominaga T, Tirumala VR, Lin EK, Gong JP, Furukawa H, Osada Y, and Wu W-l. Polymer 2007;48(26):7449-7454.

133. Lee S, Tirumala VR, Nagao M, Tominaga T, Lin EK, Gong JP, and Wu W-l. Macromolecules 2009;42(4):1293-1299.

134. Okumura K. EPL (Europhysics Letters) 2004;67(3):470-476.

135. Tominaga T, Tirumala VR, Lee S, Lin EK, Gong JP, and Wu W-l. The Journal of Physical Chemistry B 2008;112(13):3903-3909.

136. Nakajima T, Furukawa H, Gong JP, Lin EK, and Wu W-l. Macromolecular Symposia 2010;291-292(1):122-126.

137. Webber RE, Creton C, Brown HR, and Gong JP. Macromolecules 2007;40(8):2919-2927.

138. Brown HR. Macromolecules 2007;40(10):3815-3818.

139. Tanaka Y. EPL (Europhysics Letters) 2007;78(5):56005.

140. Wada H and Tanaka Y. EPL (Europhysics Letters) 2009;87(5):58001.

141. Yu QM, Tanaka Y, Furukawa H, Kurokawa T, and Gong JP. Macromolecules 2009;42(12):3852-3855.

142. Tanaka Y, Kawauchi Y, Kurokawa T, Furukawa H, Okajima T, and Gong JP. Macromolecular Rapid Communications 2008;29(18):1514-1520.

143. Edgecombe S and Linse P. Polymer 2008;49(7):1981-1992.

144. Jang SS, Goddard WA, and Kalani MYS. The Journal of Physical Chemistry B 2007;111(7):1729-1737.

145. Hao J, Yuan G, He W, Cheng H, Han CC, and Wu C. Macromolecules 2010;43(4):2002-2008.

146. Nishi S and Kotaka T. Macromolecules 1985;18(8):1519-1525.

147. Li Y, Li H, Chen X, Zhu F, Yang J, and Zhu Y. Journal of Polymer Science Part B: Polymer Physics 2010;48(16):1847-1852.

148. Rostovtsev VV, Green LG, Fokin VV, and Sharpless KB. Angewandte Chemie International Edition 2002;41(14):2596-2599.

149. Binder WH and Sachsenhofer R. Macromolecular Rapid Communications 2007;28(1):15-54.

150. Ossipov DA and Hilborn Jn. Macromolecules 2006;39(5):1709-1718.

151. Crescenzi V, Cornelio L, Di Meo C, Nardecchia S, and Lamanna R. Biomacromolecules 2007;8(6):1844-1850.

152. Polizzotti BD, Fairbanks BD, and Anseth KS. Biomacromolecules 2008;9(4):1084-1087.

153. van Dijk M, van Nostrum CF, Hennink WE, Rijkers DTS, and Liskamp RMJ. Biomacromolecules 2010;11(6):1608-1614.

154. Xu LQ, Yao F, Fu GD, and Kang ET. Biomacromolecules 2010;11(7):1810-1817.

155. Xu X-D, Chen C-S, Wang Z-C, Wang G-R, Cheng S-X, Zhang X-Z, and Zhuo R-X. Journal of Polymer Science Part A: Polymer Chemistry 2008;46(15):5263-5277.

156. Wei H-L, Yang Z, Chen Y, Chu H-J, Zhu J, and Li Z-C. European Polymer Journal 2010;46(5):1032-1039.

157. Ali M and Brocchini S. Advanced Drug Delivery Reviews 2006;58(15):1671-1687.

158. Qin X, Zhao F, Liu Y, Wang H, and Feng S. Colloid and Polymer Science 2009;287(5):621-625.

159. Xu K, Tan Y, Chen Q, An H, Li W, Dong L, and Wang P. Journal of Colloid and Interface Science 2010;345(2):360-368.

160. Xia L-W, Ju X-J, Liu J-J, Xie R, and Chu L-Y. Journal of Colloid and Interface Science 2010;349(1):106-113.

161. Tan Y, Wang P, Xu K, Li W, An H, Li L, Liu C, and Dong L. Macromolecular Materials and Engineering 2009;294(12):855-859.

162. Matsunaga T, Sakai T, Akagi Y, Chung U-i, and Shibayama M. Macromolecules 2009;42(4):1344-1351.

163. Akagi Y, Matsunaga T, Shibayama M, Chung U-i, and Sakai T. Macromolecules 2010;43(1):488-493.

164. Matsunaga T, Sakai T, Akagi Y, Chung U-i, and Shibayama M. Macromolecules 2009;42(16):6245-6252.

165. Jiang G, Liu C, Liu X, Zhang G, Yang M, Chen Q, and Liu F. Journal of Macromolecular Science, Part A: Pure and Applied Chemistry 2010;47(7):663 - 670.

166. Jiang G, Liu C, Liu X, Zhang G, Yang M, Chen Q, and Liu F. Journal of Macromolecular Science, Part A: Pure and Applied Chemistry 2010;47(4):335 - 342.

167. Abdurrahmanoglu S, Can V, and Okay O. Polymer 2009;50(23):5449-5455.

168. Jiang G, Liu C, Liu X, Chen Q, Zhang G, Yang M, and Liu F. Polymer 2010;51(6):1507-1515.

169. Ma J, Liu X, Yang Z, and Tong Z. Journal of Macromolecular Science, Part A: Pure and Applied Chemistry 2009;46(8):816 - 820.

170. Philippova OE, Andreeva AS, Khokhlov AR, Islamov AK, Kuklin AI, and Gordeliy VI. Langmuir 2003;19(18):7240-7248.

171. Lake GJ and Thomas AG. Proceedings of the Royal Society London A 1967;300:108-119.

172. Ahagon A and Gent AN. Journal of Polymer Science B: Polymer Physics 1975;13(10):1903-1911.

173. Baumberger T, Caroli C, and Martina D. Nature Materials 2006;5:552-555.

174. Naficy S, Razal JM, Spinks GM, and Wallace GG. Sensors and Actuators A: Physical 2009;155:120-124.

175. Abidian MR and Martin DC. Advanced Functional Materials 2009;19(4):573-585.

176. Lee SH, Lee CK, Shin SR, Gu BK, Kim SI, Kang TM, and Kim SJ. Sensors and Actuators B: Chemical 2010;145(1):89-92.

177. Fan S, Tang Q, Wu J, Hu D, Sun H, and Lin J. Journal of Materials Science 2008;43(17):5898-5904.

178. Morita S, Kawai T, and Yoshino K. Journal of Applied Physics 1991;69(8):4445-4447.

179. Donat BP, Lairez D, de Geyer A, and Viallat A. Synthetic Metals 1999;101(1-3):471-472.

180. Pepin-Donat B, Van-Quynh A, and Viallat A. Macromolecules 2000;33(16):5912-5917.

181. Pépin Donat B, Viallat A, Blachot JF, Fedorko P, and Lombard C. Synthetic Metals 2003;137(1-3):897-898.

182. Fizazi A, Moulton J, Pakbaz K, Rughooputh SDDV, Smith P, and Heeger AJ. Physical Review Letters 1990;64(18):2180.

183. González I, Vecino M, Muñoz ME, Santamaría A, and Pomposo JA. Macromolecular Chemistry and Physics 2004;205(10):1379-1384.

184. Lin J, Tang Q, Wu J, and Hao S. Reactive and Functional Polymers 2007;67(4):275-281.

185. Tang Q, Lin J, and Wu J. Journal of Applied Polymer Science 2008;108(3):1490-1495.

186. Liu K, Li Y, Xu F, Zuo Y, Zhang L, Wang H, and Liao J. Materials Science and Engineering: C 2009;29(1):261-266.

187. MacDonald RA, Voge CM, Kariolis M, and Stegemann JP. Acta Biomaterialia 2008;4(6):1583-1592.

188. Ferris CJ and Panhuis Mih. Soft Matter 2009;5(18):3430-3437.

189. Lin J, Tang Q, and Wu J. Reactive and Functional Polymers 2007;67(6):489-494.

190. Ghosh S, Rasmusson J, and Inganäs O. Advanced Materials 1998;10(14):1097-1099.

191. Dai T, Jiang X, Hua S, Wang X, and Lu Y. Chemical Communications 2008(36):4279-4281.

192. Dai T, Shi Z, Shen C, Wang J, and Lu Y. Synthetic Metals 2010;160(9-10):1101-1106.

193. Tang Q, Lin J, Wu J, Zhang C, and Hao S. Carbohydrate Polymers 2007;67(3):332-336.

194. Tang Q, Wu J, and Lin J. Carbohydrate Polymers 2008;73(2):315-321.

195. Lin J, Tang Q, Hu D, Sun X, Li Q, and Wu J. Colloids and Surfaces A: Physicochemical and Engineering Aspects 2009;346(1-3):177-183.

196. Tang Q, Wu J, Sun H, Fan S, Hu D, and Lin J. Carbohydrate Polymers 2008;73(3):473-481.

197. Bajpai AK, Bajpai J, and Soni SN. eXPRESS Polymer Letters 2008;2(1):26-39.

198. Thanpitcha T, Sirivat A, Jamieson AM, and Rujiravanit R. Carbohydrate Polymers 2006;64(4):560-568.

199. Dai T, Qing X, Wang J, Shen C, and Lu Y. Composites Science and Technology 2010;70(3):498-503.

200. Gilmore K, Hodgson AJ, Luan B, Small CJ, and Wallace GG. Polymer Gels and Networks 1994;2(2):135-143.

201. Small CJ, Too CO, and Wallace GG. Polymer Gels and Networks 1997;5(3):251-265.

202. Brahim S and Guiseppi-Elie A. Electroanalysis 2005;17(7):556-570.

203. Justin G and Guiseppi-Elie A. Biomacromolecules 2009;10(9):2539-2549.

204. Guiseppi-Elie A, Brahim S, and Narinesingh D. Journal of Macromolecular Science, Part A: Pure and Applied Chemistry 2001;38(12):1575 - 1591.

205. Aouada FA, Guilherme MR, Campese GM, Girotto EM, Rubira AF, and Muniz EC. Polymer Testing 2006;25(2):158-165.

206. Gong JP, Katsuyama Y, Kurokawa T, and Osada Y. Advanced Materials 2003;15(14):1155-1158.

207. Langer R. Science 1990;249: 1527-1533.

208. Murdan S. Journal of Controlled Release 2003;92(1-2):1-17.

209. Christine MS, Zhang M, Rizzardo E, Thang SH, Chong YK, Edwards K, Karisson G, and Muller AHE. Macromolecules 2004;37(21):7861-7866.

210. Gudeman LF, and Peppas NA. Journal of Membrane Science 1996;107(3):239-248.

211. Kwon IC, Bae YH, and Kim SW. Nature 1991;354:291-293.

212. Lira LM, and Cordoba de Torresi SI. Electrochemistry Communications 2005;7(7):717-723.

213. Abidian MR, Kim DH, and Martin DV. Advanced Materials 2006;18(4):405-409.

214. Juntanon K, Niamlong S, Rujiravanit R, and Sirivat A. International Journal of Pharmaceutics 2008;356 (1-2):1-11.

215. Vanbever R, and Preat V. Advanced Drug Delivery Reviews 1999;35(1):77-88.

216. Delgado-Charro MB, and Guy RH. STP Pharma Sciences 2001;11(6):403-414.

217. Bose S, Ravis WR, Lin YJ, Zhang L, Hofmann GA, and Banga AK. Journal of Controlled Release 2001;73(2-3):197-203.

218. Xie Y, Xu B, and Gao Y. Nanomedicine: NBM 1 2005;1(2):184-190.

219. Kim J, Kim WJ, Kim SJ, Cho CW, and Shin SC. International Journal of Pharmaceutics 2006;315(1-2):134-139.

220. Park H, and Park K, Hydrogel and Biodegradable Polymers for Bioapplicaitons, Ottenbrite RM, Huang SJ, and Park K, ACS Symposium Series, American Chemical Society, Washington DC: 1996.

221. Wichtelre O, and Lim D. Nature 1960;185:117-118.

222. Koppang R, Berg E, Dahm S, and Floystrand F. Journal of Prosthetic Dentistry 1995;73(5):486-491.

223. Venkatraman S, and Gale R. Biomaterials 1998;19(13):1119-1136.

224. Huang G, Gao J, Hu Z, John JVSt, Ponder BC, and Moro D. Journal of Controlled Release 2004;94(2-3):303-311.

225. Kim B, Flamme KL, and Peppas NA. Journal of Applied Polymer Science 2003;89(6):1606-1613.

226. Xu FJ, Kang ET, and Neoh KG. Biomaterials 2006;27(14):2787-2797.

227. Guy RH, Kalia YN, Delgado-Charro MB, Merino V, Lopez A, and Marro D. Journal of Controlled Release 2000;64(1-3):129-132.

228. Vuorio M, Murtomaki L, Hirvonen J, and Kontturi K. Journal of Controlled Release 2004;97(3):485-492.

229. Elijarrat-Binstock E, and Domb AJ. Journal of Controlled Release 2006;110(3): 479-489.

230. Chen LLH, and Chien YW. Journal of Controlled Release 1996;40(3):187-198.

231. Elvira C, Mano JF, San Roman J, and Reis RL. Biomaterials 2002;23(9):1955-1966.

CHAPTER TWO

Modulated Drug Release from Hydrogel Films: Chitosan – Carbon Nanotube

2. Modulated Drug Release from Hydrogel Films: Chitosan – Carbon Nanotube

2.1. Introduction

As briefly discussed in Chapter 1, hydrogels are a suitable candidate for drug release in applications where the release device is in direct contact with tissue [1]. Amongst various synthetic and biopolymer hydrogels, the biopolymer chitosan has been the topic of interest for drug delivery systems because of its biocompatibility. No adverse reaction is observed when chitosan is in contact with human cells [2]. Chitosan (CS) is biodegradable and the degradation products were observed to activate macrophages. Moreover, chtiosan also assists in the reconstruction of extracellular matrix components [3]. Chitosan hydrogels have been used as a matrix to control the delivery of neutral (hydrocortisone), anionic (benzoic acid), or cationic (lidocaine hydrochloride) drug molecules by electrical stimulation [2]. Being an insulating material, the applied potential for this electric field type of drug release can reach up to a several tens of volts, while the applied current can be a few milliamperes [4]. Such high voltages may not be tolerated *in vivo* and strategies are required to enhance the material conductivity and

stimulate release at lower voltages. One approach is to incorporate a conductive material in the polymer formulation using a conductive polymer [5, 6] or carbon nanotubes.

It has recently been reported that chitosan is a good dispersing agent for SWNTs [7]. SWNTs are promising material because of their excellent electrical properties including improved electrochemical activity and high surface area [8]. In a previous report, several strategies were demonstrated in transforming CS-SWNT dispersions into macroscopic structures in the form of films, hyrdogels and fibres [7, 9]. The properties of the composites were influenced by the presence of carbon nanotubes. Respectable mechanical properties (ca. 155 MPa) and electrical conductivies (ca. 21 S/cm) were achieved [30]. The composite materials have also been shown non-cytotoxic to L-929 fibroblasts cells [30]. While there is already a large body of literature on biopolymer based systems containing SWNTs in biosensor applications [10-12], reports on their application to controlled release of drugs are limited [13].

In this chapter a simple bio-polymeric composite matrix is reported that was processed from CS and SWNT dispersions. These dispersions were loaded with dexamethasone phosphate (DEX) which is a negatively charged drug. DEX is a steroid hormone, which can act as an anti-inflammatory and immunosuppressant. Corticosteroids, particularly DEX, can reduce cerebral oedema to lower intracranial pressure [14, 15]. The drug release is modulated by controlling the amplitude and polarity of the applied electric potential. Since a direct electrical stimulation is utilized (as opposed to electric field), the electric potentials used are considerably lower compared to the previous reports.

2.2. Experimental Section

2.2.1. Materials

High molecular weight chitosan (degree of deacetylation 86.6 %) and dexamethasone disodium phosphate (Scheme 2.1) were purchased from Aldrich (St. Louis, USA). Hydrochloric acid (HCl) (32 wt%, Ajax Finechem Australia) and sodium hydroxide (Chem Supply, Australia) used to adjust the solution pH were analytical grade reagents. Purified SWNT were obtained from Carbon Nanotechnologies Inc. (Houston, USA) and were used as supplied. Carbon paper (100 μm thickness) was obtained from Goodfellow (Cambridge, UK) and used as substrate for solution casting. Phosphate buffered saline (PBS) solution (0.1 M, pH 7.4 at 25 ^{o}C) obtained from Sigma Aldrich (St. Louis, USA) was used as the supporting electrolyte and as the medium for drug release.

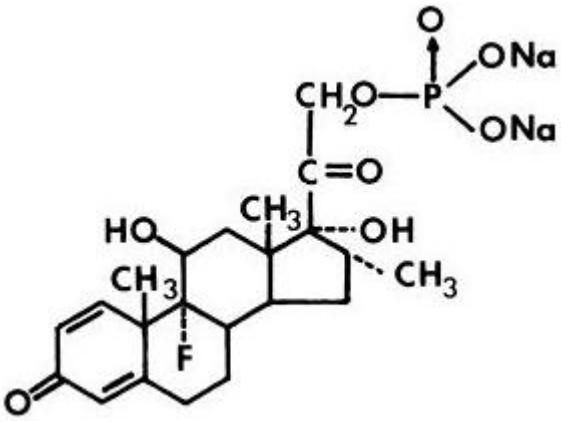

Scheme 2.1. Chemical Structure of dexamethasone disodium phosphate.

2.2.2. Preparation of CS-SWNT Films and Loading with DEX

The CS:SWNT dispersion was prepared by mixing 0.3 wt% SWNT (30 mg) and of 0.6 wt% chitosan in 0.3 M HCl. This mixture was probe sonicated (Branson Sonifier) at 150 W pulsed for one second to a total of 10 minutes. For a direct comparison, the control sample containing only chitosan was sonicated under the same conditions. Drug-loaded samples were prepared by dissolving DEX at 5 mg per 10 mL of the chitosan solution prior to the addition of SWNTs. Drop cast film was obtained by carefully pipetting 30 μL of the solution onto a carbon paper substrate (40 mm^2) and allowed to dry overnight.

2.2.3. Cyclic Voltammetry

Cyclic voltammetry (CV) and potentiostatic experiments were performed using eDAQ potentiostat ED401 connected to an e-corder recorder unit (eDAQ, Australia) using the EChem and Chart software. For all experiments, a three-electrode electrochemical set-up was used. A 0.1 M PBS solution (pH 7.4 at 25 ^oC) was used as supporting electrolyte, Ag/AgCl as reference electrode and platinum mesh as counter electrode. All potentials given are referenced to Ag/AgCl.

2.2.4. Drug Release

The amount of the DEX released was quantified using UV-visible spectroscopy (Shimadzu UV-1601) by monitoring the maximum absorbance at 240±2 nm. A 0.1 M PBS solution (pH 7.4 at 25 ^oC) was used as the release media. In a typical experiment,

the drop cast film was immersed in a 10 mL of the release media (unstimulated release) for the selected period of time. For an electrically-stimulated DEX release, the three-electrode configuration was used and constant potentials of -0.80 V, -0.40 V and 0.15 V (vs Ag/AgCl) were applied to the working electrode.

To measure the amount of the DEX released at each specific time interval, a 3 mL aliquot was taken from the release media and carefully replenished with 3 mL of the fresh PBS solution. The DEX concentration for each aliquot was compared against a calibration curve. The cumulative amount of DEX released was obtained from the amount of drug in the release media before and after a given time interval. A dilution factor is incorporated in the calculation after each 3 mL of fresh PBS was added to the release medium. The percentage of DEX release was based on the initial amount of DEX in the film.

To estimate the release rate of DEX from the hydrogel films, the initial slope of the linear section of DEX accumulative release profile was measured. Since the initial amount of DEX in the hydrogel film is known, the initial slope of the accumulative release profile indicates the total mass of DEX which has been released as a function of the time. The release rate is presented in μg/h.

2.3. Results

Cyclic voltammograms (CVs) of the different samples with and without DEX taken after 20 cycles in PBS solution are shown in Figure 2.1. The CVs of CS films with and without DEX cast on a carbon paper substrate are rather featureless, due to the absence

of any redox activity in CS or DEX over the potential range used (from 0.6 V to -0.8 V vs Ag/AgCl). There is a small redox peak observed for samples that contain SWNTs, which could be due to the presence of functional groups in the purified HiPco. The CVs are mainly dominated by double layer capacitive charging with SWNTs providing a large electroactive surface area.

The presence of DEX in the releasing medium from CS and CS-SWNT films was monitored using UV-visible spectroscopy. The absorption spectrum of DEX in PBS solutions (pH 7.4) is characterized by the maximum absorbance at 238 nm. Figure 2.2 shows that both passive release and stimulated release of DEX from chitosan did not affect the UV-visible absorbance at 238 nm, indicating that the DEX was unchanged once released from the chitosan.

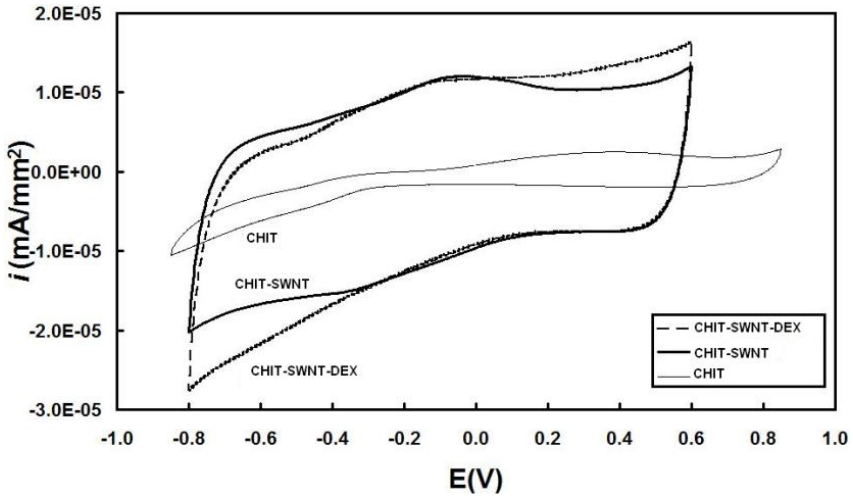

Figure 2.1. Cyclic voltammetry of DEX loaded CS-SWNT, CS-SWNT with no DEX, and DEX loaded chitosan. Scan rate of 50 mV/sec, ranging from -0.8 V to 0.6 V after 20 cycles.

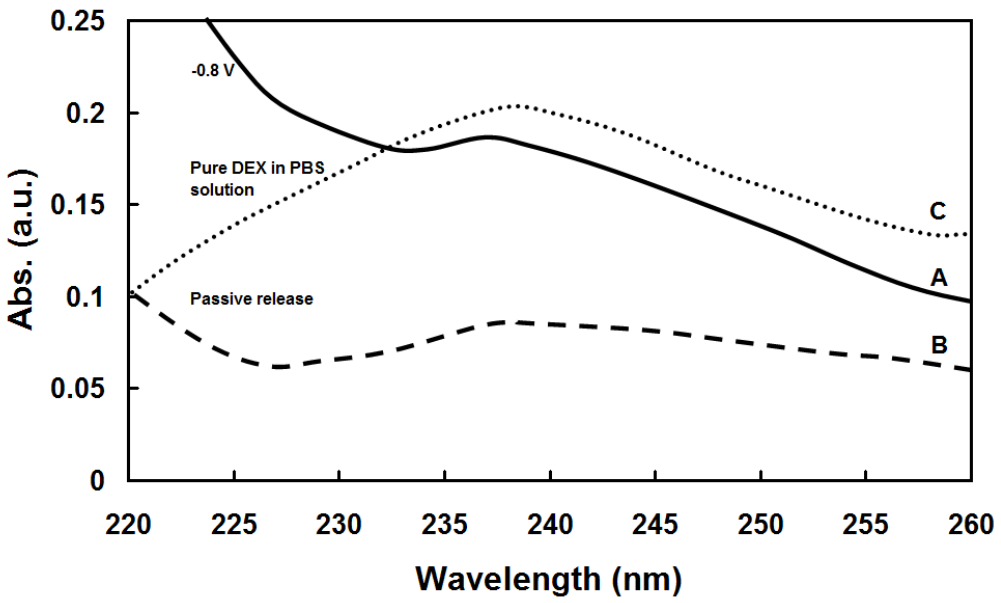

Figure 2.2. UV spectra of DEX released by electrical stimulation at -0.8V (A), and passive release (B) after 24 h release in PBS, and DEX in PBS solution (C).

DEX release was monitored over a 1800 min (30 hrs) hour period with and without electrical stimulation (Figure 2.3). More data points were collected during the first few hours until the amount of DEX released started to plateau. Each data point represents an average of independent measurements from three samples. The passive release profile from CS films showed a rapid DEX release within the first hour. The DEX release rate slowed with time and began to level off after 120 min (2 hrs) at which time approximately 60 % of the DEX had been released. This release is attributed to the passive diffusion of DEX from the CS film into the release medium. The average release

rate over the initial 120 min (2 hrs) period was 92 μg/h. At equilibrium the amount of DEX released was limited to 70 % of the DEX imbibed in the film.

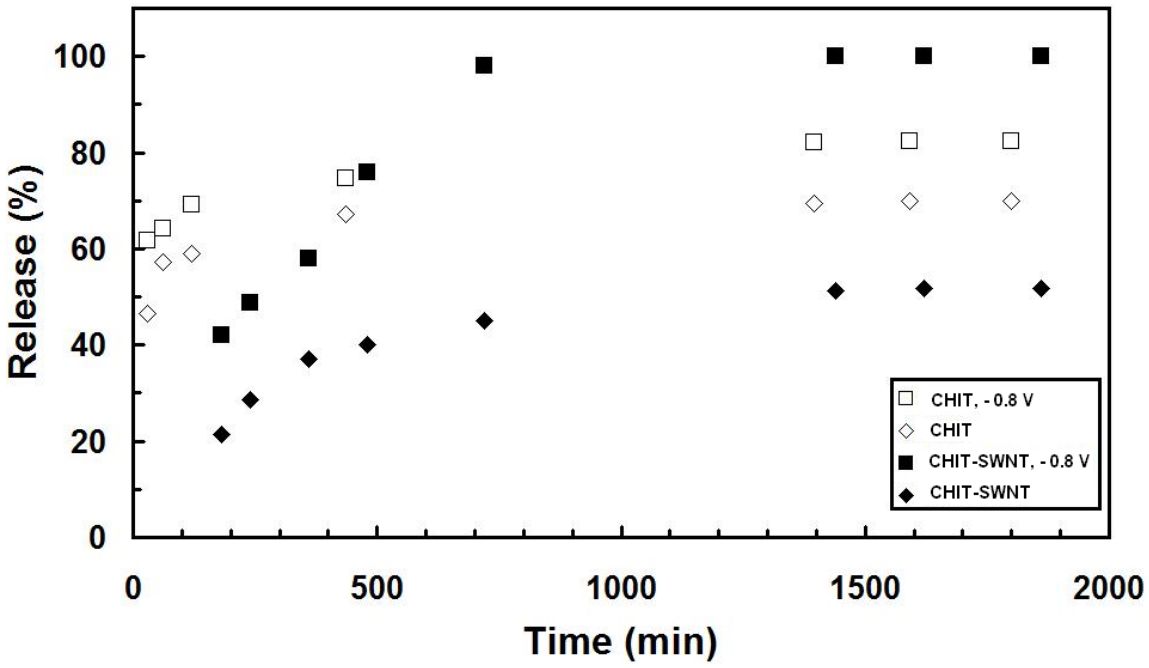

Figure 2.3. Cumulative release of DEX from chitosan without SWNT: passive release (open diamond); electrical stimulated at -0.8 V (open square); and from chitosan with SWNT: passive release (filled diamond), electrical stimulated at -0.8 V (filled square) at pH 7.4.

For samples containing carbon nanotubes (CS-SWNT film), the passive release profile clearly shows that the presence of SWNTs alters the rate of DEX release and the total amount of DEX released. The DEX release again occurred rapidly at first but started to level off at around 8 hours. The average release rate during this period was 16

μg/h. At equilibrium only 50 % of the DEX was released. The average release rate, release time period (time until the release starts to level off) and the total amount of DEX released are summarised in Table 2.1. The retardation of release of DEX from CS-SWNT films indicates a degree of attractive interaction between the DEX and the nanotubes.

Table 2.1. Release rate and maximum accumulative release of DEX from chitosan (CS) and chitosan-nanotube (CS-SWNT) hydrogels

Hydrogel / Release mode	**Initial average linear release rate[a] (μg/h)**	**Initial levelling off time (h)**	**Maximum cumulative release (wt%)**
CS / passive release	92	2	70
CS / -0.8 V	108	2	82
CS-SWNT / passive release	16	8	51
CS-SWNT / -0.8 V	26	12	100
CS-SWNT / -0.4 V	6	54	100
CS-SWNT / +0.15 V	3	4	30

[a] the linear release rate is based on the amount of released DEX from the beginning of release test till the release profile levels off.

The effect of applying an electrical potential on the release of DEX was then investigated. Since DEX is negatively charged, it was postulated that a negative potential applied to the electrode would enhance the rate of DEX release via

electromigration. Applying a negative potential of -0.8 V to the carbon substrate of the CS film produced a higher DEX release of 70 % (vs 60 % for the unstimulated sample) at a rate of 108 μg/h over the initial 120 min (2 hrs) period. When monitored over 1800 min (30 hrs) , the amount of the DEX released was consistently higher in the electrically polarized films compared to the unstimulated CS films. With the applied potential of -0.8 V, the total DEX released was 80 % at equilibrium. These results show that it is not possible to completely release DEX from the CS film even when electrically stimulated.

Electrical stimulation of samples containing SWNTs also showed an improved DEX release profile and resulted in complete 100 % release of the DEX. The measured average release rate after 720 min (12 hrs) of 26 μg/h is more than 1.5 times higher than for the passively released DEX (16 μg/h) from the same CS-SWNT material. While only 50 % drug release was achieved during passive release, with electrical stimulation the DEX could be completely released within 720 min (12 hrs).

We have further investigated the effect of electrical stimulation by varying the amplitude and the polarity of the applied potential to modulate the release the DEX from CS-SWNT films. Figure 2.4 clearly shows that the magnitude of the applied potential significantly alters the DEX release profiles. A complete DEX release can only be achieved when negative potentials (vs Ag/AgCl) were applied. Although it is possible to achieve complete DEX release at -0.4 V, the rate of release occurred considerably slower than that for -0.8 V. The initial (first 180 min) average release rates from these applied potentials were similar at 26 μg/h. However, after the initial 180 min (3 hrs) of stimulation, the release rates were quite different: 26 μg/h for -0.8V and 6 μg/h for -0.4 V. 100 % DEX was released after 720 min (12 hrs) at -0.8 V, while it required 3240 min

(54 hrs) for -0.4 V before the DEX release was completed. Also, more negative voltages were also investigated and resulted in a more rapid DEX release but because of a small amount of gas bubble formation, the results are not reported here.

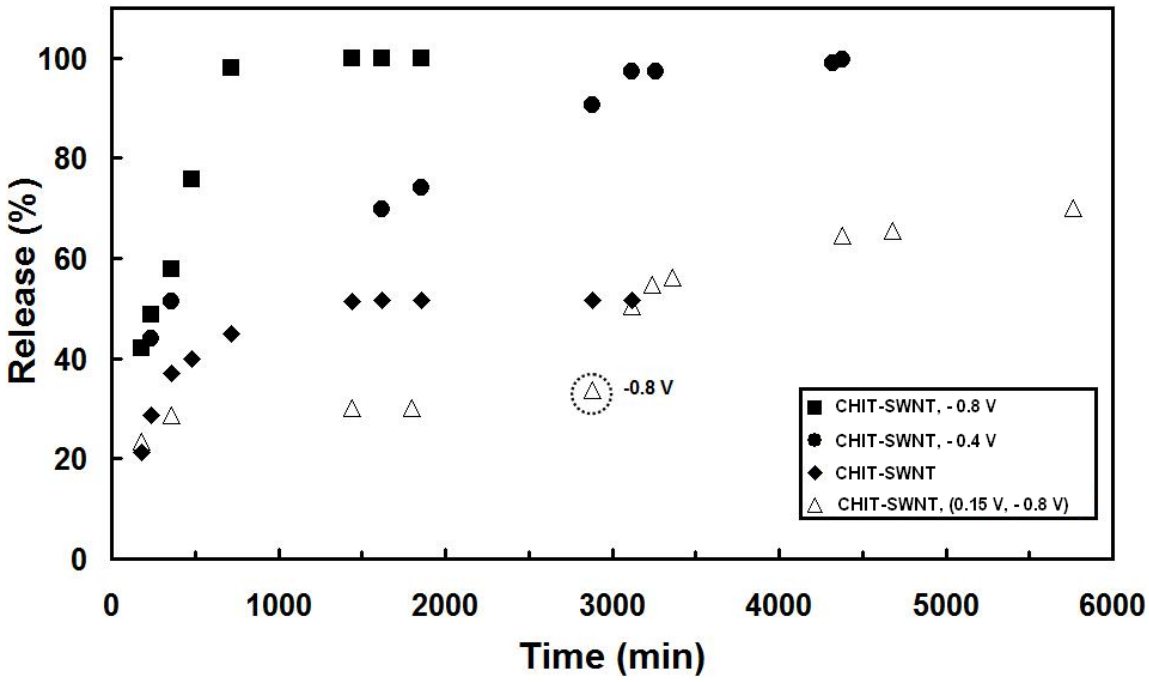

Figure 2.4. Cumulative DEX release from CS-SWNT hydrogels verses time at various applied potentials: -0.8 V (square), -0.4 V (circle), passive (diamond), +0.15 V then -0.8 V as indicated (triangles), pH 7.4.

Significantly, when a positive voltage was applied, the DEX release was much slower than at negative potentials and slower even than the passive release. Again a rapid DEX release occurred initially, with the release levelling off after 4 hours. During the first 240 min (4 hrs) of stimulation at +0.15 V, the measured DEX release of 30 % is

equivalent to that of the passively released DEX from an unstimulated CS-SWNT film after only 180 min (3 hrs). 30 % is the maximum amount of DEX that can be released from the stimulated CS-SWNT film at +0.15 V. This result suggests that the 30 % of DEX is not interacting directly with the SWNTs and a higher loading of SWNTs may be necessary to completely stop the release of DEX.

To investigate the dynamic release of DEX through electrical control, the voltage was switched from positive to negative potentials. Initially a potential of +0.15 V was applied for 2880 min (48 hrs) and then the voltage was switched to -0.8 V. The 2880 min (48 hrs) stimulation at +0.15 V ensured that the release of DEX release was limited to just 30 %. Figure 2.4 shows the DEX release profile that occurred almost simultaneously when the voltage was switched from +0.15 V to -0.8 V. The amount of DEX released doubled in about 1080 min (18 hrs) after the voltage switch and continued to increase over time. It should be noted, however, that the average rate of DEX release at -0.8 V occurred slower in this experiment (9 μg/h) compared with the initial study (26 μg/h) where a voltage of -0.8 V was applied from the beginning.

2.4. Discussion

This study evaluated the use of SWNTs to control the electrical stimulation and release of a negatively-charged drug (DEX) from a conducting composite matrix. The DEX-loaded CS (with and without SWNTs) was cast onto an inert electrode material and immersed in PBS buffer. The release of DEX into the buffer was monitored periodically. In all cases, an initial rapid release of some of the DEX occurred that is attributed to the

passive diffusion of DEX from the matrix. Without electrical stimulation, approximately 70 % of the DEX was released passively from CS over 1380 min (23 hrs). The presence of SWNTs resulted in a decrease of the amount of DEX released passively to about ~ 50 % demonstrating that SWNTs act to limit the diffusion of DEX through the CS matrix. With electrical stimulation, it was found that the drug release could be modulated to either increase or decrease the release rate compared with passive diffusion. With negative applied potentials, the rate of DEX release could be enhanced and the DEX could be completely expelled from the host polymer. The release process was faster at more negative potentials: 720 min (12 hrs) for -0.8 V and 3240 min (54 hrs) for -0.4 V before the DEX was released completely. The application of a positive potential of +0.15 V caused the DEX release to level off at just 30 %, which was lower than the amount released passively.

Several mechanisms have been considered for drug release from polymer-based matrices, including forced convection, diffusion, electrophoresis and erosion [2,5-7]. Early drug release studies used electrical stimulation to alter the pH of the electrolyte and thereby cause pH-induced swelling and concomitant increase in diffusion rates of imbibed species [16, 17]. In chitosan-based materials the swelling ratio increases as pH decreases. While the increase in swelling at low pH may allow a greater rate of DEX diffusion, the release studies in the current investigation were performed in a buffered solution (PBS) that maintains a constant pH of 7.4 of the electrolyte bath. Furthermore, the experiments were carried out under mild electrochemical conditions, ranging from -0.8 V ($i_d < 5.5\times10^{-3}$ mA/mm^2) to +0.15 V ($i_d \sim 0$ mA/mm^2) with no evidence of redox processes shown in the CVs. Therefore, the conditions used were unlikely to alter the

surrounding pH significantly. The acidic dissociation constant of chitosan is pK_a 6.5 [18], so it seems that a change in pH from the electrical stimulation is not the main cause of DEX release from CS-SWNT matrix.

More recent studies have considered lower voltage induced release of charged molecules from hydrogels as a result of electrophoresis [2]. This process seems to be involved in the current study as the release profile of DEX changes significantly when the voltage was switched from positive to negative. The potential of zero charge (pzc) for SWNTs has been reported at 0 V (vs. Ag/AgCl) [19], so the potentials used in the current study make the SWNTs either negatively charged (below pzc) or positively charged (above pzc). The presence of SWNTs in the chitosan matrix appears to enhance the electrophoretic effect compared with CS alone. Interactions between the charged SWNTs and the negatively charged DEX can accelerate or retard the DEX release. When positively charged, the SWNTs act more efficiently as a diffusion barrier: attracting the DEX molecules and slowing their release. The high surface area of SWNTs integrated as a 3-dimensional network throughout the chitosan matrix provides ample opportunity for DEX to be retarded at the SWNT surface. When the SWNTs are negatively charged, however, the opposite occurs with the DEX being repelled from the SWNTs and their release from the CS-SWNT matrix is accelerated. Scheme 2.2 illustrates this mechanism, where negatively charged DEX molecules are retained inside the matrix when a positive potential is applied (A). By switching the potential to negative (B), negatively charged DEX molecules are forced to leave the matrix. Note that at positive voltage some of the DEX still leaves the matrix in a diffusion mechanism. A small steady-state current was measured when negative potentials were

applied to the CS-SWNT indicating a reduction process was occurring. It is not known, however, whether that process was directly related to the release of DEX or was caused by some parasitic reaction, such as the reduction of oxygen.

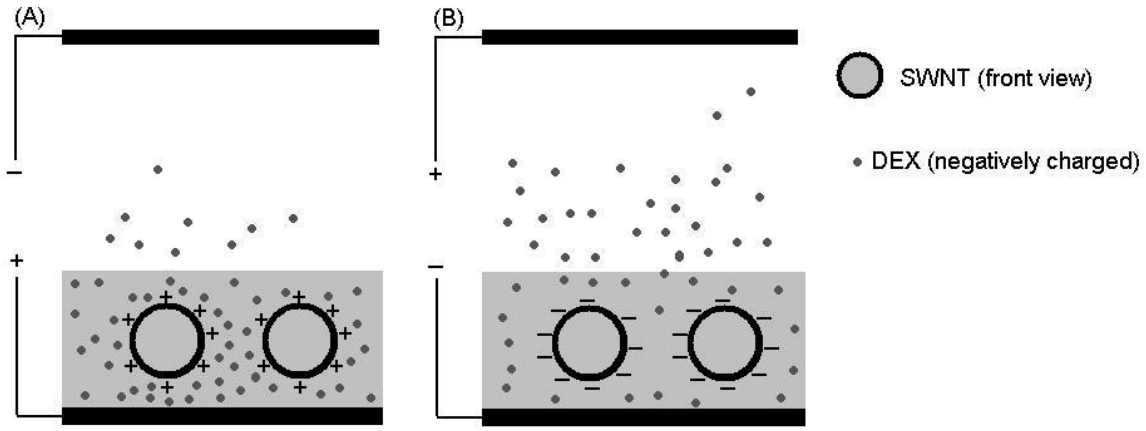

Scheme 2.2. Schematic illustration of modulated drug release from CS-SWNT matrix when the applied voltage polarity is (A) positive or (B) negative.

2.5. Conclusions

Dexamethasone was loaded into chitosan hydrogels with and without single walled carbon nanotubes and the release of the drug into a surrounding PBS solution determined. The SWNTs acted as a diffusion barrier to DEX, slowing down its release when no electrical potential was applied (passive release). This retardation effect was enhanced when the SWNTs were positively charged due to the electrostatic attraction between the SWNTs and the negatively-charged DEX. Furthermore, the release of DEX could be accelerated compared with the passive diffusion rate by negatively charging the SWNTs and inducing electrostatic repulsion. In this way, the release of DEX could be

effectively turned on and off by controlling the applied electrochemical potential. It is possible that similar control can be achieved with other charged molecules. The rate at which DEX was released from the carrier film was larger than previous reports, although direct comparisons are difficult due to the varying experimental conditions used. Faster drug release may be achieved by using thin films or fibers, however, these structures would require improved mechanical properties. Methods to enhance the strength of chitosan based hydrogel fibres are considered in the next chapter.

2.6. References

1. Park H, and Park K, Hydrogel and Biodegradable Polymers for Bioapplicaitons, Ottenbrite RM, Huang SJ, and Park K, ACS Symposium Series, American Chemical Society, Washington DC: 1996.
2. Ramanathan S, and Block LH. Journal of Controlled Release 2001;70(1-2):109-123.
3. Ravi Kumar MNV, Muzzarelli RAA, Muzzarelli C, Sashiwa H, and Domb AJ. Chemical Reviews 2004;104(12):6017-6084.
4. Murdan S. Journal of Controlled Release 2003;92(1-2):1-17.
5. Lira LM, and Cordoba de Torresi SI. Electrochemistry Communications 2005;7(7):717-723.
6. Abidian MR, Kim DH, and Martin DV. Advanced Materials 2006;18(4):405-409.
7. Razal JM, Gilmore KJ, and Wallace GG. Advanced Functional Materials 2008;18(1):61-66.
8. Iijima S. Nature 1991;354:56-58.
9. Lynam C, Moulton SE, and Wallace GG, Advanced Materials 2007;19:1244-1248.
10. Zhang M, Smith A, and Gorski W. Analytical Chemistry 2004;76(17):5045-5050.

11. Luo XL, Xu JJ, Wang JL, and Chen HY. Chemistry Communications 2005;16:2169-2171.

12. Tkac J, Whittaker JW, and Ruzgas T. Biosensors and Bioelectronics 2007;22(8):1820-1824.

13. Bianco A, Kostarelos K, and Prato M. Current Opinion in Chemical Biology 2005;9(6):674-679.

14. Koda-Kimble MA. Applied Therapeutics: The Clinical Use of Drugs 9th edition, Young LY, Kradjan WA, Guglielmo BJ, Alldredge BK, and Corelli RL, Lippincott Williams & Wilkins: 2008.

15. Elijarrat-Binstock E, Raiskup F, Frucht-Pery J, and Domb AJ, Journal of Controlled Release 2005;106(3):386-390.

16. Tanaka T, Nishio I, Sun ST, and Ueno-Nishio S, Science 1982;218:467-469.

17. Tomer R, Dimitrijevic D, and Florence AT. Journal of Controlled Release 1995;33:405-413.

18. Wang QZ, Chen XG, Liu N, Wang SX, Liu CS, Meng XH, and Liu CG. Carbohydrate Polymers 2006;65(2):194-201.

19. Barisci JN, Wallace GG, Chattopadhyay D, Papadimitrakopoulos F, and Baughman RH. Journal of Electrochemistry Sociecty 2003;150:E409-E415.

CHAPTER THREE

Tough Hydrogel Fibres: Chitosan – PAAm

3. Tough Hydrogel Fibres: Chitosan–PAAm

3.1. Introduction

Chitosan (CS), a linear polysaccharide consisting of β (1 → 4) linked D-glucosamine residues with a variable number of randomly located *N*-acetyl-glucosamine groups, is a semi-crystalline polymer with relevant biocompatibility and biodegradability [1]. CS has been extensively used as a building block in a wide range of biomedical applications such as drug delivery carriers, wound healing agents, tissue engineering scaffolds, and nerve repair conduits [2-5]. It was shown in the previous chapter that chitosan combined with carbon nanotubes can be used as an effective medium for the controlled release of drugs. While CS possesses appropriate biocompatibility and biodegradability, some applications are limited by the brittleness of CS hydrogels. For example, some tissue engineering applications (i.e. muscle and/or nerve regeneration) requires a fibrillar architecture with mechanical performances similar to surrounding tissues to serve as directional cues for cell growth [4]. An ideal material for such applications can be a biocompatible hydrogel fibre with modulus matched to the surrounding tissue and adequate strength.

CS fibres have been prepared in the past via a wet-spinning method. This method typically involves injecting a lightly acidic solution of CS (pH ~ 4) into a

highly basic (pH ~ 10) coagulation bath. Post-processing steps (e.g. crosslinking) are necessary to generate fibres with usable mechanical properties in the wet state [6-9]. Because of its semi-rigid polymeric chain [10], CS by nature is more rigid than many other synthetic hydrogels. While the modulus can be modified by adjusting the degree of crosslinking, chitosan hydrogels in the swollen state are typically very brittle like most other synthetic hydrogels [11].

One approach to achieve hydrogels with tunable mechanical properties is to introduce another polymer network into the system, typically following the methods used to prepare interpenetrating polymer network (IPN) hydrogels [9, 12, 13]. This approach also improves the ability of CS hydrogels to hold water for an extended period. IPN hyrdogel made from CS and poly(acrylic acid) (PAA) shows improvement in dry mechanical properties [14, 15]. However, the elongation-at-break in the wet state was greatly reduced compared to wet CS fibres [14]. The brittleness of the CS-PAA IPN has been attributed mainly to the strong CS-PAA interactions. CS is positively charged at acidic pHs (< 6.5) while PAA is anionic at pH > 4. Ionic interactions between partially positively charged CS and partially negatively charged PAA results in low elongation-at-break. Moreover, due to the interaction between PAA and CS a relatively low swelling ratio over solution pH 3 to pH 8 was measured [14, 15]. While there are a vast number of examples of CS polymeric blends or IPN structures in the literature [16, 17], most of these studies aim to address specific properties like pH sensitivity, drug release properties, etc. Their mechanical properties in a fully immersed state have not been verified as broadly as their biological properties. Poly(acrylamide) (PAAm) is another polymer which has been used with CS. The network made from PAAm is a very well-known hydrogel, with swelling capacity which is not sensitive to solution pH at moderate

pHs. The CS-PAAm hydrogels have been reported before as graft structures (PAAm-*g*-CS) or CS-PAAm IPN systems.[13, 18-21] Electrospun CS-PAAm fibres were formed by modifying spinning conditions and electrospinning unit in which polymer solution can be spun at temperatures above 100 ^{o}C [22].

In this chapter, the preparation of tough CS-PAAm hydrogel fibres made by the double network technique first introduced by Gong and co-workers [23] as reviewed in Chapter 1 is presented. These tough fibres show tunable swelling ratio and consequently mechanical properties as a function of pH and PAAm volume fraction. The PAAm neutral network was selected on the basis of integrating a neutral and loosely crosslinked second network in a pre-formed tightly crosslinked polyelectrolyte first network which is a typical requirement of a DN hydrogel [24]. Along with the crosslinking density of two networks, the molar ratio of two networks is another crucial parameter [24-26] that has also been investigated here by varying the concentration of AAm monomer solution.

3.2. Experimental Section

3.2.1. Materials

High molecular weight chitosan (degree of deacetylation 86.6 %), acryl amide (AAm) (electrophoresis grade in ultra pure water, 40 wt%), potassium persulfate (KPS) as initiator and *N,N'*-methylene MBAAacrylamide (MBAA) as crosslinking agent were purchased from Sigma-Aldrich and used without further purification. Sodium hydroxide (Chem Supply, Australia) and acetic acid (glacial, Ajax Finechem, Australia) were used to prepare the coagulation bath and adjust the pH of

CS solution, respectively. Glutaraldehyde (aqueous solution, 50 wt%, Sigma-Aldrich) was used to crosslink the CS fibres. Chemical structures of reagents used to prepare the hydrogels are shown in Scheme 3.1.

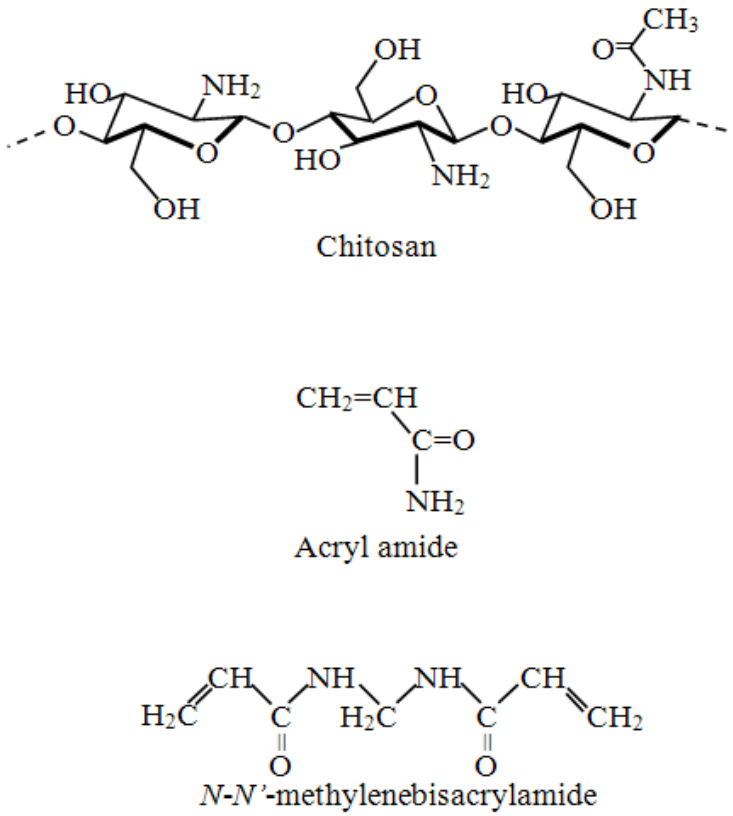

Scheme 3.1. Chemical structure of reagents.

3.2.2. Preparation

CS fibres

CS was dissolved in acetic acid solution (1 wt%) to make up 2 wt% CS solution. This solution was then wet-spun into a sodium hydroxide solution (0.1 M, pH ~ 13) as the coagulation bath. To spin the fibres, CS solution was injected in to

the rotating sodium hydroxide coagulation bath at an appropriate injection rate and spinning speed to obtain uniform CS fibres of ~ 150 μm (dry) in diameter. The CS fibres were allowed to remain in sodium hydroxide solution for 24 hrs, and then washed thoroughly. The crosslinking bath was made from glutaraldehyde solution (5 mM), wherein CS fibres were immersed for another 24 hrs. The crosslinked CS fibres then were washed extensively and stored in deionised water (Figure 3.1a).

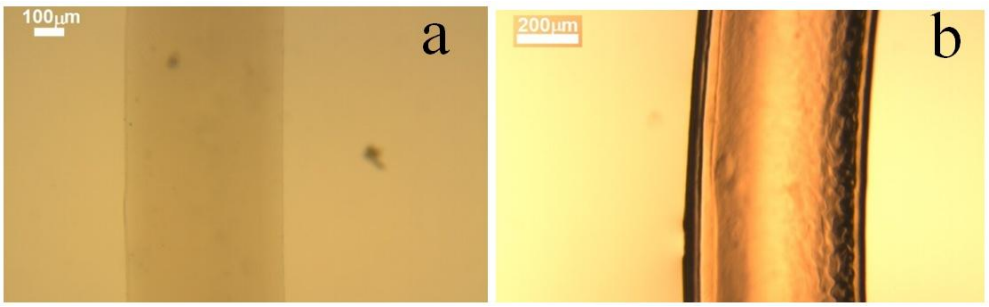

Figure 3.1. Microscopic photographs of a) crosslinked CS fibre, and b) CS-PAAm hydrogel fibre, both in their fully swollen state.

CS-PAAm IPN fibres

To develop the DN structure in CS fibres, a two step process was employed as follows: first, the CS fibres were immersed in AAm monomer solution for 24 hrs. The monomer solution consisted of a varying concentration of AAm (1, 2, 3, or 4 M) in deionised water. This solution also contained MBAA (crosslinking agent) and KPS (initiator) at concentration of 0.1 mol% based on AAm monomer. In the second step, the fully swollen fibres were transferred to a sealed container. To keep the humidity at the saturated level during the process, deionised water was added to the containers beneath the fibres (Scheme 3.2a). Polymerization was carried out at 60 ^{o}C

for 6 hrs. The obtained CS-PAAm fibres were washed with deionised water several times to remove unreacted components, and then stored in deionised water for further experiments (Figure 3.1b).

PAAm hydrogel

To compare the properties of CS-PAAm fibres with its constituent components, PAAm hydrogel sheets were synthesized following a similar approach as in the second step of the process discussed above to make PAAm network within CS fibres. Briefly, AAm solution, with an identical composition to the AAm monomer solution used to form PAAm network in CS-PAAm fibres, was poured into disc shape plastic containers, then sealed and polymerized at 60 ^{o}C for 6 hrs. The PAAm hydrogels were washed with deionised water to remove unreacted monomers and stored in deionised water.

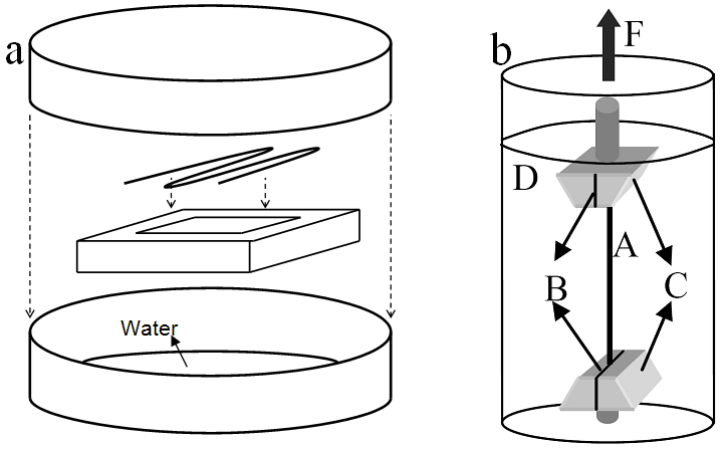

Scheme 3.2. Schematic illustrations of a) second network polymerization process within the CS fibres in a humidified container, b) fully immersed CS-PAAm fibre in a tensile test: (A) hydrogel fibre, (B) rubber spacers, (C) clips, (D) water.

3.2.3. Tensile Test

A laboratory set up was made to measure the tensile properties of fully swollen fibres while immersed in deionised water with a mechanical tester (Shimadzu EZ-S, Japan). The CS-PAAm hydrogel fibres were mounted between two grips, whereas one of the grips was attached to the bottom of a cylindrical container (100 mL, 2 cm in diameter) and the other one was connected to the upper clamp of the tensile machine (Scheme 3.2b). The container was fixed on the lower plate of the machine, filled with deionised water, while the upper clamp was connected to a load cell and crosshead. The crosshead displacement rate was 10 %/min. To measure the tensile properties of PAAm hydrogels, samples were cut into strips (5 mm × 10 mm × 50 mm), mounted between grips and tested in the air. The weight of samples was monitored before and after the test to estimate the water loss during the test. For the thicker PAAm strips the mass loss was negligible, so it was possible to conduct tensile testing of fully swollen sheets in air. Sand paper was used between hydrogel and grips to prevent any slippage from the clamps.

3.2.4. Fourier Transform Infrared (FT-IR) Spectra

Transmission infrared spectra of CS films, PAAm, and CS-PAAm fibres were measured using a FT-IR spectrometer (IRPrestige-21, Shimadzu, Japan). Different FT-IR techniques including Ge-ATR component and KBr powder were used to characterize the structure of CS-PAAm fibres and compare with dried CS and PAAm networks.

3.2.5. Swelling Ratio

Considering the homogeneous swelling of a long cylindrical gel, the volumetric swelling ratio (q) of fibres could be estimated as:

$$q = {}^{V}/_{V_o} \sim ({}^{d}/_{d_o})^3 \qquad (3.1)$$

where d and d_o are, respectively, the diameter of fully swollen fibre and dried fibre. An optical microscope was used to measure the diameter change of fibres over the drying process.

3.3. Results and Discussions

3.3.1. Hydrogel Formation

Shown in Figure 3.1 are microscopic photographs of a crosslinked CS fibre, and a CS-PAAm hydrogel fibre, both in their fully swollen state in deionised water. The crosslinking step in preparing the CS fibres was necessary to prevent them from dissolving in acidic solutions. This step, however, had a complex effect on the swelling ratio of CS fibres (Figure 3.2) where the swelling degree in deionised water passed through a maximum as the concentration of glutaraldehyde increased. The aqueous solution of glutaraldehyde is acidic with pH decreasing as glutaraldehyde concentration increases. It is seen clearly from Figure 3.2 that all crosslinked CS fibres had a higher swelling ratio in deionised water than the as-prepared, uncrosslinked fibre. Since glutaraldehyde solution in water is acidic, some of the chitosan starts to dissolve from the surface of the as-prepared chitosan fibres immersed in acidic glutaraldehyde before the crosslinking reaction takes place. At

lower concentration of glutaraldehyde the crosslinking reaction is slow and as a result more chitosan will be removed from the surface before the crosslinking prevents the dissolution process. The resulting crosslinked chitosan fibre is more porous than the as-spun chitosan fibres which consequently exhibits higher swelling ratio. By increasing the concentration of glutaraldehyde the crosslinking process takes place faster and less chitosan will dissolve off from the surface, resulting a smaller swelling ratio.

It was also observed that the diameter of dry crosslinked CS fibres was smaller than that of dry uncrosslinked CS fibre (Figure 3.3). This drop in the diameter of dry crosslinked fibres compared to dry uncrosslinked fibres indicates that CS fibres start to dissolve in acidic glutaraldehyde solution before crosslinks form. In 5 mM and 10 mM glutaraldehyde solutions the crosslinking reaction is slow and more dissolution occurs before crosslinks form. However, as the concentration of glutaraldehyde increases the crosslinking time decreases considerably [27]. At 20 mM glutarladehye solution the crosslinking reaction occurs much faster limiting the extent of CS dissolution. Since the CS fibres crosslinked at 10 mM and 20 mM glutaraldehyde were very brittle and difficult to handle, 5 mM glutaraldehyde solution was chosen to crosslink the CS fibres for further studies.

Following the typical DN synthesis steps, CS hydrogel fibres crosslinked with 5mM glutaraldehyde were immersed in a monomer solutions of increasing AAm monomer concentrations. This method allows different amounts of AAm to be impregnated within the CS hydrogel structure. Subsequent polymerization of the PAAm network is then expected to lead to different swelling ratios, hence different mechanical properties along with pH sensitivity which originates from the CS component.

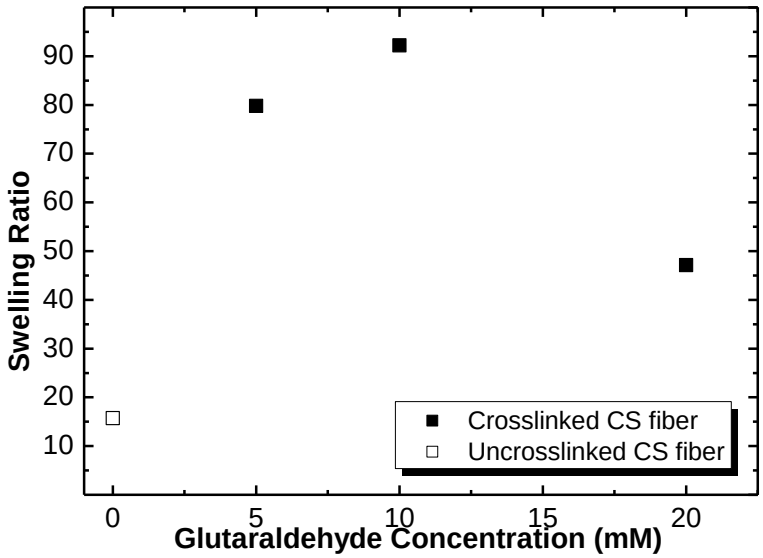

Figure 3.2. Effect of glutaraldehyde concentration on the swelling ratio in deionised water of crosslinked CS fibres (filled square) compared with as-spun CS fibre (open square).

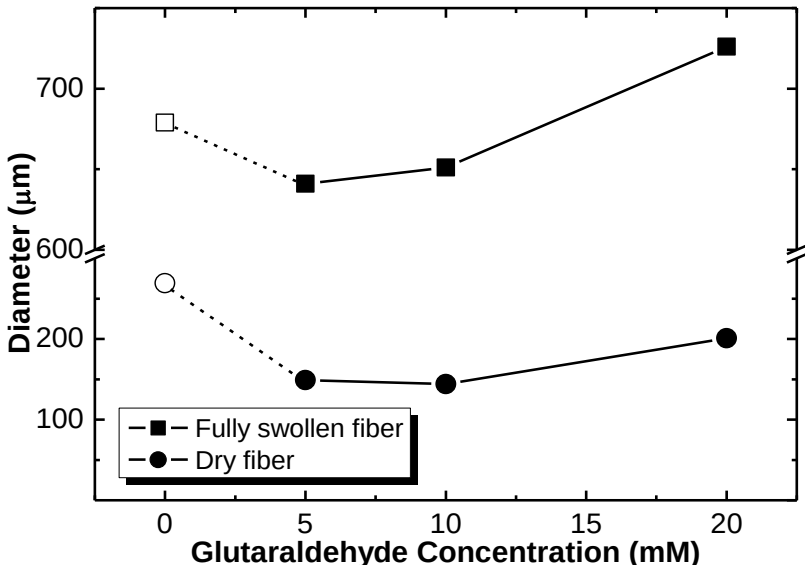

Figure 3.3. Diameter change of (filled symbols) crosslinked CS fibres (fully swollen in deionised water and dry) and (open symbols) as-spun CS fibres as a function of glutaraldehyde concentration.

3.3.2. FT-IR spectra

Figure 3.4 displays FT-IR spectra of CS-PAAm fibre, dried PAAm gel and crosslinked CS film from wave numbers 900 to 3900 1/cm. Curve B in Figure 3.4 shows the IR bands of crosslinked CS, including a characteristic band at 1650 cm^{-1}, which corresponds to an imine bond (N=C) formed by the reaction of amino groups in CS with aldehyde groups of glutaraldehyde to form a Schiff base. The peak at 1578 cm^{-1} is associated with the N-H deformation of primary amines (amide II), and the band at 1378 cm^{-1} is attributed to C-H of CH_3 group of acetamide, which suggests that CS is not fully deacetylated. The band at 1072 cm^{-1} corresponds to the C-O stretching of primary alcohols. In the FT-IR spectrum of PAAm (curve C), the two bands appearing around 3352 and 3198 cm^{-1} are associated with the N-H stretching vibration. The nature of the PAAm network can be derived by monitoring the vibrations of amide groups. The characteristic C-O stretching vibration in amide group occurs at around 1660 cm^{-1} (amide I). The medium intensity band at around 1420 cm^{-1} can be assigned to C-N stretching (amide III) vibrations of acrylamide. Also, the peaks at 1188 and 1126 cm^{-1} IR bands are contributed by C-C stretching in acrylamide species. The FT-IR spectrum of CS-PAAm fibre (curve A) has characteristic features of both CS and PAAm samples. Similar C-H stretching vibration band appears around 2920 cm^{-1} in CS-PAAm spectrum as for CS film. Furthermore, the 1660 cm^{-1} band corresponding to C-O stretching vibration of acrylamide species distinctly appears in CS-PAAm FT-IR spectrum, similar to PAAm spectrum.

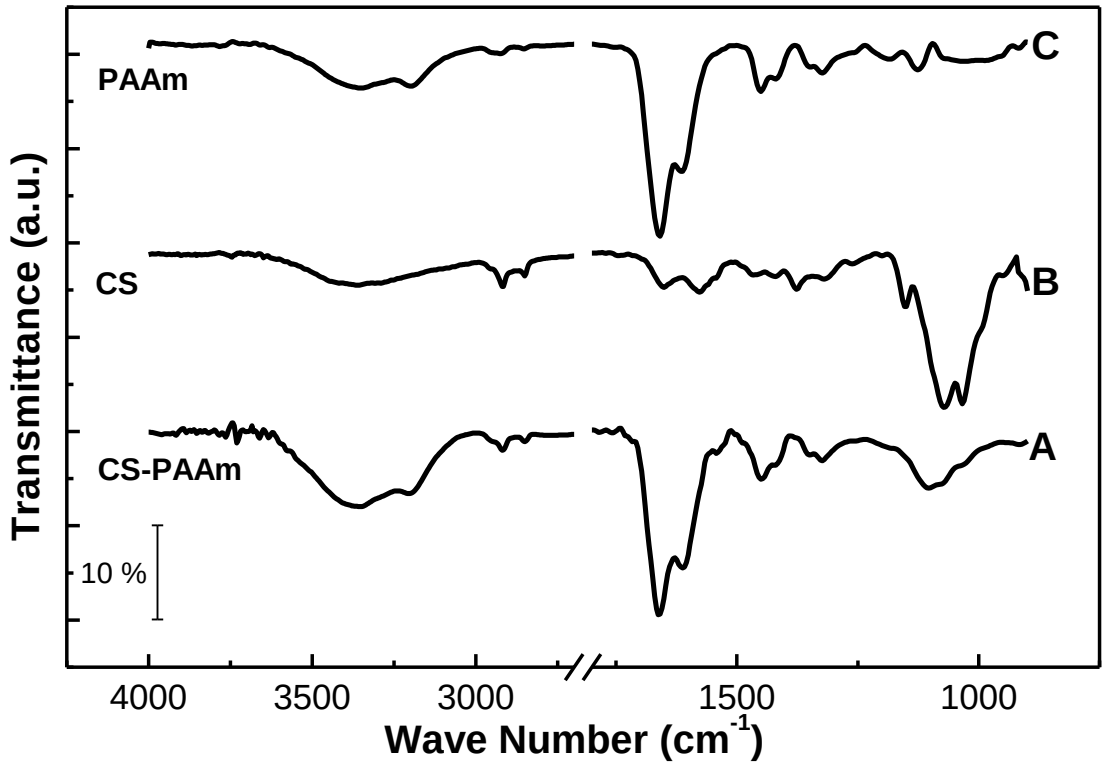

Figure 3.4. FT-IR spectra of (A) CS-PAAm fibre, (B) crosslinked CS film, (C) PAAm gel.

3.3.3. Swelling Ratio

The swelling ratio of the resulting CS-PAAm hydrogel fibres prepared from different AAm concentration is shown in Figure 3.5 as a function of AAm monomer concentration. It is clear that the swelling ratio of CS-PAAm hydrogel (q ~ 10 to 25) fibres is lower compared to that of CS fibres (q ~ 80). Likewise, the swelling ratio of the CS-PAAm hydrogel fibres in deionised water decreases with increasing AAm concentration, following almost a linear behaviour. As has been demonstrated for PAAm hydrogels elsewhere [28], the monomer concentration influences the swelling ratio of hydrogels with increasing concentration leading to smaller swelling. At low

monomer concentrations, the crosslink density is reduced due to the formation of closed loops and dangling chains [28].

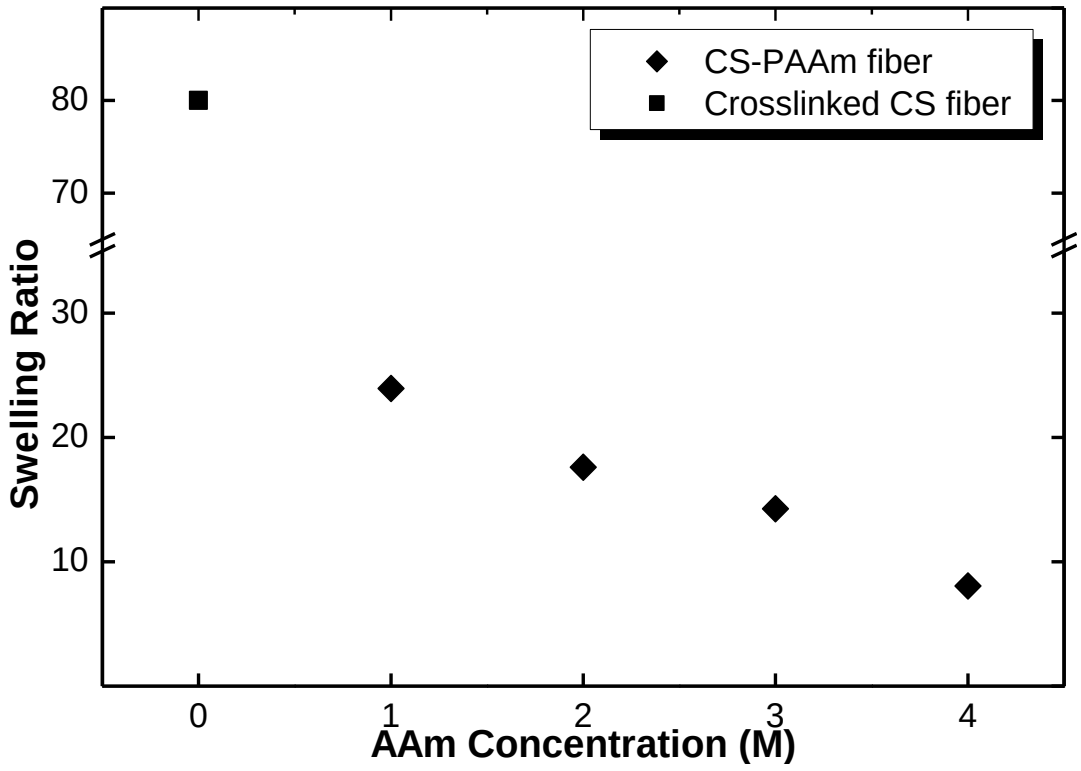

Figure 3.5. Swelling ratio of (diamond) CS-PAAm hydrogel and (square) starting crosslinked CS fibres in deionised water as a function of AAm monomer concentration.

3.3.4. Mechanical Properties

Figure 3.6 compares the typical tensile stress-strain curves of fully swollen samples from CS-PAAm hydrogel fibre, CS fibres and PAAm hydrogel. The PAAm hydrogel was prepared in an identical manner to that used to make the second PAAm network in the CS-PAAm fibre. It is clear that the CS-PAAm hydrogel fibre has a

significantly higher tensile strength (150 kPa) than the PAAm hydrogel (20 kPa). Although, the fracture strain of CS-PAAm hydrogel fibre (~ 40 %) is ~ 7 times lower than that of PAAm hydrogel (~275 %), the CS-PAAm slightly outperforms the PAAm in the overall breaking energy (area under the curve), 31 vs. 28 kJ/m^3. Note that the fully swollen CS fibre without PAAm was not possible to mount the fibre for tensile testing. However, after drying and rehydrating the CS fibre, the fibres became slightly stronger (with a lower swelling degree) and the tensile test was performed on these fully rehydrated CS fibres (Figure 3.6). The rehydrated CS fibre still showed lower tensile strength (36 kPa) than CS-PAAm fibres, but slightly higher elongation-at-break (~ 75 %). The area under the tensile curve of CS-PAAm fibre was more than 7 times higher than the rehydrated CS fibre (4 kJ/m^3). The measured mechanical properties here are lower than those of wet CS-PAAm interpenetrating network films reported elsewhere. [13] However, the samples in the present study were tested totally immersed in water, and their swelling ratio (q > 10) was much higher than that of CS-PAAm films (q < 3.7) reported previously [13].

Mechanical properties of hydrogels are very sensitive to their water content. For example, the tensile testing of wet CS-PAAm fibres performed in air resulted in much higher mechanical performance than when the same fibres were tested fully immersed in water. The fibres tested in air were weighed before and after the test to monitor the amount of water lost during the test. The CS-PAAm fibre with 90 % water content in the beginning of the test was reduced to just 70 % water content by the end of the test. The measured strength was as high as 200 kPa, with elongation-at-break of 120 %. The area under the curve was calculated to be 120 kJ/m^3, which is 4 times higher than fully immersed fibre.

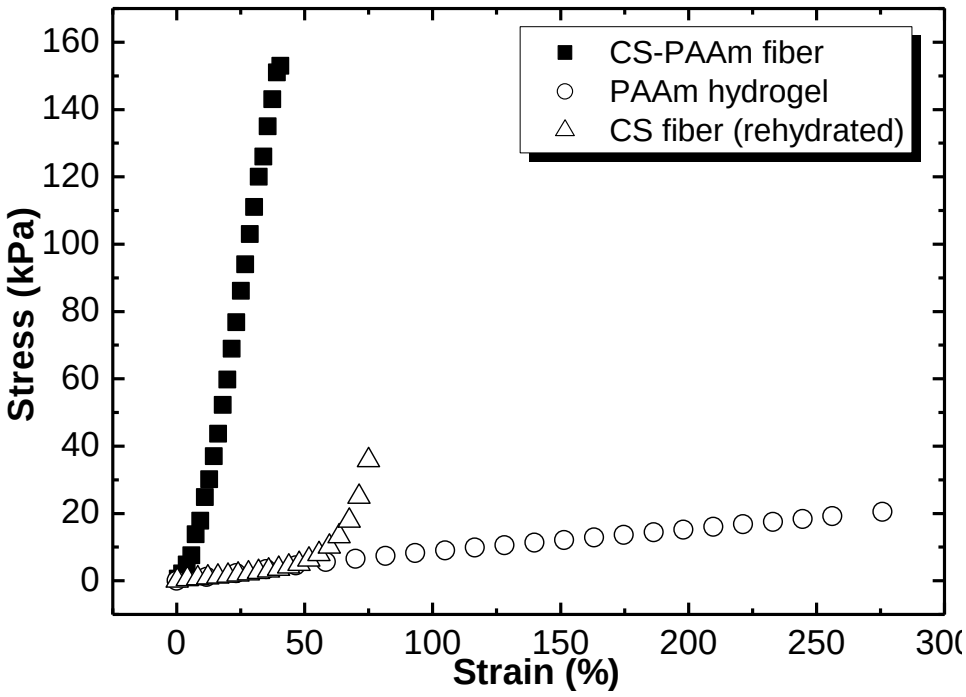

Figure 3.6. Tensile stress-strain curve of fully swollen CS-PAAm hydrogel fibre and PAAm hydrogel sheet. AAm monomer concentration was 3 M. CS fibre (re-hydrated) represents the crosslinked CS fibre after drying and then re-hydrating again.

Table 3.1 lists tensile strength and Young's modulus of fully swollen CS-PAAm fibres and PAAm hydrogels prepared with different AAm concentrations. Again, the lack of mechanical strength of the fully swollen CS fibres prevented us obtaining any data from them. The highest tensile strength that could be achieved was ~ 290 kPa for CS-PAAm hydrogel fibre made from 4 M AAm monomer solution, with Young's modulus of around ~ 80 kPa. The measured tensile strength and Young's modulus for the corresponding PAAm hydrogel was approximately 41 kPa and 10 kPa, respectively. The strength and modulus of the hydrogels (both single network PAAm and double network CS-PAAm) increased with increasing AAm

concentration with also a concomitant decrease in swelling ratio. These results also suggest that the PAAm network incorporated within the CS-PAAm hydrogel fibre functions as an effective reinforcement to enhance the mechanical performance of hydrogel fibres.

Table 3.1. Tensile mechanical properties and swelling ratio of CS-PAAm hydrogel fibres (immersed) and PAAm hydrogels (in air) with various AAm monomer concentrations.

Material	AAm (mol/L)	q	E (kPa)	σ_b (kPa)
CS-PAAm fibre (immersed)	1	24	24	35
	2	18	38	71
	3	14	55	153
	4	8	79	293
PAAm hydrogel (in air)	1	37	2	4
	2	18	3	13
	3	13	5	21
	4	11	10	41

The effects of swelling ratio on the mechanical properties of CS-PAAm hydrogel fibres and PAAm hydrogels are shown in Figure 3.7. These plots highlight how the mechanical properties of CS-PAAm fibres and PAAm hydrogels depend on their swelling ratio as the primary parameter rather than AAm monomer concentration which is a synthesis parameter. It can be observed that the strength and modulus of both hydrogels decrease with increasing water content. The Young's modulus of PAAm hydrogels are generally more sensitive to the water content, as

suggested by the slope of the best-fit line, than the CS-PAAm hydrogel fibres. A similar trend was observed in bacteria cellulose (BC)-gelatin DN hydrogels, where the BC-gelatin hydrogels were considerably less sensitive to the swelling ratio than glatin [29]. Also, the Young's modulus of CS-PAAm is almost one order of magnitude higher than that of PAAm over the range of swollen states of the hydrogels (Figure 3.7a). Moreover, the CS-PAAm fibres demonstrate higher tensile strength than PAAm hydrogels (Figure 3.7b). The measured strength for CS-PAAm is more 5 to 8 times higher than that of PAAm (Table 3.1) and displayed less sensitivity to water content (Figure 3.7b). In general, Figure 3.7 suggests that CS-PAAm fibres retain their mechanical properties even when fully immersed over a wide range of water content.

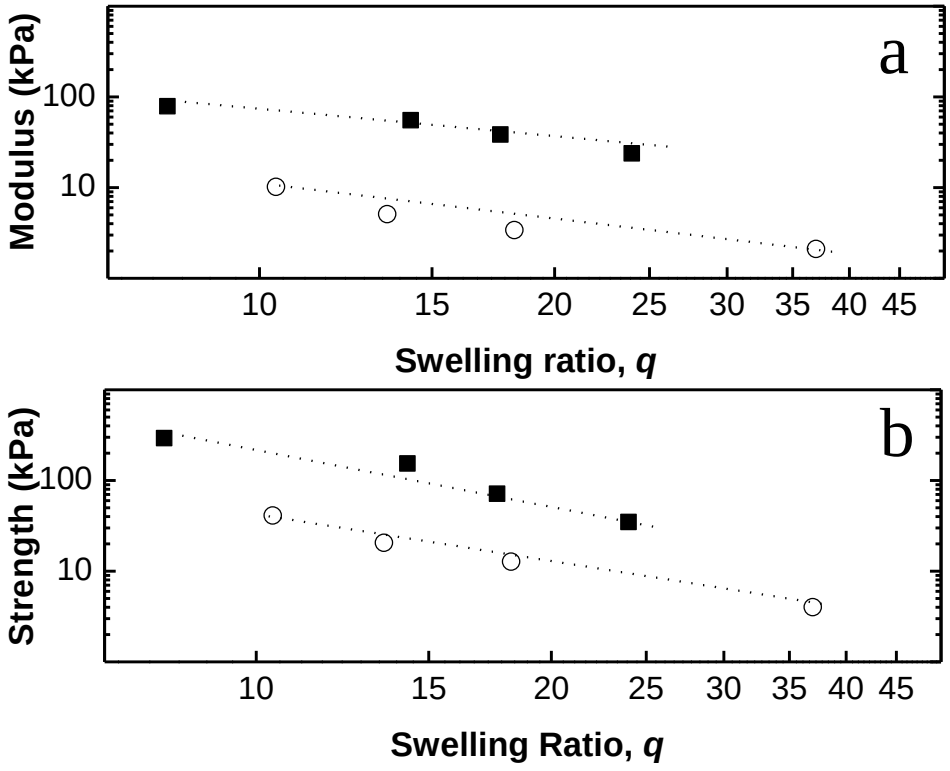

Figure 3.7. Tensile mechanical properties of CS-PAAm fibres and PAAm hydrogels vs. swelling ratio: a) Young's modulus, b) tensile strength. Dotted lines are power-law best fits.

3.3.5. pH Sensitivity

The CS-PAAm hydrogel fibres also respond to changes in solution pH. Figure 3.8 shows the change in swelling ratio of both CS and CS-PAAm hydrogel fibres as the surrounding pH environment changes from acidic (pH 2) to basic (pH 13). There was no observable change in swelling ratio of the PAAm hydrogel in this pH range. On the other hand, the CS hydrogel, as a weak polybase, exhibited pH sensitivity when pH is lower than its dissociation constant (pK_a 6.5) [30]. At lower pH, the amino groups in the CS backbone becomes protonated causing the CS hydrogel to swell (expand) with q of up to ~180. A slow increase in pH neutralizes the CS backbone and results in a decrease in swelling ratio (contraction occurs). More hydrogen bonding forms between neutral amino groups and less repulsion takes place between remaining protonated amino groups. At its neutral state (when pH slightly exceeds the pK_a value), the CS hydrogel contracts to its original state (q ~ 40). No further contraction is observed at pHs well above the pK_a since all of the amino groups have been neutralized. A similar pattern is observed for CS-PAAm hydrogel fibres when pH is lower than the pK_a value of CS. The swelling ratio at its fully swollen (expanded) state (pH 2) is ~ 85, almost two times lower than that of CS. The swelling decreases sharply at around pH 6 due to the de-protonation of the chitosan network. Swelling of CS-PAAm hydrogel fibres remains low at higher pH values above the CS pK_a. Interestingly, however, the CS-PAAm hydrogel fibres swell again at pH 13, unlike CS. Although this result is in contrast to other reports[31], this behaviour can be attributed to the alkaline hydrolysis of PAAm. The response time to pH change is ~ 30 sec when the fibres swell at acidic pHs, and almost twice of that when fibres deswell at more basic pHs.

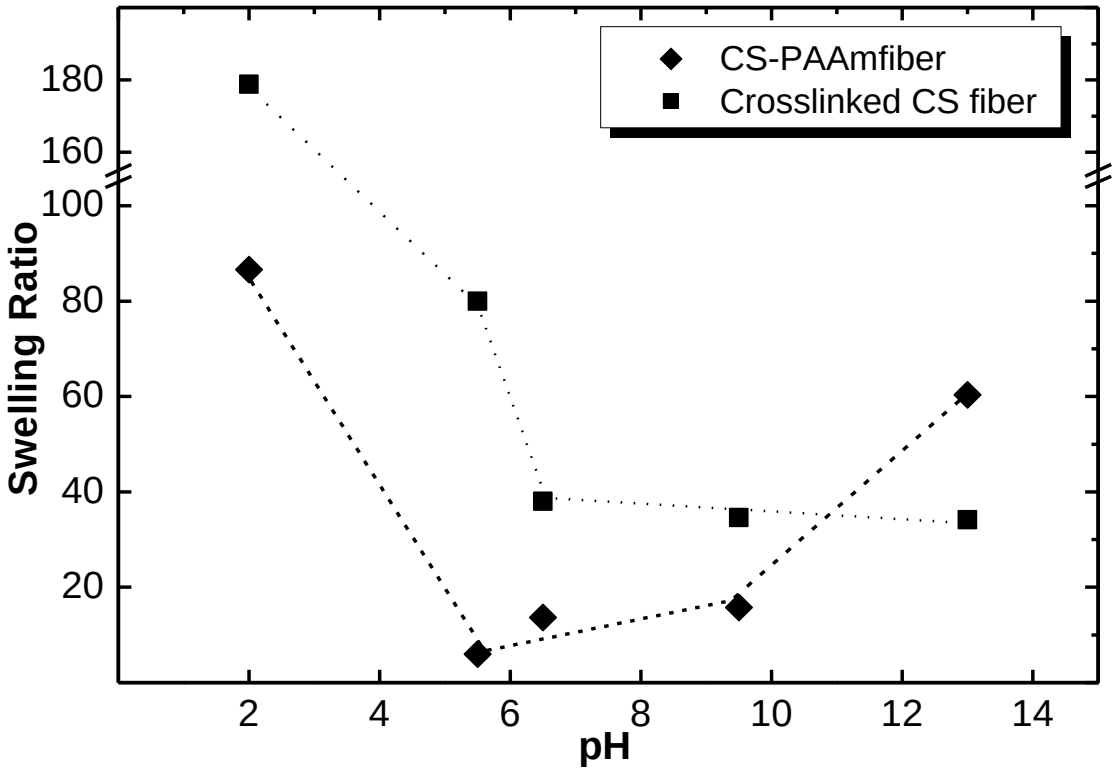

Figure 3.8. Swelling ratio of (diamond) CS-PAAm fibre and (square) crosslinked CS fibre as a function of solution pH.

3.4. Conclusion

It has been shown that it is possible to prepare fibres from a double network-like hydrogel. This method takes advantage of the spinnability of CS fibres, which provided the platform for infusion of the PAAm network. A considerable improvement in tensile strength (up to 6 times) and modulus (up to 9 times) in the fully swollen state were achieved compared with polyacrylamide. The DN gel fibres were also considerably stronger than the CS fibres, since the latter were too brittle to test when fully swollen. The amount of PAAm network in the hydrogel fibre can be controlled to tune properties such as swelling ratio, mechanical properties and pH sensitivity. Higher amounts of PAAm yielded higher mechanical strength and

stiffness and lower swelling ratio. A typical power-law relation was observed for both modulus and tensile strength of CS-PAAm fibres. The degree of swelling was influenced by the PAAm content of CS-PAAm fibres. However, the pH sensitivity was influenced by the chitosan network. These new hydrogel can have potential applications in which pH sensitivity can be employed as a means to respond to the environmental signals (e.g. in sensors, actuators and drug delivery systems).

3.5. References

1. Seo H, Mitsuhashi K, and Tanibe H. ANTIBACTERIAL AND ANTIFUNGAL FIBRE BLENDED BY CHITOSAN. In: Brine CJ, Sandford PA, and Zikakis JP, editors. 5th International Conf on Chitin and Chitosan. Princeton, Nj: Elsevier Appl Sci Publ Ltd, 1991. pp. 34-40.
2. Ramanathan S and Block LH. Journal of Controlled Release 2001;70(1-2):109-123.
3. Francis Suh JK and Matthew HWT. Biomaterials 2000;21(24):2589-2598.
4. Cheng M, Deng J, Yang F, Gong Y, Zhao N, and Zhang X. Biomaterials 2003;24(17):2871-2880.
5. Tuzlakoglu K, Alves CM, Mano JF, and Reis RL. Macromolecular Bioscience 2004;4(8):811-819.
6. Wei YC, Hudson SM, Mayer JM, and Kaplan DL. Journal of Polymer Science Part A: Polymer Chemistry 1992;30(10):2187-2193.
7. Knaul JZ, Hudson SM, and Creber KAM. Journal of Applied Polymer Science 1999;72(13):1721-1732.
8. Knaul JZ, Hudson SM, and Creber KAM. Journal of Polymer Science Part B: Polymer Physics 1999;37(11):1079-1094.
9. Hirano S, Zhang M, Nakagawa M, and Miyata T. Biomaterials 2000;21(10):997-1003.
10. Brugnerotto J, Desbrières J, Roberts G, and Rinaudo M. Polymer 2001;42(25):09921-09927.
11. Lee S-H, Park S-Y, and Choi J-H. Journal of Applied Polymer Science 2004;92:2054-2062.

12. Chen X, Li WJ, Zhong W, Lu YH, and Yu TY. Journal of Applied Polymer Science 1997;65(11):2257-2262.

13. Xia Y-q, Guo T-y, Song M-d, Zhang B-h, and Zhang B-l. Biomacromolecules 2005;6(5):2601-2606.

14. Lee JW, Kim SY, Kim SS, Lee YM, Lee KH, and Kim SJ. Journal of Applied Polymer Science 1999;73(1):113-120.

15. Wang HF, Li WJ, Lu YH, and Wang ZL. Journal of Applied Polymer Science 1997;65(8):1445-1450.

16. Kim SJ, Park SJ, and Kim SI. Reactive & Functional Polymers 2003;55(1):53-59.

17. Lee SJ, Kim SS, and Lee YM. Carbohydrate Polymers 2000;41(2):197-205.

18. Risbud MV and Bhonde RR. Drug Delivery 2000;7(2):69-75.

19. Bonina P, Petrova T, and Manolova N. Journal of Bioactive and Compatible Polymers 2004;19(2):101-116.

20. Singh V, Tiwari A, Tripathi DN, and Sanghi R. Polymer 2006;47(1):254-260.

21. Zeng X, Wei W, Li X, Zeng J, and Wu L. Bioelectrochemistry 2007;71(2):135-141.

22. Desai K and Kit K. Polymer 2008;49(19):4046-4050.

23. Gong JP, Katsuyama Y, Kurokawa T, and Osada Y. Advanced Materials 2003;15(14):1155-1158.

24. Na Y-H, Kurokawa T, Katsuyama Y, Tsukeshiba H, Gong JP, Osada Y, Okabe S, Karino T, and Shibayama M. Macromolecules 2004;37(14):5370-5374.

25. Tsukeshiba H, Huang M, Na Y-H, Kurokawa T, Kuwabara R, Tanaka Y, Furukawa H, Osada Y, and Gong JP. The Journal of Physical Chemistry B 2005;109(34):16304-16309.

26. Huang M, Furukawa H, Tanaka Y, Nakajima T, Osada Y, and Gong JP. Macromolecules 2007;40(18):6658-6664.

27. Mi F-L, Kuan C-Y, Shyu S-S, Lee S-T, and Chang S-F. Carbohydrate Polymers 2000;41:389-396.

28. Baker JP, Hong LH, Blanch HW, and Prausnitz JM. Macromolecules 1994;27(6):1446-1454.

29. Nakayama A, Kakugo A, Gong JP, Osada Y, Takai M, Erata T, and Kawano S. Advanced Functional Materials 2004;14(11):1124-1128.

30. Wang QZ, Chen XG, Liu N, Wang SX, Liu CS, Meng XH, and Liu CG. Carbohydrate Polymers 2006;65(2):194-201.

31. Kim SJ, Shin SR, Kim NG, and Kim SI. Journal of Macromolecular Science, Part A: Pure and Applied Chemistry 2005;42(8):1073 - 1083.

CHAPTER FOUR

pH Sensitive, Double-Network Hydrogels: Poly(ethylene glycol) methyl-ether methacrylates – Poly-(acrylic acid)

4. pH-Sensitive, Double-Network Hydrogels: Poly(ethylene glycol) methyl ether methacrylates – Poly(acrylic acid)

4.1. Introduction

In the previous Chapter it was shown that the strength and toughness of chitosan based hydrogels could be substantially improved by the incorporation of a polyacrylamide network. In this chapter a different type of double network hydrogel is considered. In particular, the effect of inter-network hydrogen bonding is considered to determine whether such interactions contribute to the gel toughness. As described in Chapter 1, previous work had shown that hydrogen bonding occurs between poly(ethylene glycol) (PEG) and poly(acrylic acid) (PAA) and the hydrogen bonding can be controlled by the pH of the surrounding aqueous solution. The effect of pH on the swelling and mechanical properties of a double network containing both PEG and PAA components is considered in this chapter.

Recently, Frank *et al.* reported a DN system based on end-linked poly(ethylene glycol) (PEG) first network and poly(acrylic acid) (PAA) second network [1]. In contrast to a typical DN, this hydrogel consisted of a neutral polymer first network and a weakly charged polyelectrolyte second network. The observed strengthening effect

contrasts typical DN properties with increased strength due to complexes that form via hydrogen bonding between the interpenetrating networks. True tensile strength and initial modulus of up to ~ 8 MPa and ~ 19 MPa, respectively were measured and are much higher than those of the individual PEG and PAA components [1].

Here, a new example of a DN hydrogel is reported where the first network is a neutral polymer that forms a "bottlebrush" network and the second network is an ionisable polyelectrolyte. The bottlebrush configuration is achieved by polymerization of poly(ethylene glycol) methyl ether methacrylate (PEGMA) oligomers [2, 3], which yields a hydrophobic poly(methyl methacrylate) backbone and hydrophilic PEG side chains. It has been shown that the non-linear PEG analogues, particularly PEGMA, could be as biocompatible as linear PEG [4]. Subsequent incorporation and polymerization of acrylic acid monomer within the tightly crosslinked PPEGMA network forms the slightly crosslinked PAA second network. Our main interest was to explore the effect of inter-network interactions on the swellability and mechanical properties of double networks. It is known that PAA associates with PEG via hydrogen bonding [1, 5] and similar interactions between PEG side chains on the PPEGMA network would form with the PAA network are anticipated. The effect of pH on physical and mechanical properties of this unique DN hydrogel is also discussed since the PAA network is ionisable at pH above 4.3.

4.2. Experimental Section

4.2.1. Materials

Two different poly(ethylene glycol) methyl ether methacrylate (PEGMA) oligomonomers (MWs 1100 and 475 g/mol), acrylic acid (AA), potassium persulfate (KPS), and *N,N'*-methylene MBAAacrylamide (MBAA) were purchased from Sigma-Aldrich and used without any further purification. Monomer molecular structures are shown in Scheme 4.1. Buffers (McIlvaine phosphate-citrate) with various pHs and constant ionic strength (0.5 M) were prepared using citric acid (Sigma-Alrich), sodium phosphate and potassium chloride (Ajax Finechem, Australia). Hydrochloric acid (Ajax Finechem, Australia) was used in some instances to adjust the pH while investigating the effect of ionic strength.

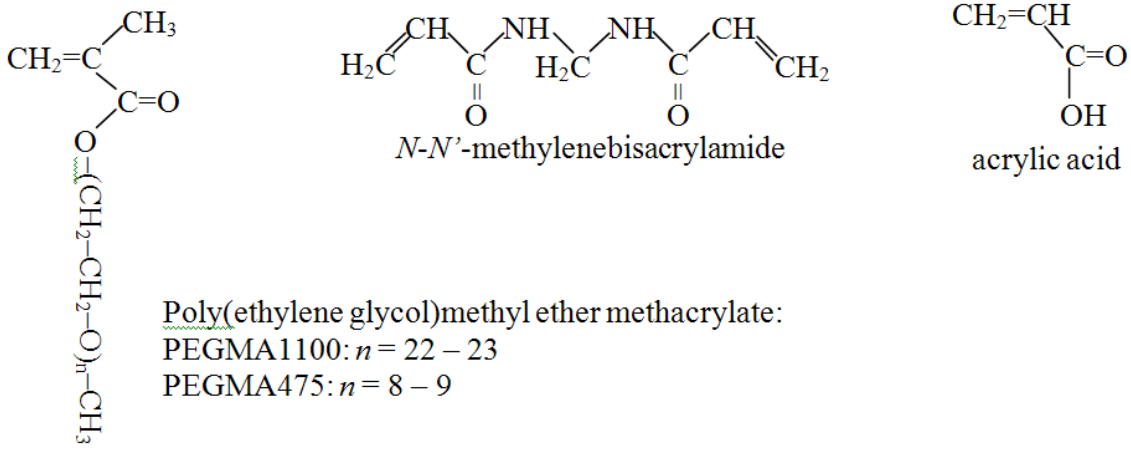

Scheme 4.1. Chemical structure of monomer and co-monomer compounds.

4.2.2. Preparation of Hydrogels

PPEGMA hydrogel network

A simple thermal radical polymerization was employed to prepare high crosslink density PPEGMA475 and PPEGMA1100 single network hydrogels (the numbers indicate the molecular weight of oligomonomers, as shown in Scheme 4.1). Briefly, PPEGMA network was synthesized by dissolving PEGMA oligomonomer in deionized water (20 wt%) followed by adding MBAA as crosslinking co-monomer and KPS as initiator (4 mol% and 0.5 mol%, respectively based on PEGMA). The solution was stirred thoroughly, purged with N_2 and then transferred to a mould (plastic syringes) to fabricate cylindrical-shaped hydrogels. Hydrogel sheets were produced by injecting the first network monomer solution between two glass slides (with hydrophobic surfaces) that were separated by a 1 mm thick silicon gasket. Polymerization was carried out in a convection oven at 65 ^{o}C for 6 hrs. After polymerization, the hydrogels were removed from their moulds, rinsed with distilled water, and kept in water for three days to remove unreacted components.

PAA hydrogel network

To compare the mechanical and physical properties of PAA with PPEGMA and DN hydrogels, PAA single network hydrogels were prepared following the same process as for PPEGMA. However, to achieve a loosely crosslinked PAA network, 0.1 mol% MBAA was added (instead of 4 mol% in PPEGMA case) to the monomer solution. KPS was 0.1 mol% based on the AA monomer concentration.

PPEGMA-PAA DN hydrogels

The DN hydrogel was prepared by a two-step process in which a sequential network formation technique was employed. Following the synthesis of the PPEGMA hydrogel network described above, the PAA second network was incorporated by fully immersing the PPEGMA hydrogel in a solution containing AA monomer (20 wt%), MBAA (0.1 mol%) and KPS (0.1 mol%) for three days. The fully swollen PPEGMA hydrogel was then transferred to a humidified sealed container and polymerization of the second network was carried out at 65 ^{o}C for 6 hrs. The resulting PPEGMA-PAA DN was then washed extensively with deionized water for three days to remove all unreacted components. These DN hydrogels were allowed to reach the equilibrium swollen state in deionized water or in buffer solutions of different pHs (with constant ionic strength of 0.5 M), by storing them in the respective solutions for a minimum of one week prior to characterization.

4.2.3. Swelling Ratio

Swelling ratio was measured to evaluate the water content of the PPEGMA, PAA and PPEGMA-PAA hydrogels at various pHs. Swelling studies were carried out by comparing the fully swollen weight and the dry weight of hydrogels. The fully swollen weight was measured from hydrogels that had been immersed in buffer solutions for at least one week. Samples were patted dry with tissue before weighing. Dry weights were measured after the hydrogels were oven-dried at 60^{o}C for 24 hrs. The following equation 4.1 was used to calculate the hydrogels water content:

$$Q = \frac{w_f}{w_d} \qquad (4.1)$$

where, w_f and w_d are mass of hydrogel when fully swollen and after drying, respectively.

4.2.4. Mechanical Tests

Tensile tests (strain rate: 2 mm/min) were performed on single network (SN) and DN hydrogels cut from sheets into strips of 5 mm width × 30 mm length. A universal testing machine (Shimadzu EZ-S, Japan) was used to perform the test. Compression test (strain rate: 2 mm/min) was carried out on cylindrical-shaped samples (height ~10 mm). Sand paper was placed at upper and lower plates to prevent sample from slipping under high compressive load.

4.2.5. Transmittance

Transmittance of the hydrogels was measured at wavelength 500 nm at room temperature (~ 23^{o}C) using a UV-spectrometer (Shimadzu, UV-1601).

4.2.6. Contact Angle

The static contact angle of deionized water (0.5 μL droplet) on the surface of DN hydrogels was measured using a goniometer (Dataphysics OCA20, Germany).

Equilibrated hydrogel samples were removed from buffer solutions then patted dry before conducting the test.

4.3. Results

4.3.1. Confirmation of Double Network Properties

The compression stress-strain plots of PPEGMA1100-PAA DN hydrogel at pH 2 and its respective SN components shown in Figure 4.1 illustrate the typical behavior of a DN type hydrogel. The mechanical strength and breaking strain of the DN hydrogel was considerably greater than its individual polymer network components on their own. The PPEGMA1100 and PAA SN hydrogels break at 27 kPa and 490 kPa, respectively, while PPEGMA1100-PAA DN hydrogel (with water content as high as 64 %) sustains a breaking stress of 8.1 MPa. This strength is approximately 265 times and 14 times higher than that of the respective single network (SN) hydrogels, PPEGMA and PAA, respectively. Also, the fracture strain of 95 % is higher than its constituent SN components (64 % and 78 % for PPEGMA and PAA, respectively).

4.3.2. Effect of pH on Physical Properties of the DN Hydrogels

As a polymer with ionizable carboxylic acid side groups, PAA has a pK_a value of around 4.25 [6] and is pH sensitive. Figure 4.2a clearly demonstrates the pH sensitivity of PAA and the PPEGMA-PAA DN hydrogels. The swelling ratio changes dramatically within the pH range of the PAA pK_a value. Below pH ~ 4, the measured swelling ratio for the

PAA SN hydrogel and both of the DN hydrogels were lower than for pHs above 4. In comparison, the swelling ratios of PPEGMA1100 and PPEGMA475 SN hydrogels were only weakly dependent on pH. It is also noted that the longer PEG side chains in the case of PPEGMA1100 gave higher swelling at all pHs than the PPEDMA475 due to PEG hydrophilicity. Strikingly, the swellability of the DN hydrogels below pH ~ 4 was significantly smaller than the SN hydrogels. Above pH ~ 4, the swelling ratio of DN hydrogels approached the swelling ratio of the PPEGMA SN hydrogels but were below the PAA SN hydrogel.

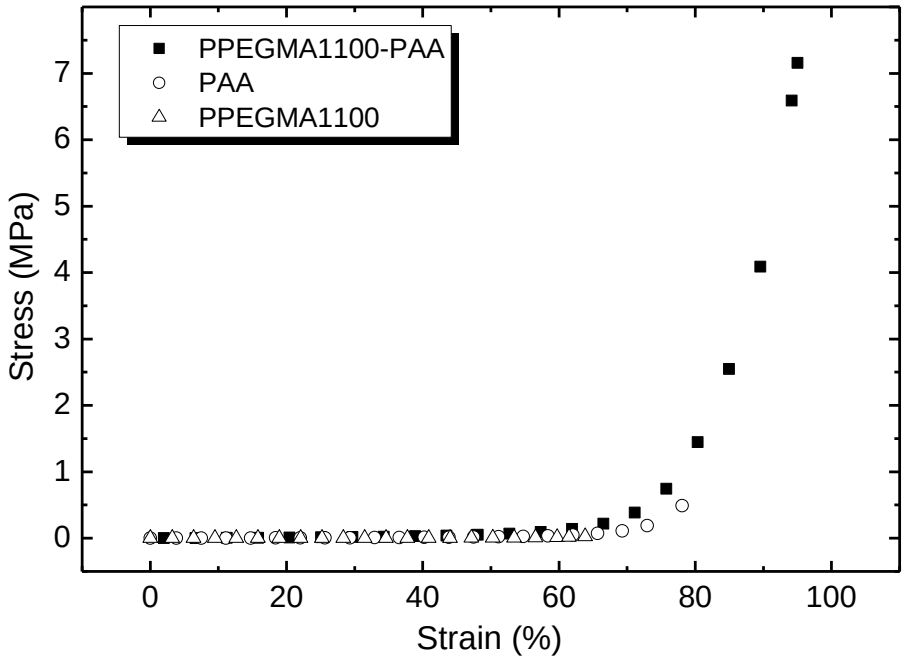

Figure 4.1. Compression stress-strain curve of PPEGMA1100-PAA hydrogel and its single network hydrogels in a pH 2 buffer.

PAA-PEG interpenetrating networks (IPN) [5] have been reported to have a strong hydrogen bonding interaction with a complex forming between the PAA and the PEG. The stability of the interaction was found sensitive to the degree of neutralization of the PAA component (which can be controlled via pH), and the ionic strength of the solution [7]. Similarly, in the PPEGMA-PAA DN hydrogels, the interaction between PEG component (side chains) of the first network and the PAA second network is pH dependent. Strongest interactions occur between PEG and the non-ionized carboxylic acid groups on PAA that exist below pH ~ 4. The reduced swelling of the DN hydrogels below pH ~ 4 can be taken as evidence of complexes that have formed due to strong hydrogen bonds that exist between two networks in this pH range. Above pH ~ 4, the hydrogen bonding is disrupted and the DN hydrogels are free to swell to the limit imposed by the more tightly crosslinked first network (PPEGMA). This swelling transition from a hydrogel with low swelling ratios at acidic pHs to more swollen hydrogels at neutral pHs is reversible. The swelling response for the DN hydrogels was observed to be dependant on the geometrical size of the samples. For a 1 mm-thick flat sheet sample, the response was less than 90 min, while it takes more than 6 hrs for a 3.6 mm-diameter cylindrical sample.

The transparency of the DN hydrogels was also affected by changing the pH of the surrounding environment. The as-prepared PPEGMA1100-PAA DN hydrogel was white and opaque and only slightly more transparent in the case of PPEGMA475-PAA DN. These gels remained white/opaque even when stored in deionized water for several weeks. The DN hydrogels, however, became transparent when the pH was raised (Figure 4.2b). Up to 80 % transparency was achieved upon neutralization in buffers at above pH

5. The transition corresponds to the swelling transition and coincides with the pK_a value of PAA. The DN made from PPEGMA475 was more transparent than the one from PPEGMA1100, while all SN hydrogels were transparent (~ 90 %) at the pH range studied here. These observations are consistent with complex formation between the PAA and PPEGMA below pH ~ 5, which result from density fluctuations that scatter visible light. The PPEGMA1100-PAA hydrogels are less transparent because the complexes which form are both larger and more stable.

The surface properties of the DN hydrogels were also investigated by measuring the contact angle of water droplet on the hydrogel surface after the samples had been equilibrated at various pH conditions (Figure 4.2c). All samples were patted dry before the test. For both DN hydrogels, the measured contact angle dropped from ~ 80 degrees (below pH ~ 4) to 40 – 45 degrees (above pH ~ 4). The transition for the change in contact angle is sharper for the DN hydrogel prepared with PPEGMA1100 than for the PPEGMA475. Also, the water contact angle for PAA SN hydrogel exhibits similar pH sensitivity but with values much lower than the DN hydrogels at all pH range. In contrast, PPEGMA1100 and PPEGMA475 SN hydrogels show no sign of pH sensitivity, with water contact angle less than 10 degrees. The hydrophobic complex acts as a surfactant and organizes at the surface to minimize the surface energy. It was not expected that the DN hydrogels maintain a contact angle > 40 degrees at pH's > 5 where the complex between the networks was expected to be destroyed.

It has been claimed that the hydrogen bond association of PAA and PEG involves "non-interrupted linear sequences of bonds" between contiguous monomer residues of the hydrogen bonding donor PAA and the hydrogen bonding acceptor PEG [8].

Similarly, copolymers of methacrylic acid and linear polymer chains of PPEGMA exhibits a cloud point which falls below 0 ^{o}C under acidic conditions [9]. This cloud point was attributed to the formation of hydrophobic H-bonded ether-acid complexes. The transition in the PPEGMA-PAA DN hydrogels transparency and surface contact angle could be mainly due to the disruption of acid-ether hydrogen bonds as pH increases. In fact, the acid-ether hydrogen bonds introduce hydrophobic zones into the hydrogel's structure which causes the DN hydrogel to contract in acidic conditions. By increasing the pH from acidic to more moderate pHs (above pK_a of PAA), these hydrophobic acid-ether complexes dissociate, and consequently, changing the swellability and surface properties of the DN hydrogels. These DN hydrogels consist of hydrophobic regions where a complex has formed between the PEG and the PAA alongside of hydrophilic regions containing PAA.

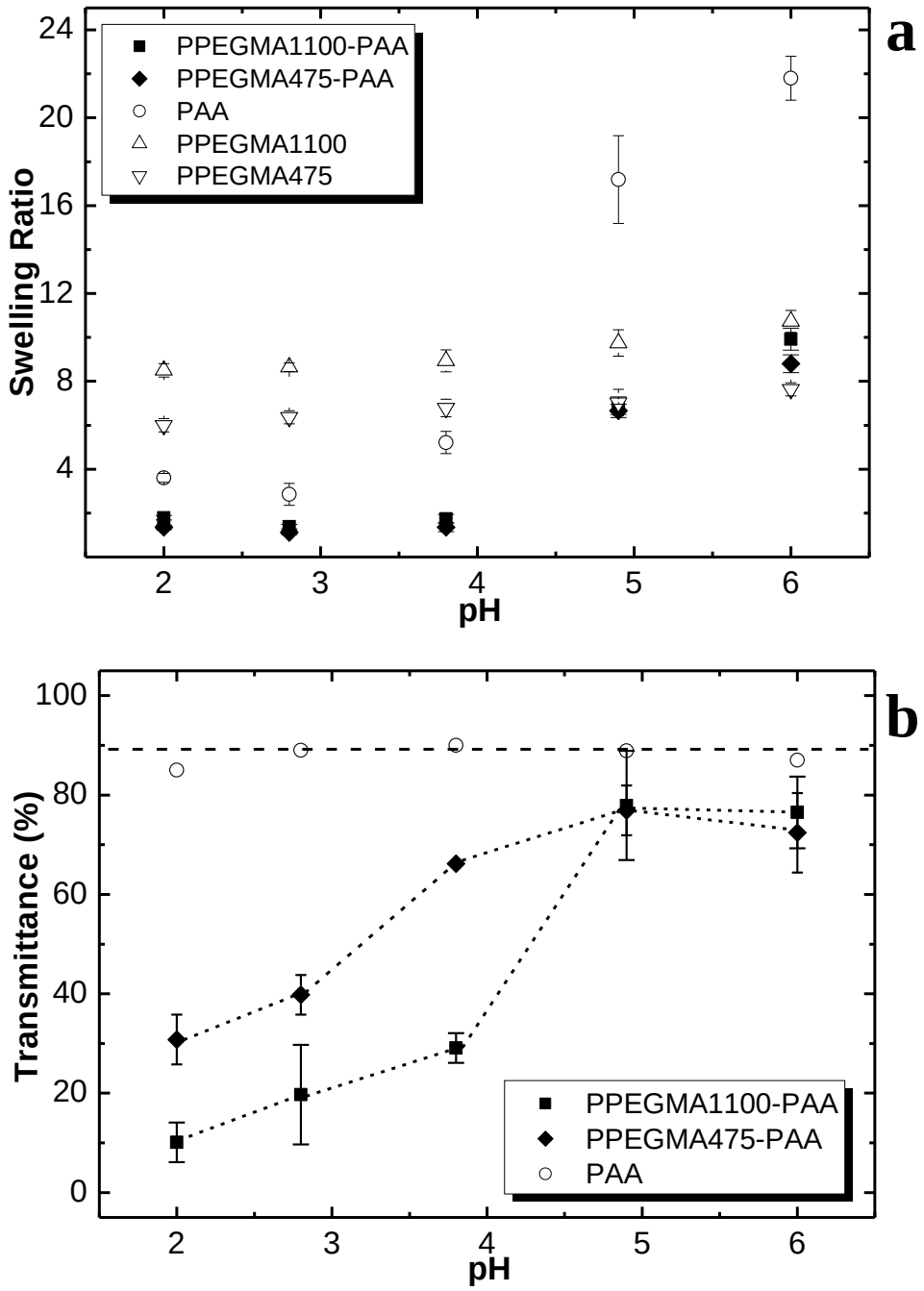

Figure 4.2. Effect of solution pH on physical properties of PPEGMA-PAA hydrogels: a) swelling ratio, b) transmittance, c) surface contact angle (next page). Lines are to guide the eye.

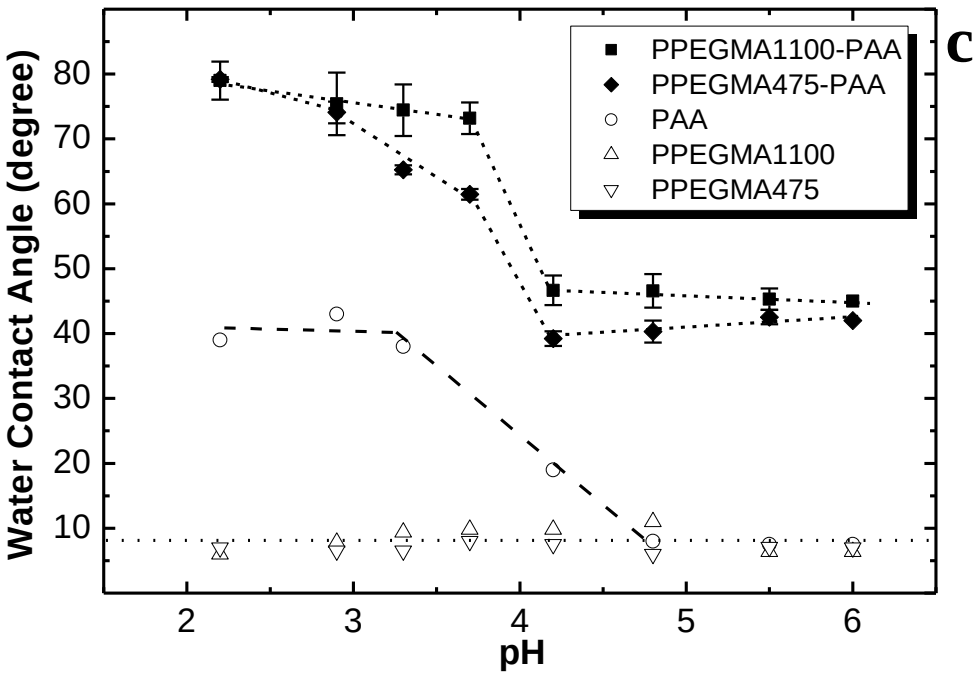

Figure 4.2. ***Continued.***

4.3.3. Effect of pH on Mechanical Properties

In crosslinked polymeric structures, the swelling ratio of the network has a direct impact on the mechanical properties of the gel [10]. Similarly, as the swelling ratio of PPEGMA-PAA DN hydrogels varies with pH, it is expected that the mechanical properties of the DN hydrogels will also depend on pH. Figure 4.3 shows the pH dependency of compression strength and modulus of all investigated hydrogels. The PPEGMA SN hydrogels showed no dependency of their mechanical properties on pH, while the PAA SN hydrogel showed a transition to lower breaking strength and modulus at pHs above 4. These behaviours are consistent with the swelling ratios, with a higher degree of swelling associated with lower strength and modulus. The DN hydrogels also

displayed a transition to higher strength at pH below 4, although the increase in strength was significantly greater than the PAA SN hydrogel (Figure 4.3a). In particular, the fracture strength of PPEGMA1100-PAA DN hydrogel at pH 2 (σ_b=8.1 MPa) was an order of magnitude higher than at pH 5.5 (σ_b=0.7 MPa). The DN hydrogels show an enhancement in strength compared with PAA SN hydrogel at all pHs. The enhancement in strength at pH < 4 of 4 – 8 MPa (for PPEGMA475-PAA and PPEGMA1100-PAA, respectively) is significantly higher than at pH > 4 (~ 0.5 MPa). The additional strengthening at low pH corresponds to the region where complexation between the interpenetrating networks was active, suggesting that the additional strengthening may be associated with the inter-network interactions. In contrast to the fracture strength, the elastic modulus of DN hydrogels (the slope of stress-strain curve at the initial part of the curve) did not show any significant pH dependence (Figure 4.3b). For the PAA SN hydrogel, a transition in elastic modulus was observed over the transition range as expected from the increase in swelling. The lack of pH sensitivity of the modulus of the DN hydrogels is particularly surprising since they display a large change in swellability with pH. The dependency of modulus on swelling ratio is considered in more details below.

To further investigate the influence of pH on the mechanical properties of PPEGMA-PAA DN hydrogels, tensile tests were performed on fully swollen DN and SN hydrogel sheets. The PPEGMA1100 and PPEGMA475 SN hydrogels were not tested under tension as they were so fragile that they fractured when mounting in the grips. Figure 4.4 shows typical tensile stress-strain curves of the PPEGMA1100-PAA and PPEGMA475-PAA DN hydrogels and PAA SN hydrogel at pH 2.

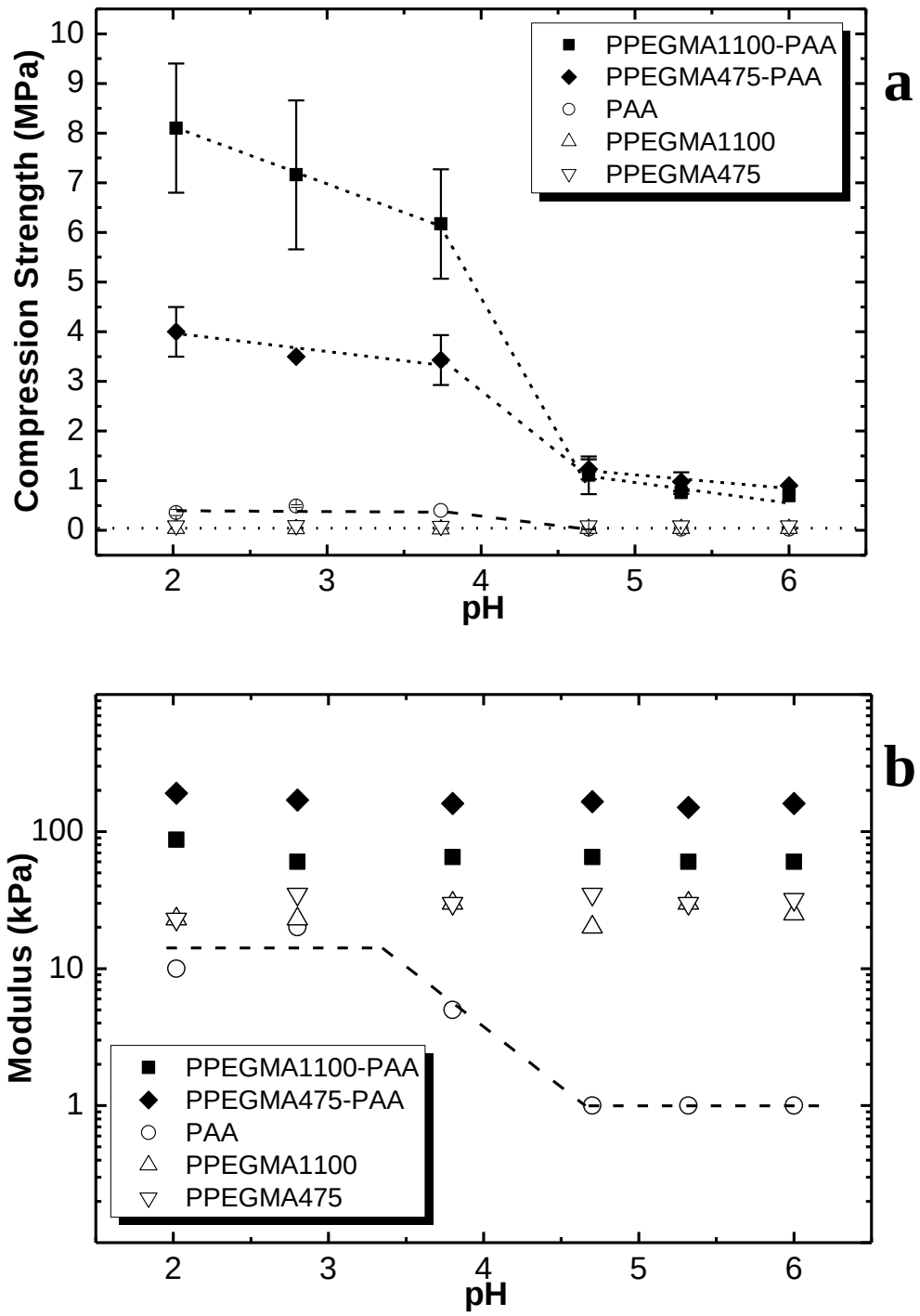

Figure 4.3. Compression properties of PPEGMA-PAA hydrogels and their constituent single networks as a function of pH: a) fracture strength, b) compression modulus.

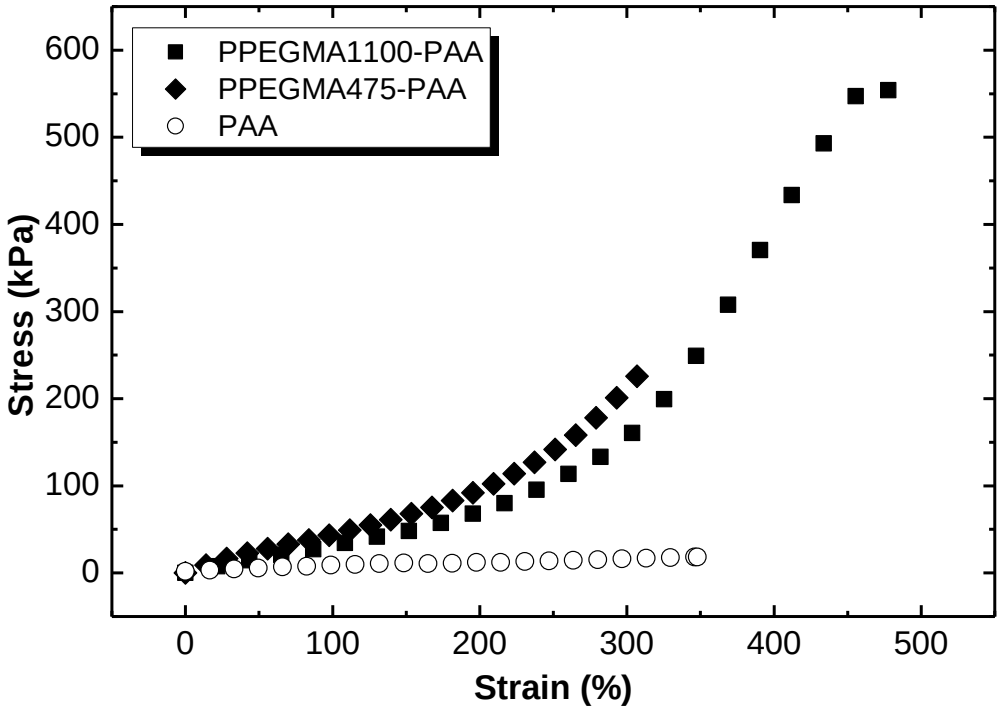

Figure 4.4. Tensile stress-strain curves of PPEGMA-PAA and PAA hydrogels at pH 2.

These curves clearly demonstrate the strengthening produced by the DN structure. Both DN and SN hydrogels show similar elongation at break (300 – 500 %) at pH 2, but the tensile strength of the DN hydrogels was more than 30 and 12 times higher than PAA (respectively for PPEGMA1100-PAA and PPEGMA475-PAA). The DN hydrogels also exhibit a J-type tensile curve indicative of strain hardening at high strains which was not evident for the PAA SN. The strain hardening is due to a reduction in entropy at high strains and is common to both hydrogels and rubbers at high strain.

The relationship of tensile strength and Young's modulus of the DN hydrogels and PAA SN hydrogel to the swelling ratio are presented in Figure 4.5a and 4.5b, respectively. Tensile strengths of DN and SN hydrogels decrease with increasing

swelling ratio, following nearly a power law trend as generally expected in swollen polymeric networks [10]. The tensile strength of the DN hydrogels was less sensitive to the swelling ratio compared to the PAA SN hydrogel, and generally showed much higher strength. A similar trend was observed by Frank *et al.* [1], where the true tensile strength of PEG-PAA DN hydrogel decreased almost one order of magnitude in its more swollen state at pH 6 (σ_{true} = 0.86 MPa) compared to its less swollen state at pH 3 (σ_{true} = 8.2 MPa).

The tensile modulus of PPEGMA-PAA DN hydrogels was observed to be much less sensitive to pH than the PAA SN, where the latter decreased with increasing swelling. However, the modulus of the DN hydrogels did not change significantly with a change in pH in agreement with Frank *et al*. for PEG-PAA interpeneterating networks. This paradox was also noted by Frank *et al.*, even though there is a significant change in water content (and hence chains per unit volume) as well as the breaking of complexes between the two networks. It should be noted that that the crosslink densities of both networks employed by Frank *et al.* are much higher than those used here as indicated by the much higher reported modulus.

At low pH, the PPEGMA network is essentially collapsed, having formed a complex with the PAA network, hence the modulus is a measure of the PAA network that is in excess. At high pH the modulus is a measure of both the PPEGMA and the PAA network. Hence, there is an increase in the number of elastic chains that corresponds with the swelling resulting from the breaking of complexes between the two networks. Overall the number of elastic chains per unit volume is close to constant, with variations expected by changing the molar ratio of ethylene glycol (EG) repeat unit to

the acrylic acid (AA) repeat unit. In this instance, the PPEGMA1100-PAA had a higher ratio of EG to AA relative to the PPEGMA475-PAA. Consequently the PPEGMA475-PAA hydrogel exhibited a small decrease in modulus with an increase of pH whilst the PPEGMA1100-PPA hydrogel did not. In the work of Frank *et al.*, the ratio of EG to AA is less than that used here (as the EG units are on the polymer back bone and not as side chains), consequently they observed a small increase in modulus with pH.

4.4. Discussion

4.4.1. Comparison with other DN Hydrogels

The PPEGMA-PAA DN hydrogels prepared in these study exhibited similar compression properties as other similar IPN and DN hydrogels. Here, under acidic conditions, the PPEGMA-PAA DN hydrogels displayed compression fracture strengths (4 – 8 MPa) that exceeds most of the other DN hydrogels [11-13] except those based on PAMPS-PAAm (17–21 MPa) [14]and PVA-PEG (12.8–25.2 MPa) DN hydrogels [15] Also, under acidic conditions, the improvement in compression strength of the DN compared to SN, $\sigma_{max}^{DN}/\sigma_{max}^{SN}$, are among the highest reported in the literature (265 and 130 for PPEGMA1100-PAA and PPEGMA475-PAA, respectively). The $\sigma_{max}^{DN}/\sigma_{max}^{SN}$ for PAMPS-PAAm and PVA-PEG DN hydrogels are 43 and 8.3, respectively; the highest reported values are 700 and 267 for P(AMPS-*co*-TFEA)-PAAm and PAMPS-TFEA, respectively [14].

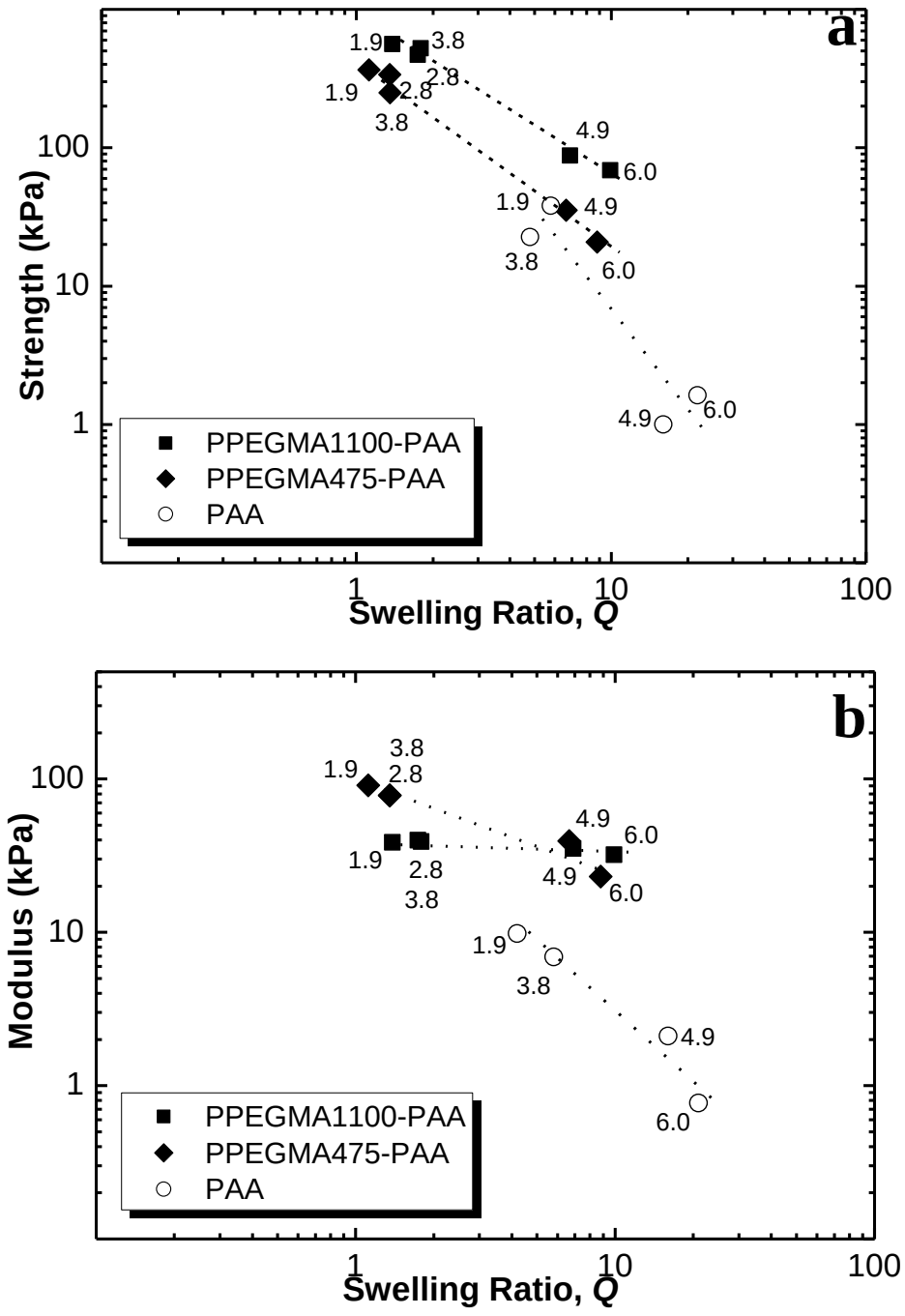

Figure 4.5. Tensile properties of PPEGMA-PAA and PAA hydrogels as a function of pH: a) Young's modulus, b) tensile strength. The numbers on each data point represent the pH of buffer solution in which the corresponding swelling ratio was achieved.

In terms of tensile behaviour, there are only a few examples in the literature that report the tensile properties of a fully swollen hydrogel. The highest reported values in the present literature for a fully swollen hydrogel is for PVA-PEG DN, which displayed a tensile strength and modulus of 6.10 MPa and 160 kPa, respectively [15]. However, the tensile strength of the PVA SN hydrogel was also fairly high (1.5 MPa) in comparison to other common synthetic SN hydrogels. The σ_{max}^{DN}/ σ_{max}^{SN} for fully swollen PPEGMA1100-PAA and PPEGMA475-PAA hydrogels in this report was measured to be ~ 23 and ~ 15 at pH ~ 2, and ~ 68 and ~ 20 at pH 6, respectively. The calculated true tensile strength, σ_{true}, of PEG-PAA DN hydrogel is around 9 MPa by Frank *et al.* [1], which is higher than what we have observed here (σ_{true} ~ 3 MPa for PPEGMA1100-PAA under acidic conditions).

4.4.2. Strengthening Mechanisms

The bottlebrush structure of first network allows the second network to interact mainly with the "side chains" of the first network. This interaction is dominantly a pH sensitive acid-ether hydrogen bonding. From the results presented here, this interaction strongly influences the behavior of the DN hydrogels when pH changes, including a significant improvement in the mechanical properties over that of the first network. At acidic pHs, although the PAA network mainly interacts with the side chains of PPEGMA network, the hydrogen bonding interaction is sufficient to induce DN-like mechanical improvement in the hydrogels. At higher pHs when the hydrogen bonding interaction is

absent, the DN still exhibits improved strength compared to either SNs. However, the strengthening effect is not as pronounced at high pH compared to lower pHs.

The main question here is whether these systems, such as PPEGMA-PAA or PEG-PAA, which are inspired by DN technique in their synthesis and possess strong hydrogen bonding between two networks, are strengthened in the same way as other double network hydrogels. In other words, is the source of strength in these hydrogels purely hydrogen bonding or topological characteristics of the networks or a combination of both? The proposed mechanism for the toughness of DN hydrogels is based on the topology of the hydrogels, where the first network will fracture first as a result of its higher crosslinking and its highly extended chains, followed by the formation of a damaged zone around the crack which has mainly the characteristics of the second network [16, 17]. Experimental evidence, such as necking and direct microscopic observation of damaged area around the crack, support this model [14, 18, 19]. However, the proposed model and all of the experimental evidence that support them totally focused on the only extensively studied DN system made of PAMPS as the first network and PAAm as the second network. Gong *et al*. in their early paper stated two main criteria for DN hydrogels which distinguish them from other IPN systems [14]. They mentioned the difference in degree of crosslinking of networks (tightly crosslinked first network and loosely crosslinked second network), and the high molar ratio of second network to the first network as two main criteria to achieve mechanical enhancement [14]. The crosslinking ratio of hydrogels can be adjusted by controlling the crosslinking agent concentration and polymerization condition of their respective polymerization reactions. The second criterion however, is mainly defined by the nature

of first network and its interaction with second network monomer solution. To achieve high molar ratio of the second network to the first network, Gong *et al*. suggested that the first network needs to preferentially be a polyelectrolyte which can then swell in the second network monomer solution and uptake second network monomers. Although it is possible to control the ratio of two networks by changing the concentration of monomer in the second network monomer solution, as demonstrated in the literature before [14], it is more difficult to manipulate it when the first network is not a polyelectrolyte. More neutral polymers do not swell in an aqueous solution as much as polyelectrolytes do. For example, to obtain a molar ratio of ~ 10 with the PAMPS first network made from a 4 M monomer solution (~ 17 wt% water), the PAMPS network should be swollen in a 1 M AAm monomer solution. Since the PAMPS first network swells in the AAm monomer solution, and in the absence of any specific interaction between first network polymer chains and second network monomer, the concentration of AAm monomers within the swollen PAMPS network is the same as the surrounding AAm monomer solution. This means that the as-prepared PAMPS hydrogel (Q_o ~ 1.21) is required to swell 40 times in AAm monomer solution to reach to the required molar ratio.

In the case of PPEGMA-PAA and PEG-PAA, the interaction between PEG and PAA is so strong that it might limit the achievable molar ratio of the two networks. It has previously been suggested that the hydrogen bonding interaction between PAA and PEG chains follows a specific pattern with the ratio of carboxylic acid groups to ethylene glycol units ranges from 1 – 3 [5, 20]. Thus, it is important to estimate the ratio of the two networks investigated in this study. Since PPEGMA and PAA networks form strong hydrogen bonding, it is not possible to simply use the swelling ratio of the first

network and the second network monomer concentration to estimate the ratio of two networks. As a result, an indirect method was employed here to measure this ratio by using the mass of networks and their corresponding swelling ratios. Briefly, as-formed PPEGMA first network hydrogels were carefully weighed (w_1) and by knowing their swelling ratio from previous measurements (Q_1) the mass of dry polymer network (W_1) can be calculated as:

$$W_1 = \frac{w_1}{Q_1} \qquad (4.2)$$

The PPEGMA hydrogels then were soaked in AA monomer solution with different monomer concentration (10 – 20 wt%), followed by polymerization of PAA second network within PPEGMA as mentioned before. The mass of fully swollen PPEGMA-PAA hydrogels were measured (w_{DN}) and by using the PPEGMA-PAA hydrogels swelling ratio (Q) the mass of dry PPEGMA-PAA networks (W_{DN}) can be estimated:

$$W_{DN} = \frac{w_{DN}}{Q} \qquad (4.3)$$

By assuming that the mass of PPEGMA network has not changed during the soaking and second network polymerization process, the difference between the mass of final dry PPEGMA-PAA and that of PPEGMA is considered as the incorporated second network's mass (W_2):

$$W_2 = W_{DN} - W_1 \qquad (4.4)$$

The number of moles of PPEGMA repeating units (X_{n1}) was calculated from the molar mass of PEGMA monomer (M_{1100} or M_{475}) and mass of dry PPEGMA networks:

$$X_{n1} = W_1/M_{1100} \quad \text{PEGMA1100 (4.5a)}$$

$$X_{n1} = W_1/M_{475} \quad \text{PEGMA 475 (4.5b)}$$

For PEGMA475 and PEGMA1100 the average number of ethylene glycol units per each monomer molecules (n_1) is 8.5 and 22.7, respectively. Thus, the number of moles of ethylene glycol units (N_1) in a PPEGMA network can be estimated as:

$$N_1 = n_1 X_{n1} \qquad (4.6)$$

A similar concept was employed to measure the number of moles of AA repeating units, and consequently carboxylic acid groups (N_2) of PAA network as:

$$N_2 = X_{n2} = W_2/M_{AA} \qquad (4.7)$$

where M_{AA} is the molar mass of acrylic acid repeating units. The molar ratio of ethylene glycol to carboxylic acid (N_2/N_1) as a function of AA monomer concentration is plotted for both PPEGMA475-PAA and PPEGMA1100-PAA in Figure 4.6a. For both systems, as the concentration of AA monomer increases in the second network monomer solution the ratio of carboxylic acid to the ethylene glycol increases in the final PPEGMA-PAA network. This ratio seems to level off around 1.1 for PPEGMA475-PAA and 2 for PPEGMA1100-PAA. These results are in agreement with previous studies that suggested a value between 1 and 3 for PAA to PEG [5, 20]. The higher concentration of AA monomer means that there is an excess of AA units so it is likely that the majority of ethylene glycol (EG) units participate in hydrogen bonding, although it is not possible to achieve all because of the defects and crosslinks.

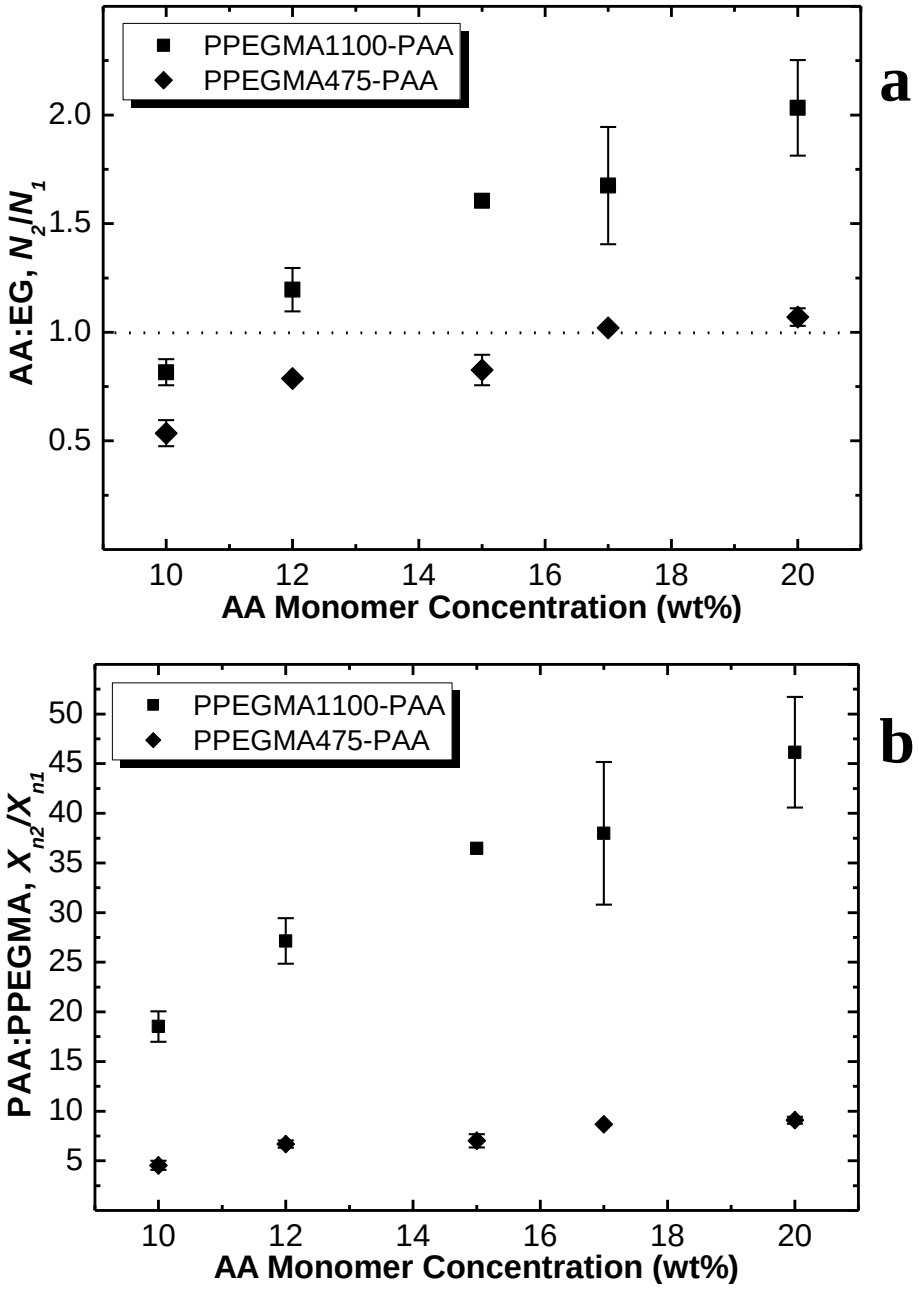

Figure 4.6. Molar ratio of a) acrylic acid (AA) and ethylene glycol (EG) side groups in PPEGMA-PAA hydrogels (N_2/N_1) and b) PAA second network to PPEGMA first network (X_{n2}/X_{n1}) vs. acrylic acid monomer concentration. Dotted line indicates the equimolar ratio. A 20 wt% solution was used for the study of hydrogel mechanical properties.

The above analysis suggests that the molar ratio of carboxylic acid groups to ethylene glycol units in the DN gels ranges between 1 and 2. However, the actual molar ratio of AA repeat unit in the second network to PEGMA repeat unit in the first network is much higher than 2. Since ethylene glycol units form the side chains of the PPEGMA network with average ethylene glycol units per methacrylate units of 8.5 and 22.7 for PPEGMA475 and PPEGMA1100, respectively, the molar ratio of PAA to PPEGMA multiplies by a factor of 8.5 or 22.7 depending on the number of ethylene glycol units of the first network. Figure 4.6b plots the molar ratio of the second network to the first network for PPEGMA475-PAA and PPEGMA1100-PAA as a function of AA monomer concentration. Consequently, for an AA monomer concentration of 20 wt% the molar ratio is well above 10 for both DN gels containing either PPEGMA475 or PPEGMA1100 (Scheme 4.2). As mentioned above, the strength and toughness of DN gels is enhanced when the second network is presented in a high molar excess [14].

The mechanisms involved in the strengthening of these hydrogen bonding DN hydrogels remains to be determined. The proposed mechanism for the toughness of non-hydrogen bonding DN hydrogels is based on the topology of the hydrogels, where the first network will fracture first as a result of its higher crosslinking and its highly extended chains, followed by the formation of a damaged zone around the crack which has mainly the characteristics of the second network [16, 17]. Experimental evidence, such as necking and direct microscopic observation of damaged area around the crack, support this model [14, 18, 19]. It is likely that similar mechanisms operate in the PEG-PAA DN gels at pH > 4, where hydrogen bonding is reduced. In this regime the PPEGMA-DN tensile strength exceeded that of the PAA SN by a factor of at least 15

times. The network topologies produced are similar to that reported to be important for achieving high toughness with the second network (PAA) lightly crosslinked and present in a molar ratio of second network to first network greater than 5. As detailed in the supporting information, the molar ratio of the two networks could be calculated from the acrylic acid monomer concentration and for both PPEGMA-PAA hydrogels the ratio exceeded 5.

The most significant strengthening of PPEGMA-PAA DN hydrogels occurred at pH <4, where hydrogen bonding induced a significant deswelling coinciding with a heterogeneous microstructure (as evidenced by the opacity). In this condition, the interactions between the two networks may provide additional toughening mechanisms by the rupture or slipping of *inter*-polymer complexes. The reduced swelling itself is likely to contribute to an increase in strength. As shown in Figure 1.2, a general trend to increased toughness has been observed in many different hydrogel systems as the swelling degree was decreased. It is likely that the enhanced strength of PPEGMA-PAA DN hydrogels at low pH is influenced by all 3 factors identified: reduced swelling; a DN topology and strong hydrogen bonded interactions.

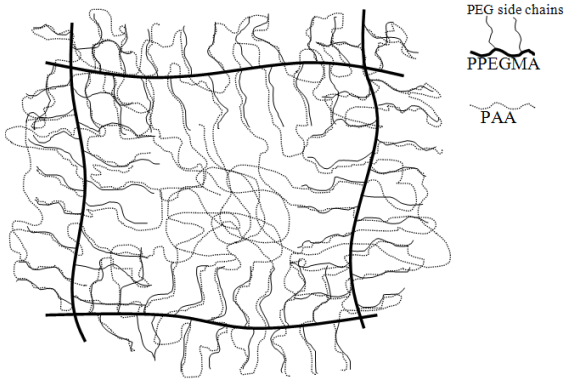

Scheme 4.2. Schematic illustration of a PPEGMA-PAA hydrogel.

4.5. Conclusions

The two PPEGMA-PAA DN hydrogels investigated here displayed true DN-properties: significant improvement in mechanical properties was measured for all DN hydrogels compared to SN hydrogels prepared from their individual components (i.e. PPEGMA1100 and PPEGMA475 first networks, and PAA second network). The DN hydrogels respond to pH similar to the PAA component. Unlike the PPEGMA1100 and PPEGMA475 single hydrogel networks, the swelling ratio of PPEGMA-PAA DN hydrogels changed at a transition pH of ~ 4. This swelling transition also corresponded to the transformation between opaque and hydrophobic hydrogels (pH < 4) to transparent and hydrophilic hydrogels (pH > 4). These changes in physical properties are related to the observed change in mechanical properties. A dramatic decrease in tensile strength occurred when pH exceeded the transition point (pH ~ 4). In contrast, the tensile modulus of DN gels was largely insensitive to pH, while the modulus of PAA SN decreased on increasing pH above 4. These observations are related to the dissociation of the acid-ether hydrogen bonds as the pH is increased above the pK_a value of the PAA network, causing the ionization of the carboxylic acid side groups of PAA. The observed enhancement in mechanical performance of PPEGMA-PAA DN hydrogels may be attributed to hydrogen bonding at pH < 4. However, it was shown that the ratio of PAA second network to the PPEGMA first network is more than ten and topological effects arising from the two networks might be responsible for additional toughening achieved at pHs above 4. The outstanding mechanical properties of the PPEGMA-PAA DN hydrogels make them potentially useful for many applications such as drug release and

actuators. The addition of electronic conductivity to these hydrogels is described in the following two chapters.

4.6. References

1. Myung D, Koh W, Ko J, Hu Y, Carrasco M, Noolandi J, Ta CN, and Frank CW. Polymer 2007;48(18):5376-5387.
2. Lutz J-F. Journal of Polymer Science Part A: Polymer Chemistry 2008;46(11):3459-3470.
3. Lutz J-F, Weichenhan K, Akdemir O, and Hoth A. Macromolecules 2007;40(7):2503-2508.
4. Lutz J-F, Andrieu J, Uzgun S, Rudolph C, and Agarwal S. Macromolecules 2007;40(24):8540-8543.
5. Nishi S and Kotaka T. Macromolecules 1985;18(8):1519-1525.
6. Perrin DD, Dempsey B, and Serjeant EP. pK_a Prediction for Organic Acids and Bases. London: Chapman & Hall, 1981.
7. Lu X and Weiss RA. Macromolecules 1995;28(9):3022-3029.
8. Iliopoulos L and Audebert R. Macromolecules 1991;24(9):2566-2575.
9. Jones JA, Novo N, Flagler K, Pagnucco CD, Carew S, Cheong C, Kong XZ, Burke NAD, and Stöver HDH. Journal of Polymer Science Part A: Polymer Chemistry 2005;43(23):6095-6104.
10. Anseth KS, Bowman CN, and Brannon-Peppas L. Biomaterials 1996;17(17):1647-1657.
11. Nakayama A, Kakugo A, Gong JP, Osada Y, Takai M, Erata T, and Kawano S. Advanced Functional Materials 2004;14(11):1124-1128.
12. Weng L, Gouldstone A, Wu Y, and Chen W. Biomaterials 2008;29(14):2153-2163.
13. Zhang Z, Chao T, and Jiang S. The Journal of Physical Chemistry B 2008;112(17):5327-5332.
14. Gong JP, Katsuyama Y, Kurokawa T, and Osada Y. Advanced Materials 2003;15(14):1155-1158.

15. Zhang X, Guo X, Yang S, Tan S, Li X, Dai H, Yu X, Zhang X, Weng N, Jian B, and Xu J. Journal of Applied Polymer Science 2009;112:3063-3070.

16. Brown HR. Macromolecules 2007;40(10):3815-3818.

17. Tanaka Y. EPL (Europhysics Letters) 2007;78(5):56005.

18. Na Y-H, Tanaka Y, Kawauchi Y, Furukawa H, Sumiyoshi T, Gong JP, and Osada Y. Macromolecules 2006;39(14):4641-4645.

19. Yu QM, Tanaka Y, Furukawa H, Kurokawa T, and Gong JP. Macromolecules 2009;42(12):3852-3855.

20. Li Y, Li H, Chen X, Zhu F, Yang J, and Zhu Y. Journal of Polymer Science Part B: Polymer Physics 2010;48(16):1847-1852.

CHAPTER FIVE

Electrically Conductive, Tough Hydrogels with pH Sensitivity

5. Electrically Conductive, Tough Hydrogels with pH Sensitivity

5.1. Introduction

As described in Chapter 1, conductive hydrogels hold significant promises in drug release (Chapter 2), bioactive electrode coating, and actuators [1, 2]. In this chapter, an electrically conductive hydrogel is reported, with pH sensitivity and improved mechanical properties. The toughness and enhanced mechanical properties along with pH sensitivity are obtained from a tough DN hydrogel system based on the poly(ethylene glycol) methyl ether methacrylates (PPEGMA) single network and poly(acrylic acid) (PAA) second network (previous chapter). The electrical conductivity and electrochemical activity are achieved by chemically polymerising EDOT with PSS dopant within the pH-sensitive tough PPEGMA-PAA DN hydrogels to form PEDOT-PSS. Conducting the EDOT polymerisation step more than once overcomes the limitations attributed to the solubility of EDOT in the PSS solution and as a result considerably higher conductivity could be reached while retaining excellent mechanical properties and pH sensitivity.

5.2. Experimental Section

5.2.1. Materials

Poly(ethylene glycol) methyl ether methacrylate (PEGMA1100) (MW 1,100 g/mol), acrylic acid (AA), potassium persulfate (KPS) and *N,N'*-methylene MBAAacrylamide (MBAA) were purchased from Sigma-Aldrich and used without any further purification to fabricate the PPEGMA1100-PAA DN hydrogels. Poly(sodium 4-styrenesulfonate) (NaPSS) (MW 70,000 g/mol), ammonium persulfate (APS) and 3,4-ethylenedioxythiophene (EDOT) were purchased from Sigma-Aldrich and used to form PEDOT-PSS within the hydrogels. Buffers (McIlvaine phosphate-citrate) with various pHs and constant ionic strength (0.5 M) were prepared using citric acid (Sigma-Alrich), sodium phosphate and potassium chloride (Ajax Finechem, Australia). To prepare glass slides with hydrophobic surfaces (that were used as moulds for the polymerisation of the hydrogels) octadecyltrichlorosilane 90 % was purchased from Sigma-Aldrich, and hexane and hydrogen peroxide 35 % solution were purchased from Ajax Finechem, Australia. The double-distilled deionised water (18.5 MΩ) was used to make up all of the aqueous solutions. The chemical structures of EDOT and PSS are presented in Scheme 5.1.

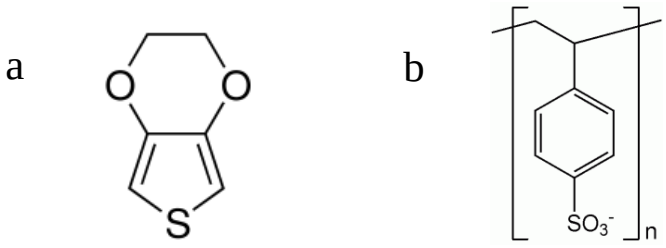

Scheme 5.1. Chemical structures of (a) EDOT and (b) PSS.

5.2.2. Preparation

PPEGMA1100-PAA DN hydrogels

The method to manufacture the PPEGMA1100-PAA DN hydrogels was described elsewhere (previous chapter). Briefly, a simple thermal radical polymerisation was employed to prepare the networks. First, the PPEGMA1100 single network (SN) was synthesized by dissolving PEGMA1100 oligomonomers in deionised water (20 wt%) followed by adding MBAA as the crosslinking comonomer and KPS as the initiator (4 mol% and 0.5 mol%, respectively, based on PEGMA1100 monomer). The solution was stirred thoroughly, purged with N_2 and then transferred to a mould. For preparing thin sheets the mould was made of two surface-treated hydrophobic glass slides separated with a silicon spacer (1 mm). In some cases a plastic syringe was used as a mould to prepare cylindrical rods. Polymerisation was carried out in a convection oven at elevated temperature (65 ^{o}C) for 6 hrs. After the polymerisation, samples removed from the moulds and were rinsed thoroughly and kept in deionised water for one week, where the water was changed on a daily basis to ensure the removal of any unreacted chemicals. In the second polymerisation stage, the PPEGMA1100 hydrogels were soaked in AA monomer solution containing AA monomer (20 wt%), MBAA (0.1 mol%) and KPS (0.1 mol%) for three days. The fully swollen PPEGMA1100 hydrogels were sealed between two hydrophobic glass slides, followed by a polymerisation reaction at 65 ^{o}C for 6 hrs. The resulting PPEGMA1100-PAA DN hydrogels ware then washed extensively with deionised water for one week to remove the unreacted components.

PPEGMA-PAA-PEDOT (PSS) hydrogels

To form the PEDOT-PSS within the PPEGMA1100-PAA DN hydrogel structure, the starting DN hydrogels were required to uptake sufficient EDOT monomer and PSS into their structure in a swelling process. Thus, the PPEGMA1100-PAA hydrogels were transferred to a buffer solution with pH 7 and ionic strength of 0.5 M for 3 days or until the hydrogels reached their equilibrium swelling ratio at this pH. After this period, the samples were removed and washed thoroughly with deionised water for another 3 days to remove the excess ions. During this final washing process the swelling ratio of samples did not change. The fully swollen samples were soaked in EDOT-PSS solution for one week as the solution was being stirred continuously. To prepare the EDOT-PSS solution, 10 g of NaPSS was dissolved in 100 mL water followed by addition of 6.5 g of EDOT monomer. The mixture was then vigorously stirred using a homogenizer (IKA T25D, Germany) for 20 min at 12000 rpm until a uniform mixture was obtained. The polymerisation of PEDOT was initiated by adding 13 g of APS to the above EDOT-PSS solution. In similar experiments KPS or Fe^{3+} were used to initiate the polymerization. In the case of KPS, the reaction started as soon as KPS was added to the mixture. This fast initiation is not desirable since the best result achieves when the polymerization starts simultaneously from within the hydrogel and the surrounding mixture. In the case of Fe^{3+}, the cationic Fe^{3+} acts as an ionic crosslinking agent and the PPEGMA-PAA DN hydrogel shrinks inside the EDOT/PSS solution before the reaction starts. As a result of this deswelling, EDOT and PSS will expel from the hydrogel and the resulting hydrogel is not conductive and becomes very brittle. Since the achieved results from KPS and Fe^{3+} were not satisfactory, APS was used to conduct the polymerization process. The

mixture was left at ambient temperature and stirring was continued for another 3 days. Since the PPEGMA-PAA hydrogels are mechanically strong this stirring process does not damage the hydrogel in general. However, minor mass loss was observed during this process without any visual damage to the hydrogel samples. This minor mass loss would cause further uncertainty in measuring the total mass of PEDOT added to the hydrogels after the polymerization. Consequently, the exact amount of PEDOT present in the samples was not obtained. At this stage, the mixture gradually turned dark and eventually the whole system turned to a gel with PEDOT-PSS forming (Scheme 5.2) both outside and inside the PPEGMA-PAA gel via radical polymerization as describe in the literature previously [3]. The PPEGMA1100-PAA-PEDOT(PSS) hydrogels were mechanically separated from the fragile surrounding PEDOT-PSS gel and washed extensively with deionised water. To increase the amount of PEDOT in the hydrogels, the PEDOT polymerisation process was repeated by immersing the fully swollen PPEGMA1100-PAA-PEDOT(PSS) hydrogels in a fresh EDOT-PSS solution, following all the aforementioned steps. This process was repeated several times to control the loading of PEDOT-PSS. To indicate the number of PEDOT polymerisation in this study, the PPEGMA1100-PAA-PEDOT(PSS) hydrogels are referred to as DN-PEDOT(PSS)-*X*, where *X* (I, II, etc.) is the number of PEDOT polymerisation steps used. For example, DN-PEDOT(PSS)-II is designated to a hydrogel which was obtained after polymerising EDOT-PSS within the DN-PEDOT(PSS)-I hydrogels and “DN” refers to the originally prepared PPEGMA-PAA double network hydrogel.

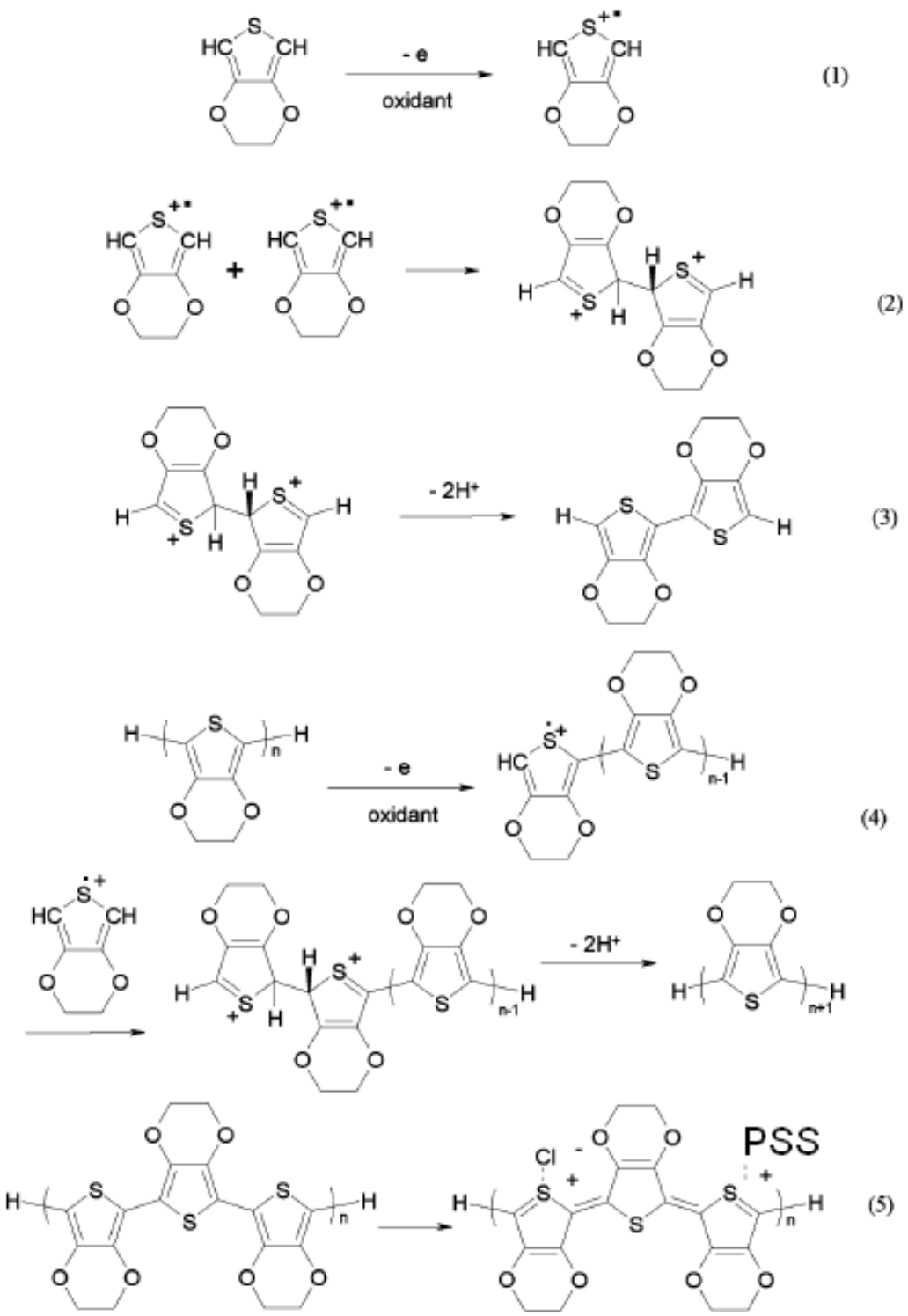

Scheme 5.2. Chemical polymerization of EDOT in the presence of PSS.

5.2.3. Swelling Ratio

Swelling ratio of various hydrogels was measured by weighing the hydrogels in their fully swollen state and after drying. Various samples were placed in pH buffer solutions at different pHs and constant ionic strength (0.5 M) for one week to reach the equilibrium. After one week, hydrogels were removed and weighed carefully. These hydrogels then dried at 75 ^{o}C for 3 days and weighed again. The mass ratio of fully swollen hydrogels to dried hydrogels was considered as the swelling ratio (Q) of hydrogels.

5.2.4. Mechanical Testing

The tensile and compression mechanical properties of hydrogels were measured using a Shimadzu mechanical tester (EZ-S, Japan). To investigate the effect of pH on the mechanical properties of hydrogels, samples were soaked in the buffer solutions at various pHs (I = 0.5 M) for one week, then cut from sheets into strip shapes for tensile testing (5 mm × 30 mm). The same procedure was carried out on cylindrical rod samples (height ~ 10 mm) for compression testing. The thickness of samples in tensile test and the diameter of samples in compression test varied as the pH changed, depending on the swelling ratio of samples. Sand paper was used in both tensile and compression tests to prevent any slippage, and the strain rate was set at 10 %/min for all samples. All the measurements were completed in air and the weight of samples was monitored before and after the test to investigate any possible water loss during testing.

The weight loss measured for each test revealed that the water loss was negligible during the course of the test.

5.2.5. Conductivity

The four point probe technique was used to measure the conductivity of hydrogel samples with a linear probe head (JANDEL, UK). The bulk resistance of samples was calculated from the applied current and voltage with at least five separate measurements made for each sample. To measure the conductivity of the inner core of the hydrogels, rod samples were cut transversely into two pieces and the inner cross section of the cut samples was used for measurements (Scheme 5.3). Before each measurement, the surface water on the samples was carefully tapped dry.

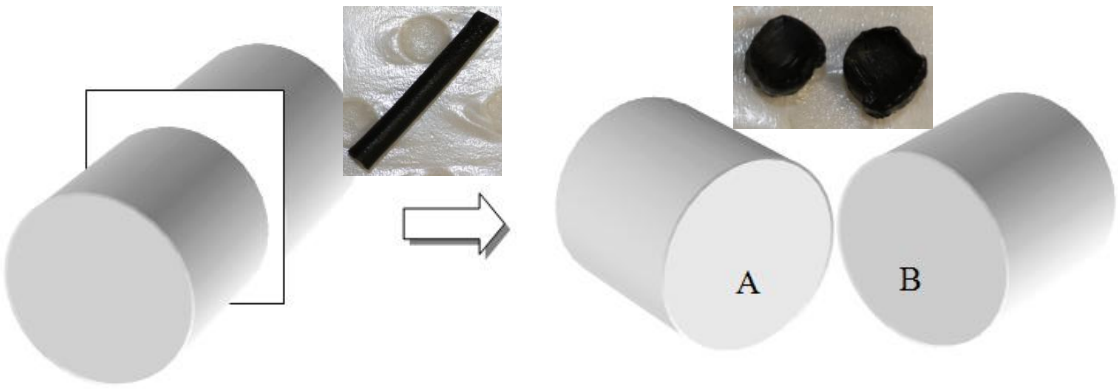

Scheme 5.3. Schematic illustration of a conducting hydrogel cut into two pieces (A and B). Electrical conductivity tests were performed on the cross sections A and B.

5.3. Results

5.3.1. Hydrogel Formation

The as-prepared PPEGMA1100-PAA hydrogels had a swelling ratio of ~ 1.5 and were opaque due to the hydrogen-bonding between carboxylic groups of PAA and ethylene glycol units of PPEGMA1100 [4]. The confirmation of tough double network formation based on PPEGMA1100 and PAA networks is presented elsewhere (previous chapter). Typical compression behaviour of DN hydrogel structures was observed for PPEGMA1100-PAA DN hydrogels with enhancements more than 15 and 270 times in compression strength compared to PAA and PPEGMA1100 SN hydrogels, respectively. Moreover, it was shown that the PPEGMA1100-PAA DN hydrogels are also pH sensitive, with their swelling behaviour and hydrophobicity changing extensively with pH. The hydrogen bonding between ethylene glycol units of PPEGMA1100 side chains and carboxylic acid groups in PAA were considered to be responsible for this pH sensitivity. As the pH increases the hydrogen bonding between PPEGMA1100 and PAA side groups dissociate and subsequently the PPEGMA1100-PAA DN hydrogels swelling ratio and hydrophilicity increase significantly. However, the as-prepared PPEGMA1100-PAA hydrogels were in their less-swollen state due to the acidic pH of the polymerisation reaction. As a result, even after immersing the as-prepared DN hydrogels in EDOT-PSS solution for one week, hydrogels were not able to absorb enough EDOT-PSS and the resulting polymerisation yielded PEDOT only at the surface of the hydrogels. To allow more EDOT monomer to diffuse into the PPEGMA1100-PAA DN structure, DN hydrogels soaked in pH 7 buffer solution were used instead of the as-prepared PPEGMA1100-PAA DN hydrogels. The fully swollen PPEGMA1100-

PAA hydrogel at pH 7 was transparent with a swelling ratio of ~ 9. This swelling ratio was 8 times as high as the as-prepared PPEGMA1100-PAA hydrogels with a much more hydrophilic nature. After the PEDOT polymerisation, visual inspection showed that the PEDOT was formed evenly through the hydrogel with no apparent difference observed at the cross section of DN-PEDOT(PSS) hydrogels.

5.3.2. pH Sensitivity

As a pH sensitive hydrogel, the swelling ratio of PPEGMA1100-PAA DN hydrogel varies considerably with pH (previous chapter). Thus, a similar pH sensitivity for PEDOT incorporated DN hydrogels was expected. The change in swelling ratio of the starting PPEGMA1100-PAA DN hydrogel, DN-PEDOT(PSS)-I and DN-PEDOT(PSS)-II hydrogels is plotted in Figure 5.1 as pH ranges from 2.2 to 6 at a constant ionic strength (0.5 M).

Clearly, both DN-PEDOT(PSS)-I and DN-PEDOT(PSS)-II hydrogels are pH-sensitive. The swelling ratio of all three systems (i.e. PPEGMA1100-PAA DN, DN-PEDOT(PSS)-I and DN-PEDOT(PSS)-II) changed dramatically within the pH range of the PAA pK_a value. All three hydrogels showed a transition point at around pH ~ 4. At pHs below ~ 4 all three systems remained in their collapsed state, although the DN-PEDOT(PSS)-I hydrogel had considerably lower swelling than either of the other two systems. This reduced swelling could be the result of additional crosslinking which was introduced into the hydrogel by adding APS to the EDOT-PSS solution during the polymerisation of PEDOT. Since APS is a radical generator it is likely that not only

EDOT was polymerised but also some radicals were formed on the PPEGMA1100 and PAA networks and additional crosslinking resulted.

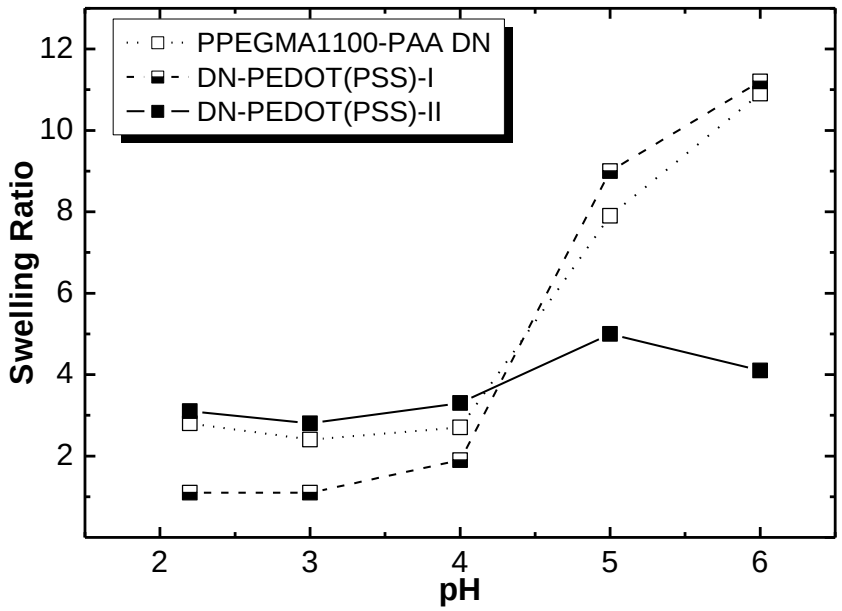

Figure 5.1. Swelling ratio of PPEGMA1100-PAA DN, DN-PEDOT(PSS)-I and DN-PEDOT(PSS)-II hydrogels as a function of pH buffer solution (I = 0.5 M). Error bars are smaller than the size of symbols.

However, in DN-PEDOT(PSS)-II case, considerably more PEDOT was present in the system and the swelling of hydrogels is closer to that reported previously for a PEDOT-PSS hydrogel (Q ~ 5) [5]. For pHs above ~ 4, the measured swelling ratio of the PPEGMA1100-PAA DN and DN-PEDOT(PSS)-I hydrogels increased with increasing pH. The swelling behaviour of the DN-PEDOT(PSS)-I hydrogel was quite similar to the starting DN hydrogel with swelling ratio increasing more than 10 times after the pH

transition point. The increase in the swelling ratio for the DN-PEDOT(PSS)-II hydrogel was not as significant as DN-PEDOT(PSS)-I, showing only a slight increase with pH around the transition point. Both PPEGMA1100-PAA DN and DN-PEDOT(PSS)-I hydrogels reached a maximum swelling ratio of around 11 at pH 6, while the maximum swelling ratio of the DN-PEDOT(PSS)-II hydrogel was only ~ 5 at this pH, which is close to reported values for PEDOT-PSS gels [5]. These results suggest that although the DN-PEDOT(PSS) hydrogels remain pH-sensitive, their overall response to pH has decreased as more PEDOT was introduced to the system. Not shown in Figure 5.1 are the swelling ratios of PPEGMA1100 and PAA SN hydrogels. The PPEGMA1100 SN hydrogel is not pH sensitive with swelling ratio around 10 over the pH range studied here. The PAA SN hydrogel is, on the other hand, is pH sensitive, with its swelling ratio jumps from 5 at pH 2.2 to 23 at pH 6.

5.3.3. Mechanical Properties

To investigate the effect of PEDOT formation on the mechanical behaviour of hydrogels, compression and tensile tests were performed on the various gel systems. Figure 5.2 compares the compression stress-strain curves of the DN-PEDOT(PSS)-II hydrogel with the PPEGMA1100-PAA DN, PPEGMA100 SN and PAA SN hydrogels at pH 3. Although the maximum compression strain did not show any considerable difference between these networks (~ 75 – 80 %), the compression strength of DN-PEDOT(PSS)-II and PPEGMA1100-PAA DN hydrogels exhibited enhancements of more than 250 and 15 times compared to PPEGMA1100 and PAA SN hydrogels,

respectively. The measured compression strength for DN-PEDOT(PSS)-II (11.6 MPa) was also higher than that of the starting DN hydrogel (8.3 MPa), with a similar failure strain of ~ 80 %. From Figure 5.1 it can be seen that at pH 3 both hydrogels possess comparable swelling ratios (3.1 and 2.8 for DN-PEDOT(PSS)-II and PPEGMA1100-PAA DN hydrogels respectively). Thus, the higher compression strength of DN-PEDOT(PSS)-II is not because of a lower swelling ratio, and most likely the presence of PEDOT and PSS chains had a positive impact on the mechanical properties of gels to cause additional strengthening.

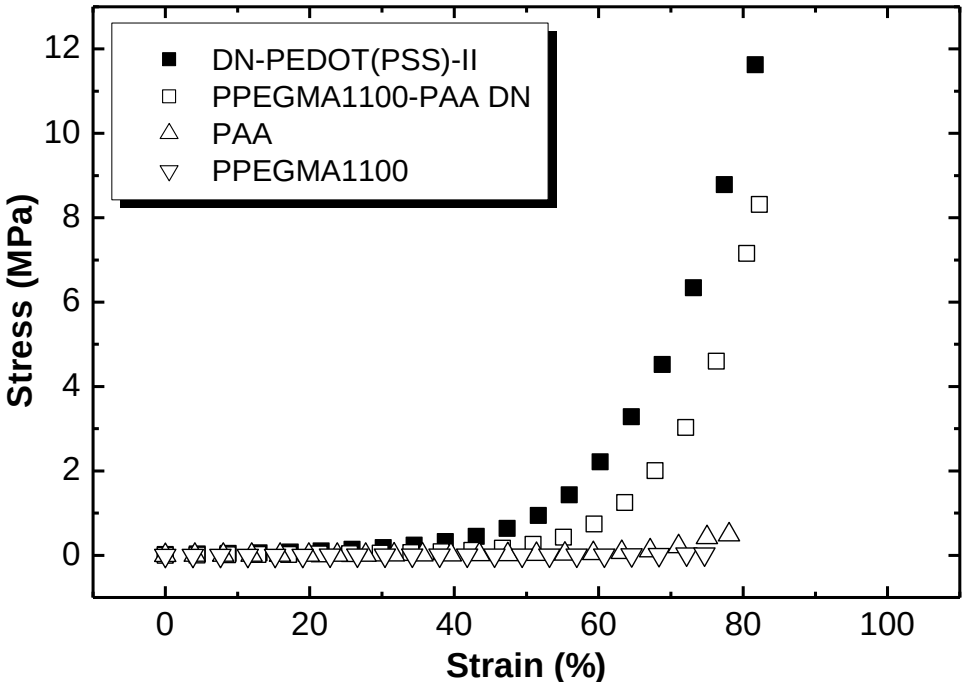

Figure 5.2. Compression stress-strain curves of fully swollen DN-PEDOT(PSS)-II, PPEGMA1100-PAA DN, PAA and PPEGMA1100 hydrogels at pH 3**.**

The effect of pH on the compression mechanical behaviour of DN-PEDOT(PSS)-II hydrogels was also studied by measuring the mechanical properties of the fully swollen hydrogels at various pHs. Figure 5.3 plots the compression stress-strain curves of DN-PEDOT(PSS)-II hydrogels at various pHs with a constant ionic strength (0.5 M). Clearly, all hydrogels over the range of pH studied here had significantly improved compression strength than the individual SN constituents (i.e. PPEGMA1100 and PAA), with their compression strengths remained always above the starting DN at the same pH. As pH increased from 3 to 6, the compression strength of DN-PEDOT(PSS)-II decreased with a significant drop around the transition point. The results showed that after a slight decrease in strength from pH 3 to pH 4 (11.6 MPa to 10.3 MPa), at pH 5 the strength dropped to 4.2 MPa followed by 1.8 MPa at pH 6. However, even at this pH, the fracture strength of DN-PEDOT(PSS)-II in its more swollen state was almost two times higher than that of PAA in its collapsed state at pH 2.2.

Tensile properties of the DN-PEDOT(PSS)-II hydrogels were also measured at different pHs. Shown in Figure 5.4 are typical tensile stress-strain curves of the PPEGMA1100-PAA DN and DN-PEDOT(PSS)-II hydrogels compared with the PAA SN hydrogel at pH 3. Noted here, the tensile properties of the PPEGMA1100 SN hydrogel was not measured because of the technical difficulties in mounting these very fragile samples. Again, considerable enhancement can be seen in strength of fully swollen PPEGMA1100-PAA DN and DN-PEDOT(PSS)-II hydrogels compared to the PAA SN hydrogel, with the DN-PEDOT(PSS)-II having even higher tensile strength than the starting PPEGMA1100-PAA DN hydrogel.

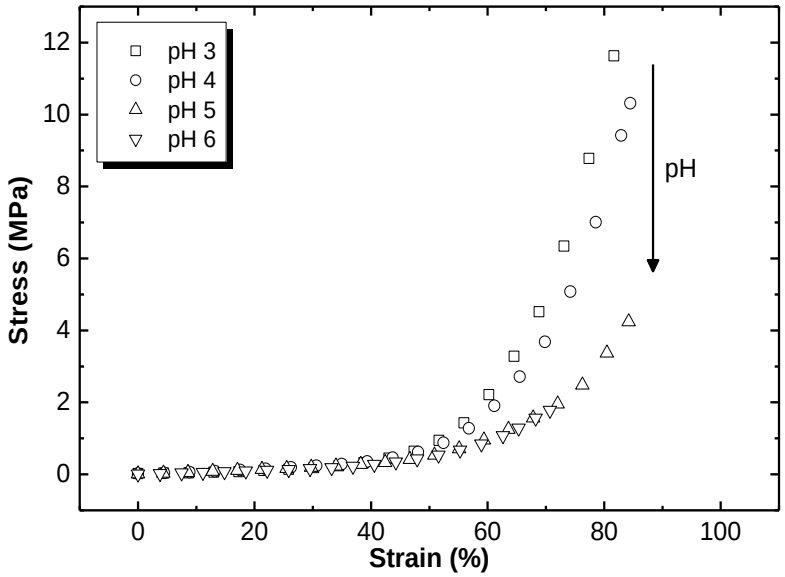

Figure 5.3. Compression stress-strain curves of fully swollen DN-PEDOT(PSS)-II hydrogels at various pH (I = 0.5 M).

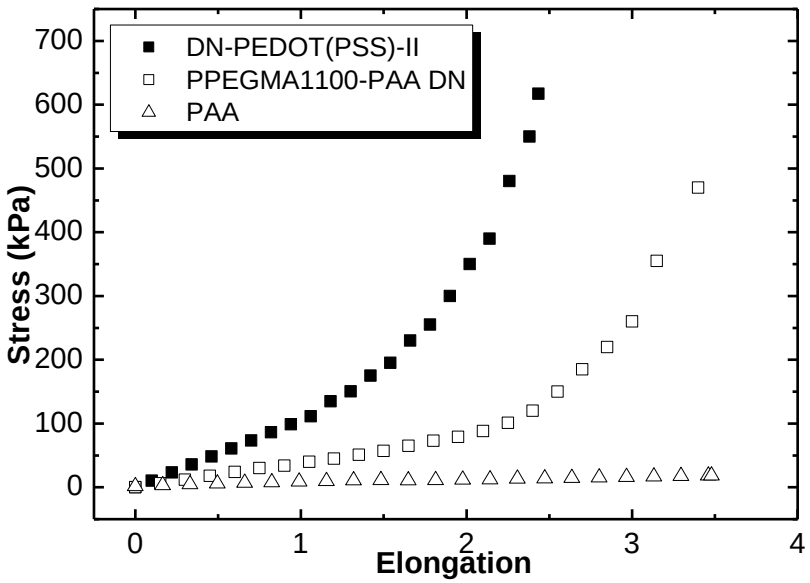

Figure 5.4. Tensile stress of fully swollen DN-PEDOT(PSS)-II, PPEGMA1100-PAA DN and PAA hydrogels (pH 3, I = 0.5 M) as a function of elongation.

To compare the tensile properties of the PPEGMA1100-PAA DN and DN-PEDOT(PSS)-II hydrogels as pH changes, Figure 5.5 illustrates the elongation at break, Young's modulus and tensile strength of PPEGMA1100-PAA DN and DN-PEDOT(PSS)-II hydrogels as a function of pH.

A similar trend to that shown by the compression properties is observed here as pH increases from 3 to 6. The tensile fracture strength of the DN-PEDOT(PSS)-II hydrogels is slightly higher than PPEGMA-PAA DN at low pHs, then drops to similar values at pHs above the pH transition. In particular, the PPEGMA1100-PAA DN hydrogels had a strength of about 500 kPa at low pHs and less than 100 kPa at higher pHs. The strength was slightly higher for DN-PEDOT(PSS)-II hydrogels reaching to more than 600 kPa at low pHs, then dropped to 60 kPa at pHs higher than 4. However, in terms of elongation at break, the PPEGMA1100-PAA DN hydrogels always showed higher elongation than DN-PEDOT(PSS)-II hydrogels, while both systems were pH sensitive with elongation decreasing as pH exceeds the transition point. Interestingly, the Young's modulus of the DN-PEDOT(PSS)-II hydrogels was almost 2 – 3 times higher than that of the starting PPEGMA1100-PAA DN hydrogels at all pHs. The Young's modulus of the PPEGMA1100-PAA DN hydrogels was around 40 kPa at low pHs then decreased to 30 kPa as pH increased. The DN-PEDOT(PSS)-II hydrogels, on the other hand, had a modulus as high as 110 kPa at low pHs and ~ 80 kPa at higher pHs.

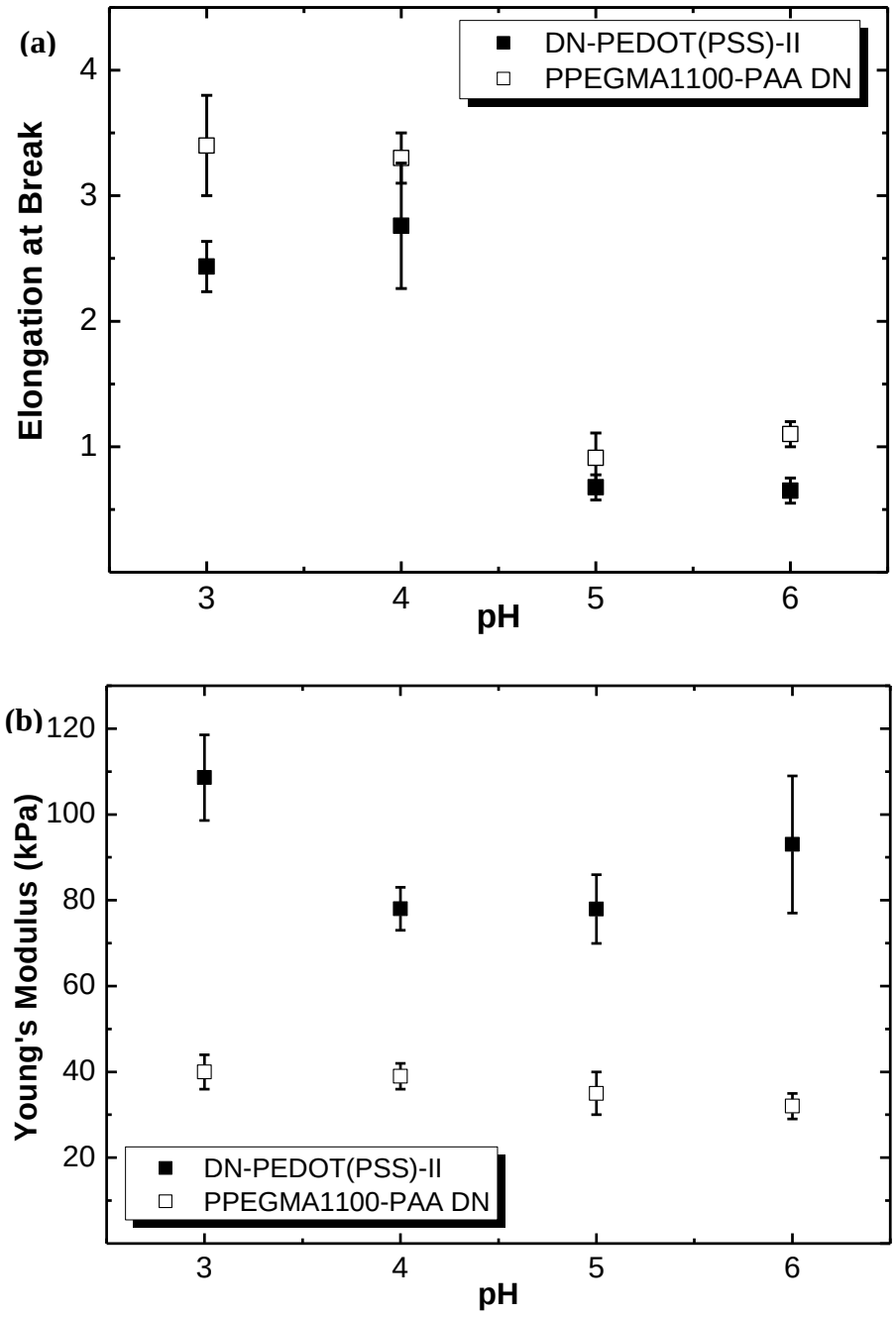

Figure 5.5. Tensile mechanical properties of fully swollen DN-PEDOT(PSS)-II and PPEGMA1100-PAA DN hydrogels as a function of pH (I = 0.5 M): a) elongation at break, b) Young's modulus, c) tensile strength (next page).

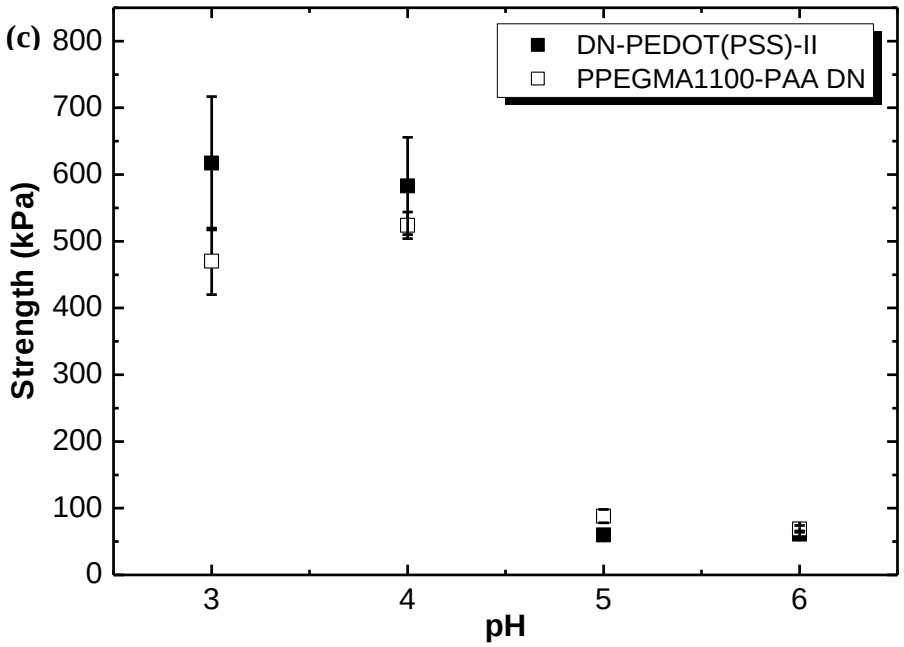

Figure 5.5. ***continued***

5.3.4. Electrical Conductivity

The main purpose of incorporating a conducting polymer such as PEDOT into the structure of tough PPEGMA1100-PAA DN hydrogels was to enhance the electrical properties of the system. The bulk DC electrical conductivity of DN-PEDOT(PSS)-I samples was measured using a four point probe technique. Figure 5.6 illustrates conductivity and swelling ratio of DN-PEDOT(PSS)-I hydrogels as pH changes from acidic to neutral (pH 2.2 – 6). Clearly, the conductivity decreases with increasing pH and subsequently the swelling ratio. As the swelling ratio rises from Q ~ 1 at pH 2.2 to Q ~ 11.2 at pH 6, the conductivity drops almost one order of magnitude from 3.7×10^{-3} S/cm at pH 2.2 to 2.8×10^{-4} S/cm at pH 6.

It was expected that the conductivity could significantly improve by repeat polymerisations of PEDOT within the DN gels to make DN-PEDOT(PSS)-II and DN-PEDOT(PSS)-III hydrogels. After the second polymerisation of PEDOT, the electrical conductivity was enhanced 3 orders of magnitude, increasing from 3.7×10^{-3} S/cm for DN-PEDOT(PSS)-I to 3.4 S/cm for DN-PEDOT(PSS)-II at pH 2.2. At this pH, DN-PEDOT(PSS)-III had a conductivity of 4.3 S/cm. The effect of pH on the conductivity of DN-PEDOT(PSS)-I and DN-PEDOT(PSS)-II hydrogels is shown in Figure 5.7. Both systems show a decrease in conductivity corresponding to the pH induced swelling transition. However, at all pHs the DN-PEDOT(PSS)-II hydrogel had a conductivity at least 3 orders of magnitude larger than the DN-PEDOT(PSS)-I hydrogels.

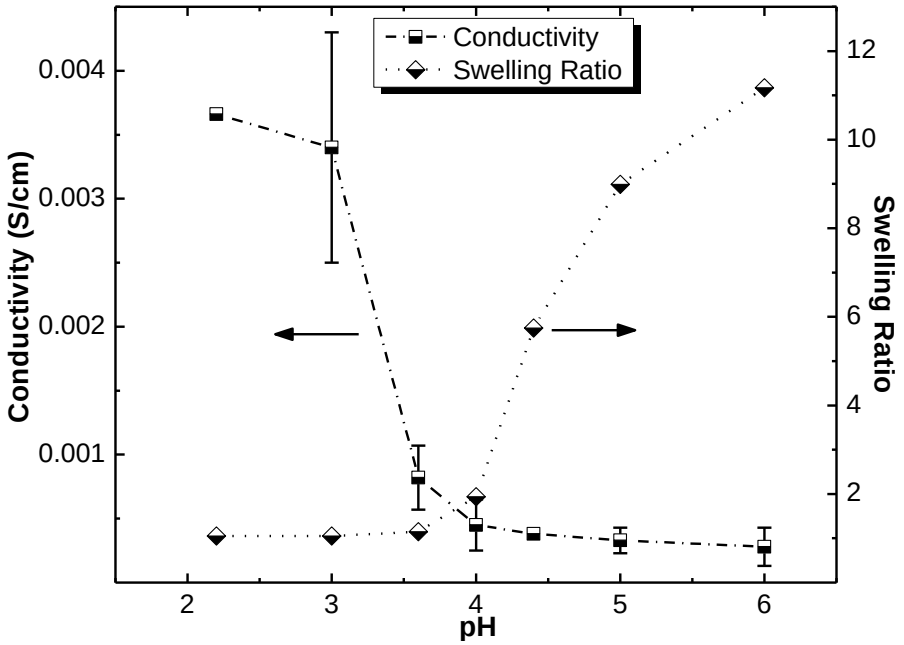

Figure 5.6. Conductivity/swelling ratio of fully swollen DN-PEDOT(PSS)-I vs. pH (*I* = 0.5 M).

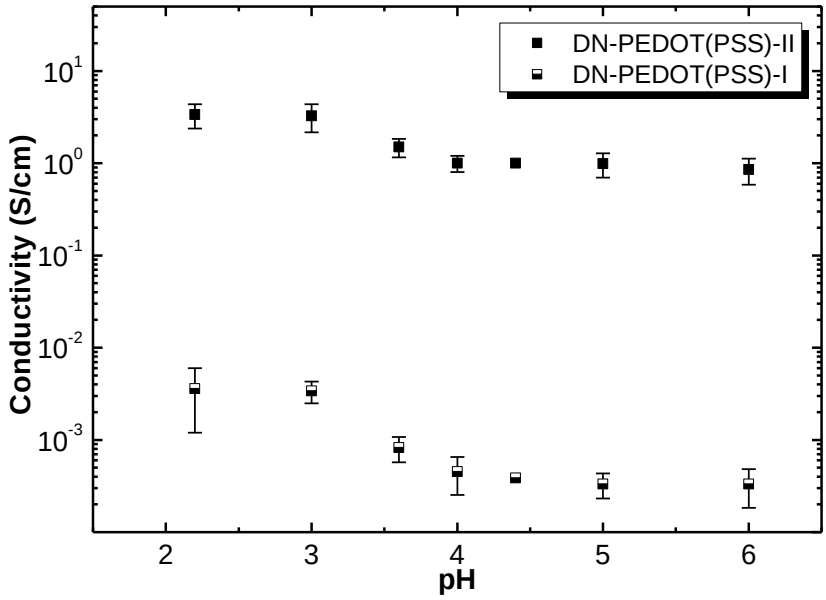

Figure 5.7. Conductivity of fully swollen DN-PEDOT(PSS)-II and DN-PEDOT(PSS)-I vs. pH (I = 0.5 M).

5.4. Discussions

The compression and tensile properties of PEDOT incorporated hydrogels obtained in this study are comparable with other typical DN hydrogels. Also, a slight improvement was observed in the mechanical properties of DN-PEDOT(PSS) hydrogels compared to the starting PPEGMA1100-PAA DN hydrogels. In terms of compression strength, these DN-PEDOT(PSS) hydrogels exhibited high strengths (11 MPa at acidic pHs) which put them amongst the strongest hydrogels obtained by employing DN method (17 MPa for PAMPS-PAA) [6]. At the same time, DN-PEDOT(PSS) hydrogels showed high electrical conductivity by controlling the amount of PEDOT within the network via chemical polymerisation. To compare the electrical conductivity and mechanical

performance of DN-PEDOT(PSS) hydrogels obtained in this study with various systems available in the literature, Figure 5.8 plots the conductivity of fully swollen hydrogels [5, 7-10] as a function of their compression strength in their fully swollen state. The data has been extracted from the literature where both mechanical properties and electrical conductivity was available. As can be seen from Figure 5.8, both compression strength and electrical conductivity of the DN-PEDOT(PSS)-II hydrogels is significantly higher than other conducting hydrogels.

Several hydrogel systems have been described as electrically conducting, but with no information regarding their mechanical properties. The results we obtained here for conductivity (3.4 and 4.3 S/cm for DN-PEDOT(PSS)-II and DN-PEDOT(PSS)-III at acidic pH) is slightly lower than that of PEDOT-PSS films (~ 7 ± 2 S/cm), and similar to dehydrated PEDOT-PSS gels prepared via ionic crosslinking [11]. As for DN-PEDOT(PSS)-I, the measured electrical conductivity (3.7×10^{-3} S/cm at pH 2.2 to 2.8×10^{-4} S/cm at pH 6) is comparable with most previously described IPN hydrogel / conjugated polymer systems.

In the present study, it was observed that the conductivity dramatically increased from ~ 10^{-4} – 10^{-3} S/cm for DN-PEDOT(PSS)-I hydrogels to ~ 3.4 S/cm for DN-PEDOT(PSS)-II and then to 4.3 S/cm for DN-PEDOT(PSS)-III hydrogels. It seems, therefore, that after the second PEDOT polymerisation in the already-formed DN-PEDOT(PSS)-I hydrogels, the amount of PEDOT has reached a critical threshold to cause a significant and saturated enhancement in conductivity. Moreover, the conductivity of DN-PEDOT(PSS) hydrogels showed a clear drop as the pH changed from acidic to neutral pH corresponding to a increase in swelling. Figure 5.9 plots the

conductivity of DN-PEDTO(PSS)-I and DN-PEDOT(PSS)-II hydrogels as a function of Q to understand whether the change in conductivity is a dilution effect of swelling or the results of a structural change in the system.

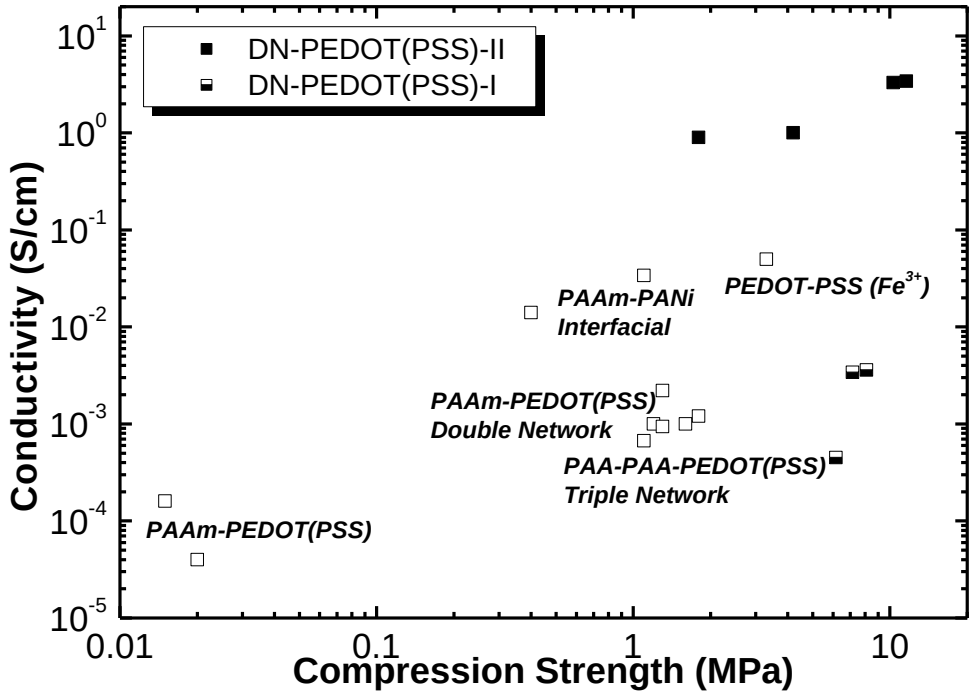

Figure 5.8. Conductivity of (open square) various conductive hydrogel systems vs. their compression strength in fully swollen state compared with (bottom-filled square) DN-PEDOT(PSS)-I and (filled square) DN-PEDOT(PSS)-II hydrogels developed in this study. The range of values reported for these systems relates to the effect of pH on mechanical strength and conductivity.

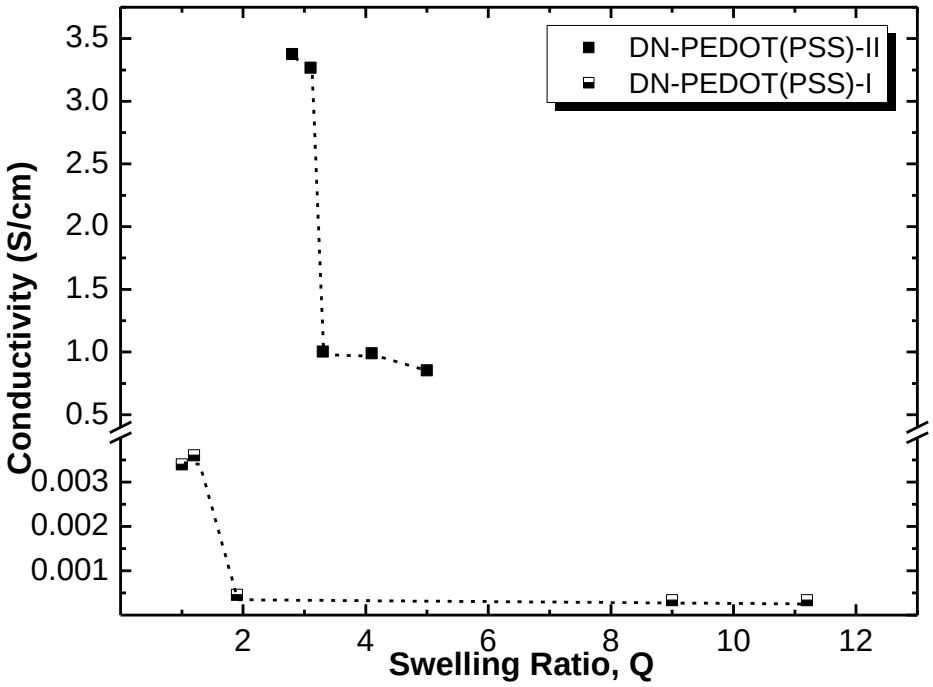

Figure 5.9. Conductivity of DN-PEDOT(PSS)-I and DN-PEDOT(PSS)-II hydrogels as a function of Q. The change is swelling ratio is corresponded to the pH change.

A threshold of Q_c ~ 1.9 and ~ 3.3 was observed for DN-PEDOT(PSS)-I and DN-PEDOT(PSS)-II, respectively, where the conductivity dramatically drops from a higher plateau to lower values. The behaviour suggests that the swelling disrupts the percolation network of conductive pathways within the gel. Since the actual amount of PEDOT within these two hydrogels is not known, the direct comparison between the threshold values is not valid. However, it is obvious that the conductivity suddenly drops after a reaching to a certain threshold as swelling ratio changes, and this threshold depends on the number of times PEDOT had been polymerised within the hydrogel.

5.5. Conclusions

The conductivity of PPEGMA1100-PAA DN hydrogels was significantly enhanced by polymerising EDOT within an already formed tough PPEGMA1100-PAA hydrogel. The DN hydrogels without PEDOT respond to pH changes in a similar way as the PAA component. By incorporating PEDOT into the structure of the hydrogels, the hydrogels remain pH sensitive, with mechanical properties and electrical conductivity changing considerably with pH. The change in pH also caused changes in swelling ratio, and this swelling transition corresponds to the transformation between highly conductive hydrogels (pH < 4) to less conductive hydrogels (pH > 4). Also, a dramatic decrease in tensile and compression strength occurred when pH exceeded the transition point (pH ~ 4).

5.6. References

1. Abidian MR and Martin DC. Advanced Functional Materials 2009;19(4):573-585
2. Lee SH, Lee CK, Shin SR, Gu BK, Kim SI, Kang TM, and Kim SJ. Sensors and Actuators B: Chemical 2010;145(1):89-92.
3. Jonas F and Schrader L. Synthetic Metals 1997;41-43:831-836.
4. Lu X and Weiss RA. Macromolecules 1995;28(9):3022-3029.
5. Dai T, Shi Z, Shen C, Wang J, and Lu Y. Synthetic Metals 2010;160(9-10):1101-1106.
6. Gong JP, Katsuyama Y, Kurokawa T, and Osada Y. Advanced Materials 2003;15(14):1155-1158.
7. Dai T, Qing X, Zhou H, Shen C, Wang J, and Lu Y. Synthetic Metals 2010;160(7-8):791-796.
8. Dai T, Qing X, Lu Y, and Xia Y. Polymer 2009;50(22):5236-5241.

9. Aouada FA, Guilherme MR, Campese GM, Girotto EM, Rubira AF, and Muniz EC. Polymer Testing 2006;25(2):158-165.

10. Dai T, Qing X, Wang J, Shen C, and Lu Y. Composites Science and Technology 2010;70(3):498-503.

11. Dai T, Jiang X, Hua S, Wang X, and Lu Y. Chemical Communications 2008(36):4279-4281.

CHAPTER SIX

CNT Containing DN Hydrogels

6. CNT Containing DN Hydrogels

6.1. Introduction

Previous studies have successfully demonstrated the fabrication of conductive hydrogels with enhanced mechanical performances by incorporating a conducting polymer (CP) within the structure of a DN hydrogel to make a triple network [1] or using the CP as one of the networks in the DN structure [2]. In the previous chapter (Chapter 4), the fabrication of a pH sensitive DN hydrogel based on poly(ethylene glycol) methyl ether methacrylate (PEGMA) oligomers and acrylic acid (AA) as the first network and second network building blocks, respectively, was reported. It was also shown that with incorporation of a CP (poly(3,4-ethylenedioxythiophene) (PEDOT)) into the already formed PPEGMA-PAA DN hydrogel, the conductivity increased several orders of magnitude (Chapter 5). Also, in Chapter 2, the modulated drug release from CNT loaded chitosan (CS) hydrogels was modulated by tuning the polarity and strength of the voltage applied to the CS-CNT hydrogel films. Here, to combine the high mechanical properties of DN hydrogels with conductivity and possible controlled release

performance of a CNT-incorporated hydrogel system, single walled carbon nanotubes (SWNTs) are added to the DN hydrogel structure.

6.2. Experimental Section

6.2.1. Materials

Acrylic acid (AA), acrylamide (AAm), poly(ethylene glycol) methyl ether methacrylate (PEGMA) (Mw 1,100 g/mol) were used as monomers and purchased from Sigma-Aldrich. Potassium persulfate (KPS) and *N,N'*-methylene MBAAacrylamide (MBAA) were used as initiator and crosslinking agent, respectively (Sigma-Aldrich). Single walled carbon nanotubes (SWNT) were obtained from Carbon Nanotechnologies Inc. (Houston, USA) and used as received. Sodium lauryl sulfate (SDS), 4-dodecylbenzenesulfonic acid (SDBS), and Triton X100Buffers were used as surfactants and purchased from Sigma-Aldrich. Buffers (McIlvaine phosphate-citrate) with various pHs and constant ionic strength (0.5 M) were prepared using citric acid (Sigma-Alrich), sodium phosphate and potassium chloride (Ajax Finechem, Australia).

6.2.2. Preparation

CNT-incorporated first network

Various single network (SN) hydrogels with CNT incorporated were prepared by mixing the monomers with a stable dispersion of SWNTs in water. To disperse the SWNTs in water different surfactants including SDS, SDBS and Triton X100 were used

to investigate any possible effect of surfactant on the final hydrogel system. In general, the SWNT dispersion was prepared by adding the surfactant to deionised water (10 mg/mL) followed by stirring. This amount was much higher than the critical micelle concentrations (cmc) of each of the surfactants. Then, different amount of SWNTs (1 – 4 mg/mL) was added to the solution and mixture was ultrasonicated (Sonics) for 90 mins (1 min on/1 min off) to disperse the SWNTs in the presence of surfactants. The SWNT dispersions made using these three surfactants were stable for the range of SWNT concentration used. All SWNT dispersions were then centrifuged at 4,400 rpm for 90 mins to separate large CNT bundles from the dispersion. The absorption peak of CNT dispersions at 655 nm before and after centrifuge was compared to estimate the amount of CNTs remaining in dispersion after centrifugation. The resulting samples obtained after centrifuging the CNT dispersions with 1, 2, 3, and 4 mg/mL SWNT had a SWNT concentration of 0.95, 1.45, 2.6 and 3.45 mg/mL, respectively. The first network monomer solution (e.g. AA, AAm and PEGMA) was made by dissolving the monomer in deionised water (various concentration), followed by adding KPS (4 mol%, based on monomer) and MBAA (various concentration). Then, the first network monomer solution was added to the SWNT dispersion (1:1 v/v) and mixed thoroughly. After this stage, monomer-SWNT dispersions with lower SWNT content (0.5 and 1 mg/mL) remained stable for days, however those with higher amount of SWNT (1.5 and 2 mg/mL) were unstable with aggregation of CNTs occurring. As a result, CNT-incorporated SN samples were manufactured from monomer-SWNT dispersions with only 0.5 mg/mL SWNT in the final composition. The monomer-SWNT dispersions were then injected between two glass slides separated with silicon spacers (1 mm) to make sheets, or sucked in plastic syringes to make cylindrical samples. The polymerization

was performed at 65 ^{o}C for 7 hrs, followed by removing the CNT-incorporated SN hydrogels from their moulds. Samples were washed extensively and stored in deionised water for at least one week to remove all unreacted reagents. The water was changed on a daily bases.

CNT-incorporated interpenetrating networks

The second polymer network was formed from either PAAm or PAA and was polymerized within the CNT-incorporated SN hydrogels by soaking the aforementioned hydrogels in AAm or AA monomer solutions, followed by polymerization. The monomer solution was made of monomer (e.g. AAm or AA) (various concentration), KPS (0.1 mol%) and MBAA (various concentration) all dissolved in deionised water. Samples of CNT-SN were allowed to remain in the second network monomer solution for at least 3 days. Since a phase segregation was observed when the second network was introduced into the CNT-SN hydrogels according to normal double network procedure, two different techniques were employed to polymerize the second network monomers within the CNT-incorporated SN hydrogels as illustrated in Scheme 6.1. Briefly, in method A (Scheme 6.1), the fully swollen samples were removed from the second network monomer solution and carefully sealed by wrapping a polyethylene plastic film around it. Some samples were placed between two sheets of different materials to investigate the effect of surface energy on the possible surface phase segregation. These materials included poly(methyl methacrylates) (PMMA), high density polyethylene (HDPE), poly(tetrafluoroethylene) (PTFE), polystyrene (PS) and

glass. After being placed between the two sheets, samples were sealed in plastic containers as well. Also, some samples were submerged in hydrophobic silicon oil and then sealed to reduce any possible monomer loss during the polymerization. The polymerization was performed at 65 ^{o}C for 7 hrs. In method B (Scheme 6.1), the CNT-incorporated SN samples were left in a bath of the second monomer solution, and the polymerization was performed while the samples were still in the second network monomer solution. A similar procedure was used to polymerize both fully swollen CNT-incorporated hydrogels within the surrounding second network monomer. In both cases, samples were removed from the mould and washed thoroughly. For samples made from method B, the CNT-incorporated hydrogels were cut out from the surrounding second network SN hydrogels. Samples were stored in deionised water with water being changed on a regular basis.

6.2.3. Methods

An optical microscope (Leica, Germany) was used for visual observations, and scanning electron microscopy was used for further investigations. To measure the mechanical properties of hydrogels, compression tests were performed on the cylindrical hydrogels using a mechanical tester (Shimadzu EZ-S, Japan). Compression tests were carried out at 2 mm/min, on samples with 10 mm height.

Conductivity test was performed on hydrogel samples using a four point probe technique. However, no significant enhancement was observed in the conductivity,

suggesting that the amount of SWNT is far less than the critical threshold which is needed to improve the conductivity.

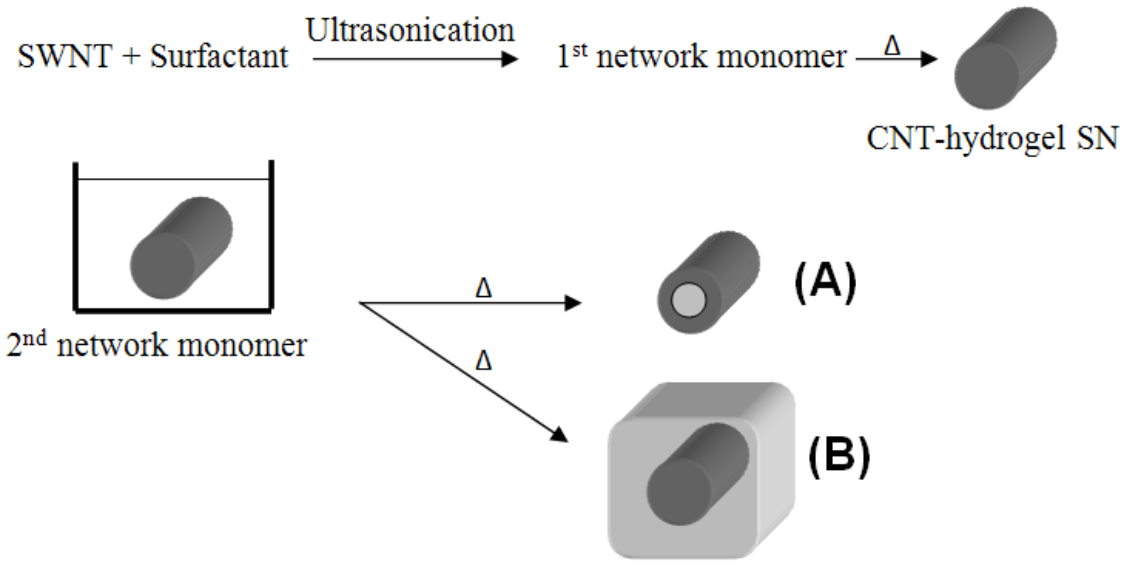

Scheme 6.1. Schematic illustration of preparing CNT-incorporated hydrogels. CNT-hydrogel SN is obtained by polymerizing CNT-monomer dispersion, followed by soaking it in the 2nd network monomer. (A) samples were polymerized outside the monomer solution (phase segregation occurred), (B) samples were polymerized within the 2nd network monomer (no phase segregation occurred).

6.3. Results

The final CNT-incorporated hydrogels manufactured here were based on different polymer networks including PPEGMA-PAA, PAAm-PAAm, PAAm-PAA and PAA-

PAA with various compositions in each network. The PPEGMA-PAA pair was chosen to consider the effect of hydrogen bonding as a strong interaction is known to occur between the two networks. The other two pairs (i.e. PAAm-PAAm and PAA-PAA) had no specific interaction between the networks. While PAA is a negatively charged polymer, PAAm has neutral polymer chains and as a result the effect of network charge could be described as well. As mentioned above two different techniques were used to form the second network within the PPEGMA-CNT, PAAm-CNT or PAA-CNT SN hydrogels. However, the method used to make these CNT-incorporated SN hydrogels was the same for all three hydrogels as mentioned before. The resulting first network hydrogels with CNT incorporated were all uniformly black in appearance as shown in Figure 6.1a for PAAm-CNT. By observing the cross section of hydrogels using the optical microscope while immersed in the second network monomer and before the polymerization no significant change was observed.

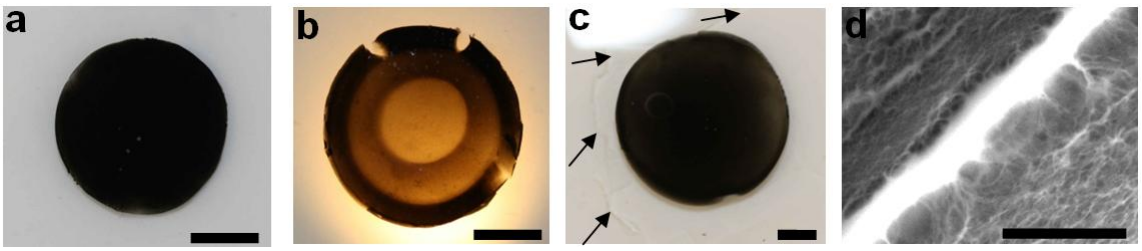

Figure 6.1. Cross sections of a) PAAm-CNT SN, b) PAAm-PAAm-CNT (method A), c) PAAm-PAAm-CNT (method B) with arrows indicating the remaining of PAAm 2nd network, d) SEM of the boundary between CNT-rich sheath and the inner layer of a phase segregated PAAm-PAAm-CNT hydrogel prepared via method A. The scale bars in a, b and c are 2 cm, and in d is 5 μm.

Surprisingly after the second polymerization process, visible phase segregation occurred for nearly all samples that were prepared via method A, with a CNT-rich phase forming in the outer wall of the hydrogel around the inner core (Figure 6.1b). In most cases the inner core was completely transparent indicating the absence of CNTs and a distinct boundary was often observed between the core and the outer CNT-rich sheath. In Figure 6.1b, there is an intermediate layer between the DN core and the CNT-rich sheath, which was not observed in all of the cases. Regardless of occurrence of this intermediate layer, the CNT-rich sheath was almost always formed around the inner core of samples prepared via method A. This phenomenon happened for different DN polymers, including PAA-PAA, PAAm-PAAm, PAA-PAAm and PPEGMA-PAA pairs, regardless of the type of surfactant used to disperse the SWNTs. Moreover, various materials ranging from hydrophilic to very hydrophobic was used as the mould and no meaningful effect was observed on the formation of the CNT-rich sheath. Furthermore, by changing the composition of each of the networks, e.g. crosslink density and monomer concentration, the size of the CNT-rich sheath varied but the phase segregation almost always happened during the second polymerization (method A). SEM micrographs showed a distinct boundary between the CNT-rich sheath and the core of samples with phase segregated (method A), as can be seen in Figure 6.1d. Phase segregation also occurred when other nanoparticles (such as gold nanoparticles) were used in place of the CNTs.

It was discovered that visible phase segregation could be prevented when method B was used for the second network formation, and the cross section of the CNT-incorporated interpenetrating network hydrogels was uniform (Figure 6.1c). The arrows

in Figure 6.1c indicate the edges of remaining *second* network SN hydrogel around the CNT-incorporated hydrogel. Again, no visible phase segregation was observed by using this technique when the composition of networks was changed. Closer examination of the DN gels made by method B, however, suggested that small-scale (< 100 μm) phase separation may still be occurring. Thin slices of the gel examined using an optical microscope showed small regions of CNT rich gel surrounded by gel of lower CNT content (Figure 6.2).

To investigate the formation of the CNT-rich sheath using method A, we performed a series of experiments in which the cross sections of CNT-incorporated PAA and PPEGMA hydrogels both fully swollen in AA (as their second network monomer) were optically monitored over the polymerization time. Figure 6.3 shows the photographs taken by an optical microscope from the cross sections of these hydrogels during the polymerization.

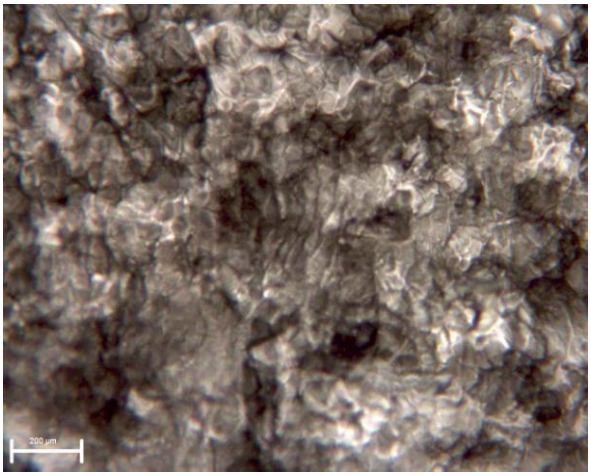

Figure 6.2. Optical micrograph of PAAm-PAAm-CNT gel produced by method B.

Lines in Figure 6.3 have been added to the photomicrographs to delineate the different phases. The solid line represents the gel-air surface and the dashed line is the phase boundary between the core and sheath. The CNT-rich sheath started to appear as the second polymerization progressed as was clearly seen within 15 minutes of the commencement of the second network polymerization (Figure 6.3a). With continued second network polymerization, the thickness of the outer sheath decreased and the colour contrast between the core and sheath increased (Figure 6.3a-f). The change in the thickness of CNT-rich sheath over the polymerization time (Figure 6.4) indicates that the sheath contracts as the polymerization progresses while the final sample (after polymerization stopped) is larger than the initial SN hydrogel. This means that the hydrogel has expanded during the polymerization and the sheath size has constantly decreased during the polymerization.

Figure 6.5 shows the change in the sheath to core size ratio l_s/l_c in phase segregated samples based on PAAm-PAAm hydrogels as a function of second network monomer (AAm) and crosslinking comonomer (MBAA) concentrations. By increasing the AAm monomer or MBAA concentration the l_s/l_c ratio continuously decreases. However, this decrease is more dramatic for AAm concentration compared to MBAA concentration. In the MBAA case, the l_s/l_c ratio drops slightly in the beginning, then levels off around 0.4, where both the sheath and core thicknesses (l_s and l_c respectively) remain almost constant. It is noted that phase segregation occurred at a MBAA concentration of zero showing that the segregation was not dependent on crosslinks forming in the second "network". For increasing AAm monomer concentration the l_s/l_c ratio drops considerably from 1 (where no DN core was formed) to ~ 0.1, with l_s

constantly decreasing. This indicates that the l_s/l_c ratio is much more sensitive to the second network monomer concentration than the crosslinking ratio of the second network. Surprisingly, the first network crosslinking or monomer concentration had no significant effect on the size of the CNT-rich sheath in phase segregated samples and the l_s/l_c remained around ~ 0.15±0.02 as the first network composition changed.

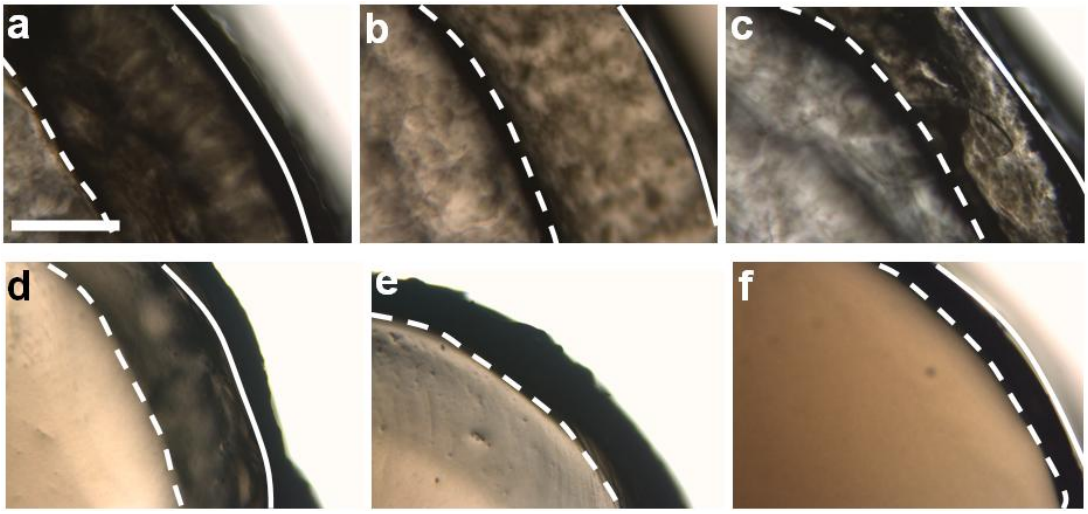

Figure 6.3. Optical microscopic pictures of a, b, c) PAA-CNT and d, e, f) PPEGMA-CNT SN hydrogels at various 2nd network (PAA) polymerization time: a) 15 min, b) 120 min, c) 240 min, d) 60 min, e) 120 min, f) 240 min. The scale bar is 500 μm for all pictures. Dashed lines separate the outer sheath from the inner core, solid lines indicate the edge of the hydrogel.

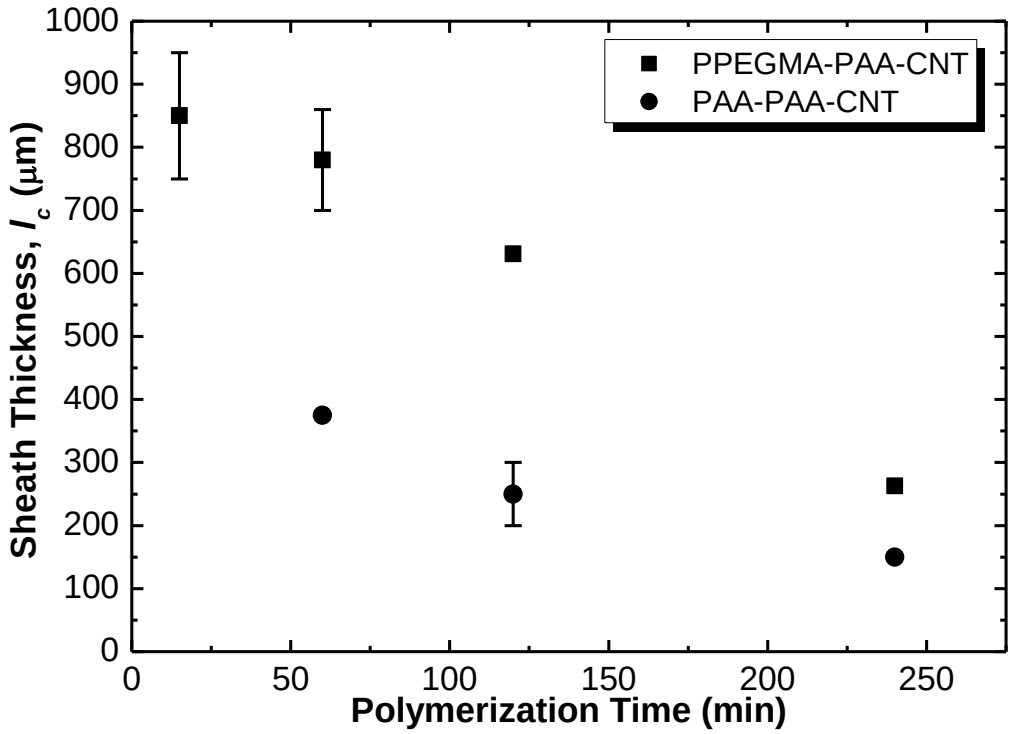

Figure 6.4. Sheath thickness l_c in phase segregated samples (method A) as a function of polymerization time.

Although the phase separation was clearly observed for different polymer networks, to ensure that the interaction between networks does not influence the phenomenon, PAAm-PAAm pair was chosen to perform further experiments. Unlike PAA, PAAm hydrogel is a neutral network and the interaction between two PAAm networks as the first and second network is assumed to be the same as between PAAm chains within a PAAm SN hydrogel.

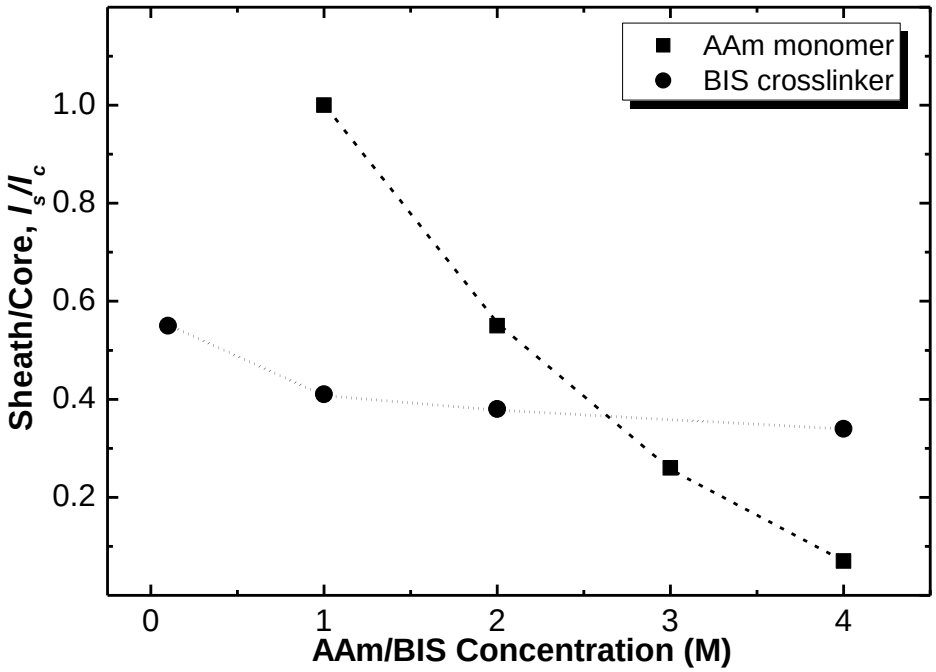

Figure 6.5. Sheath/core size ratio l_s/l_c of phase segregated samples (method A) as a function of 2nd network monomer (AAm) concentration and second network crosslinker (MBAA) concentration. Lines are to guide the eye.

A swelling study was performed on samples made from different second network monomer concentrations (AAm; 1 – 4 M). Swelling ratios of SN hydrogel [16] and DN hyrdogels (Chapter 4) with no added CNT tends to decrease with increasing monomer concentration. The decreased swelling was attributed to the reduction of defects in the network structure as a result of higher monomer concentration. Swelling ratios were measured for the PAAm-PAAm-CNT hydrogels obtained from method B and for the

CNT-rich sheath and the DN core of phase segregated hydrogels (method A). As shown in Figure 6.6 the swelling ratio of CNT-rich sheath remained almost constant at around 22, regardless of the second network monomer concentration and this swelling degree is similar to the starting PAAm-CNT SN hydrogel (19.8). In contrast, the DN core hydrogel showed a decrease in swelling with increasing AAm monomer concentration. For hydrogels made using method A and from 1 M AAm second network, the samples were visibly uniform and no core structure was observed in the middle of the hydrogels. For these samples the swelling ratio remained close to that of the PAAm-CNT single network hydrogel. Interestingly, the PAAm-PAAm-CNT hydrogels obtained from method B exhibited higher swelling ratio than the DN core and CNT-rich sheath of phase segregated samples. For these hydrogels the swelling first increased and then decreased with increasing AAm concentration. This behaviour is unusual and not understood at this stage, although it suggests changes to the crosslink density of the first network.

The swelling of the PPEGMA-PAA hydrogels prepared by method A were also measured. The core exhibited the same pH sensitivity as was observed for PPEGMA-PAA DN hydrogels in previous studies (Chapter 4) with a dramatic increase in swelling occurring above the pK_a of the PAA component (pH ~ 4). The core was optically transparent at pHs above the transition point, but were opaque (white) below this pH due to the hydrogen bonding interactions that occur between the PPEGMA and the protonated PAA and as reported previously. Interestingly, the swelling ratio of the CNT-rich sheath remained independent of pH, suggesting a low concentration of PAA in the outer sheath.

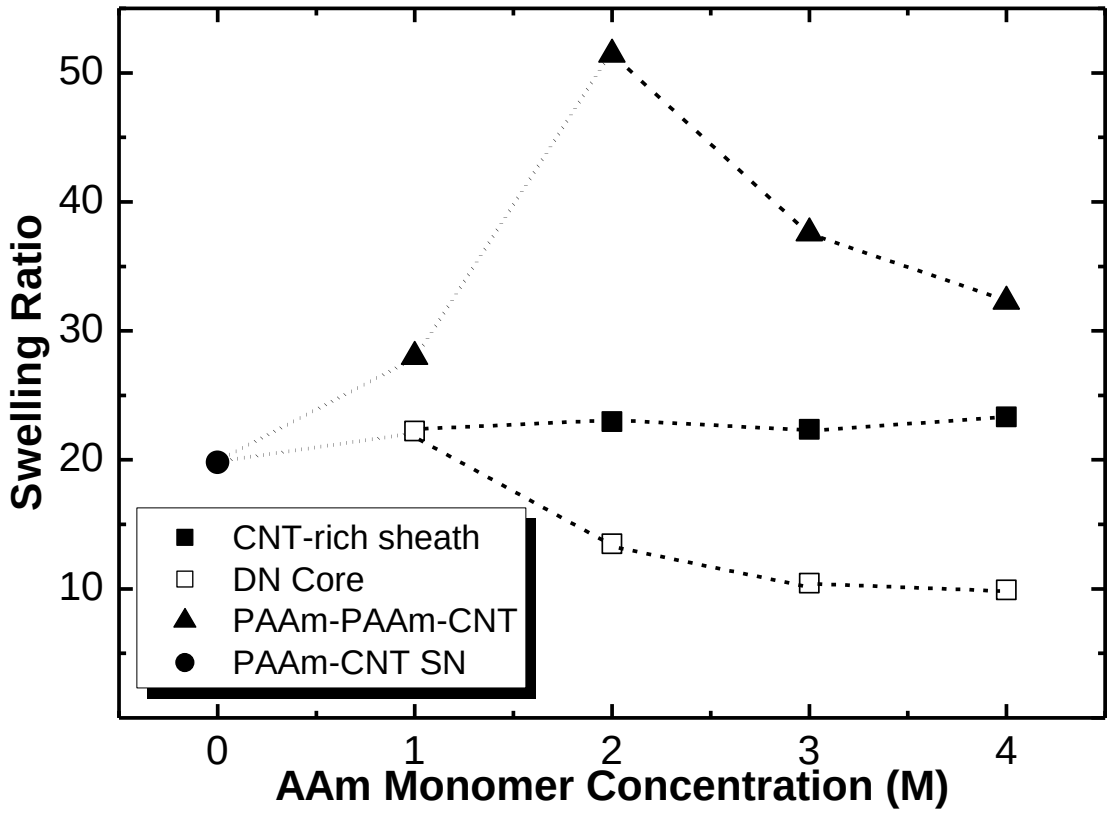

Figure 6.6. Swelling ratio of core-sheath (method A) and visibly homogeneous (method B) PAAm-PAAm-CNT hydrogels as a function of AAm 2nd network monomer concentration. Lines are to guide the eye.

To examine the nature of these hydrogels and study the effect of phase segregation on the mechanical properties of hydrogels, compression tests were performed on the DN core of phase segregated samples made via method A and on the homogenous samples made be method B. These tests were performed on samples prepared with varying second network monomer concentration and constant crosslinker concentration (Figure 6.7). The measured compression strength of both systems increased considerably as

AAm monomer concentration increased, as is typical of DN hydrogels (Chapter 4). The compression strengths of the DN core in phase segregated samples were always higher than the method B PAAm-PAAm-CNT hydrogels prepared at the same monomer concentration. The lower strength of the latter could be the result of the higher swelling ratios of the method B PAAm-PAAm-CNT hydrogels compared to the DN core of phase segregated hydrogels (Figure 6.6). Noted here, the compression strength of the method B PAAm-PAAm-CNT hydrogels was even lower than a PAAm SN hydrogel without CNT for AAm concentration of 1 and 2 M, indicating that no effective DN structure exists at these concentrations. On the other hand, the DN core of phase segregated hydrogels exhibited high compression strength which was always significantly higher than the PAAm SN hydrogel for all AAm concentration except for 1 M, where no phase segregation was observed and the strength was almost equal to PAAm SN hydrogel. This is in agreement with one of the DN criteria, suggesting that the molar ratio of the second network to the first network is required to be more than 5 [3]. This observation was interesting since it implies that no effective DN structure would form in the presence of SWNTs in visibly homogeneous PAAm-PAAm-CNT hydrogels (at least at lower concentrations), while the core of phase segregated hydrogels displays DN-like mechanical properties with lower amount of SWNTs.

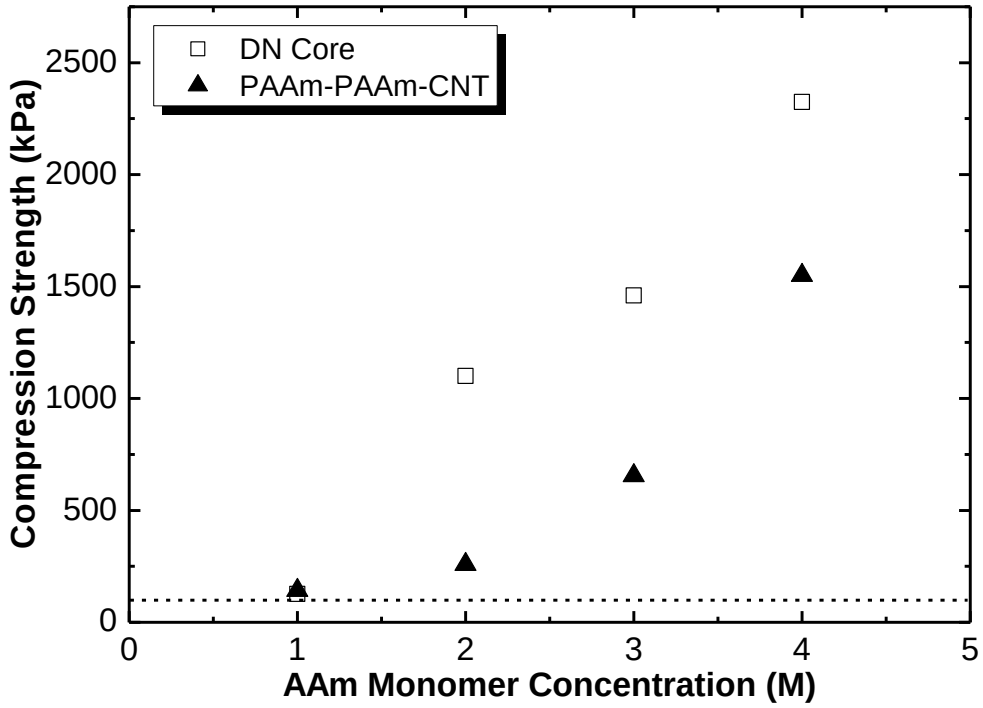

Figure 6.7. Compression strength of DN core of core-sheath hydrogels (method A) and visibly homogeneous PAAm-PAAm/CNT hydrogels (method B) as a function of AAm 2nd network monomer concentration. The dashed line indicates the compression strength of PAAm/CNT SN hydrogel.

6.4. Discussion

Although the occurrence and hindrance of phase segregation phenomenon during the second polymerization was characterized and reported here, the actual reason for this behaviour is not clear at this stage. The fact that the phase segregation happens regardless of the nature of the networks and their interactions with each other can indicate that this phenomenon is general to all double networks and may even occur in the absence of CNTs or other nanoparticles.

The hindrance of the large scale phase segregation when the CNT-incorporated SN hydrogel was polymerized while still immersed in the second network monomer (method B) provides valuable clues to the phase segregation process. Previously, a similar technique called monomer immersion polymerization was used to produce an interpenetrating network membrane based on poly(dimethylsiloxane) (PDMS) and poly(methacrylic acid) (PMAA) [4]. It was shown that when the PDMS films were immersed in MAA monomer throughout the synthesis an even monomer concentration profile would be obtained ensuring a uniform bi-continuous morphology of PMAA in PDMS throughout the membrane. This morphology was indicative of spinodal decomposition. Sequential polymerization of PDMS-PMAA IPN against various solid mould surfaces resulted in a varying morphology ranging from dispersed PMAA domains close to the surface (20 – 50 μm) to a bicontinuous morphology below the surface (> 60 μm). The volume fraction of PMAA was much smaller near the surface (<60 μm) than farther away from the surface.

Similar small scale composition variations have been noted previously in single network hydrogels that were polymerized against surfaces with various surface energies [5, 6]. It was found that the gelation process was suppressed at the hydrophobic surface and an inhomogeneous distribution of hydrogel network density was observed close to the more hydrophobic surface. However, in our work the scale of phase segregation observed here is much larger (0.1 – 1.5 mm) and the segregation occurs even when both networks are made from the same polymer (PAAm-PAAm and PAA-PAA).

The swelling study results showed that the CNT-rich sheath had a similar swelling behaviour to the PAAm-CNT SN hydrogels. However, both the DN core of the phase

segregated hydrogels prepared by method A and the PAAm-PAAm-CNT hydrogels made via method B displayed swelling ratios that were quite different to the PAAm-CNT SN hydrogels and which vary with the monomer concentration and crosslink density. The mechanical tests suggested that whenever the phase segregation has taken place, the core with visually less SWNTs than the sheath exhibits DN mechanical behaviour. In contrast, no effective DN structure is believed to form in the visibly homogeneous PAAm-PAAn-CNT hydrogels at least at lower monomer concentrations. Moreover, in the PPEGMA-PAA case, where the DN without SWNT is pH sensitive, only the core of phase segregated hydrogels was pH sensitive. As a result, it is very likely that both networks are present in the core of the core-sheath phase segregated samples. Since the SWNTs were present in the starting SN hydrogel, it is also very likely that the sheath is mainly a SN hydrogel and in fact is part of the initial CNT-incorporated hydrogel.

The illustration in Scheme 6.2 shows a proposed mechanism for the formation of the core-sheath structure. In this illustration, before the start of the second polymerization ($t_p = 0$) the CNT-incorporated SN hydrogel shows no phase segregation. As the second network polymerization proceeds, a gradient in the concentration of polymer chains of the second network develops with a higher concentration in the core and lower concentration at the surface. The reasons for the formation of this concentration gradient are not known, but the experimental evidence confirms its occurrence. Secondly, it seems that the CNTs become excluded from the gel structure when the polymer concentration of the second network exceeds some value. Again, the theromodynamic basis of this phase separation is not known. Because of the “inside-out”

formation of the second network, the SWNTs are pushed to the outer surface. In the end, a CNT-incorporated SN is left around the DN core that is devoid of CNTs. The fact that no core was observed in the samples prepared via method A with the second network monomer of 1 M indicates the importance of the polymer concentration to the CNT stability. Similarly, when the CNT-containing SN hydrogels are polymerized within the monomer solution (method B) the CNTs also phase separate during the second network formation. However, in this case the CNT form small size aggregates evenly dispersed throughout the final gel structure. Consequently, the method B gels appear homogeneous to the unaided eye. In method B the concentration of growing chains will almost remain constant across the cross section because of the surrounding monomer solution.

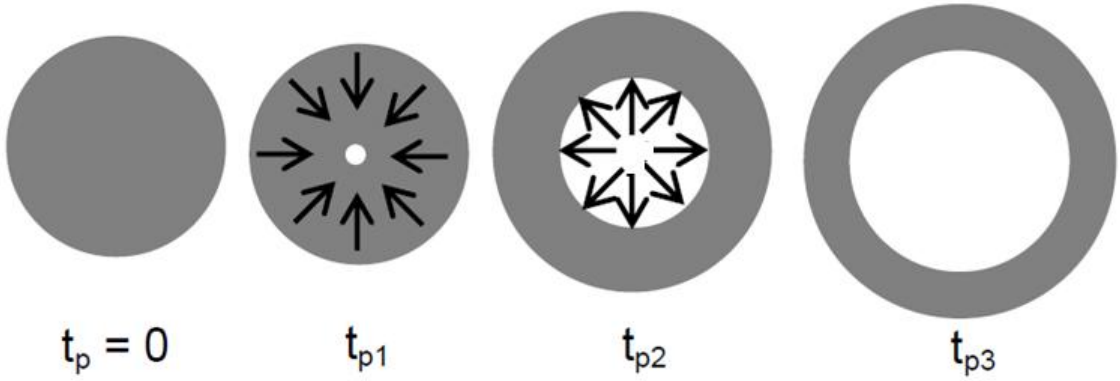

Scheme 6.2. Schematic illustration of the cross section of a hydrogel (method A), showing the formation of DN core and CNT-rich sheath over the 2nd network polymerization time (t_p): $0 < t_{p1} < t_{p2} < t_{p3}$. See text for details.

The proposed mechanism is speculative and incomplete. Further work is required to establish the reasons for the "inside-out" polymerization that occurs in method A. Secondly, the conditions that govern the phase separation of CNTs from gel need to be identified and explained.

6.5. Conclusions

The original aim of this work was to produce a conductive, tough hydrogel using carbon nanotubes as the conducting network. The study, however, diverted to a different direction with the observation of the phase separation phenomenon that occurred during the second network formation. It is important to understand this surprising observation, as the process by which it occurs may occur generally in other double network systems. The core-sheath structure may occur in other double networks but go unnoticed due to the optical transparency of both networks. In the present work it was clearly shown that the core and sheath behave differently due to their different structures. It is not known at this stage, whether the carbon nanotubes are responsible for the formation of such phase separated structures or whether the carbon nanotubes are simply a marker for the phase separation phenomenon. Many details of the phase separation process are not yet known and are left for future work, as they are beyond the scope of the present thesis.

6.6. References

1. Dai T, Qing X, Lu Y, and Xia Y. Polymer 2009;50(22):5236-5241.

2. Dai T, Qing X, Zhou H, Shen C, Wang J, and Lu Y. Synthetic Metals 2010;160(7-8):791-796.

3. Gong JP, Katsuyama Y, Kurokawa T, and Osada Y. Advanced Materials 2003;15(14):1155-1158.

4. Turner JS and Cheng Y-L. Macromolecules 2000;33:3714-3718.

5. Xianmin Zhang, Jian Xu, Kaori Okawa, Yoshinori Katsuyama, Jianping Gong, Osada Y, and Chen K. Journal of Physical Chemistry B 1999;103(15):2888-2891.

6. Akishige Kii, Jian Xu, Jian Ping Gong, Yoshihito Osada, and Zhang X. Journal of Physical Chemistry B 2001;105(20):4565-4571.

CHAPTER SEVEN

Conclusion and Future Work

7. Conclusion and Future Work

7.1. Summary and Conclusions

The aim of this thesis was to develop mechanically strong hydrogel systems mainly based on the double network concept. These hydrogels are preferably conductive as well. A series of studies have been undertaken to develop hydrogel materials that are potentially useful as electroactive devices for applications such as controlled drug release. The principal problem investigated in this thesis was the way to produce thin gel materials (for fast response) that combined both high strength / toughness with adequate electrical conductivity.

The feasibility of employing conductive hydrogels for the drug release purposes was studied (Chapter 2) using a model drug and a model conductive hydrogel. The model drug was negatively charged dexamethasone sodium phosphate (DEX) and the conductive hydrogel was based on chitosan (CS) hydrogel films. The conductivity of hydrogels was obtained by incorporating single walled carbon nanotubes (SWNT) into the structure of the hydrogel. The resulting system displayed clear potential for modulated drug release under electrical stimulation. The CS-SWNT hydrogel films

loaded with DEX exhibited slow release behaviour in passive release of DEX (no electrical voltage was applied), compared to those without SWNTs. Moreover, when an external voltage was applied on the CS-SWNT hydrogels the release pattern changed in a controllable manner. Significantly faster drug release was observed when negative (-0.4, -0.8 V) voltages were applied while the voltage strength controlled the rate of release. Also, it was possible to achieve100 % release by applying negative voltages. On the other hand, a positive voltage (+0.15 V) showed considerable retardation effects on release with accumulative release reaching only to around 30 % after 4 hrs then levelled off. The release was switched on again by applying a negative voltage. The release rate was also measured which reflected the overall retardation effects of SWNTs on the release process, and the effect of voltage polarity and strength on the release rate. Measured diffusion coefficients were also revealed to be much smaller for hydrogel films with SWNTs compared to samples with no nanotubes, which was attributed to the barrier effect of SWNTs. The modulated release imposed by voltage polarity and strength was considered to be the result of electrostatic interactions between the charge applied to the conductive network and the negatively charged DEX. The experimental observations in Chapter 2 suggested that although the SWNTs play a central role in slowing down the release in this system, it is possible to achieve similar modulated release from other conductive hydrogels by implementing the concepts which were framed in Chapter 2.

To expand the applicability of conductive hydrogel systems to broader application areas, various structures of hydrogels such as fibres, rods and sheets are required. In particular, small thickness films and fibres are desirable to minimise diffusion distances

and to increase the rate of response such as drug release. Moreover, as mentioned in Chapter 1, it is essential in some applications for hydrogels to sustain external forces during their usage. As a result, fabrication of a hydrogel fibre based on CS with enhanced mechanical properties was studied and described in Chapter 3. The fibres were made by a wet spinning process and to enhance their mechanical properties PAAm was synthesized within the CS fibres. The tensile properties of fully swollen CS-PAAm fibres showed clear enhancement in modulus and tensile strength of hydrogel fibres compared to PAAm hydrogels with, respectively, 11 and 8 times increase in Young's modulus and tensile strength. The overall breaking energy of the CS-PAAm hydrogel fibres also showed a maximum of 8 times enhancement compared to rehydrated CS fibres. Maximum Young's modulus and tensile strength of ~ 80 and ~ 300 kPa was achieved for fully swollen CS-PAAm fibres with swelling ration of ~ 8 (swell ratio here represents the volume ratio of fully swollen hydrogel fibre to dry fibre). Also, CS-PAAm hydrogel fibres exhibited pH sensitivity where swelling ratio dropped with increasing pH as pH approached neutral values, then increased again at more basic pHs (pH > 9). The effect of PAAm content on the Young's modulus and tensile strength of CS-PAAm hydrogel fibres was studied as well. As AAm monomer concentration increased the swelling ratio decreased and the tensile mechanical properties increased. In general, the CS-PAAm hydrogel fibres made in Chapter 3 possessed higher Young's modulus and tensile strength compared to PAAm hydrogels and CS fibres, but the elongation at break was considerably lower than PAAm. This means that the hydrogels are not able to sustain large external deformation when the sample is bent or stretched.

In order to produce a hydrogel system with more robust mechanical performance, the double network (DN) concept was employed to make DN hydrogels with hydrogen bonding (Chapter 4). The DN hydrogels were made from a tightly crosslinked first network based on poly(ethylene glycol) methyl ether methacrylate (PEGMA) oligomers and a loosely crosslinked network of poly(acrylic acid) (PAA). After polymerization, the PEGMA oligomers will produce bottlebrush chains, PPEGMA, with hydrophobic backbones and hydrophilic poly(ethylene glycol) (PEG) side chains. These specific components were chosen as it is known that hydrogen bonding interactions operate between PAA and PEG and such interactions may affect the DN toughness. The resulting PPEGMA-PAA DN hydrogels exhibited significantly higher compression and tensile performance compared to both PPEGMA and PAA single networks. Compression strength could reach to ~ 8 MPa, where tensile strength was ~ 550 kPa for fully swollen samples (pH 2). Moreover, the elongation at break was up to 500 % in tensile tests. The length of PEG side chains also had a clear impact on the physical and mechanical performance of achieved hydrogels, where hydrogels made of PPEGMA with longer side chains (PPEGMA1100-PAA) showed higher tensile and compression mechanical properties than those made of PPEGMA with shorter side chains (PPEGMA475-PAA).

In addition to the improved mechanical properties these DN hydrogel were pH sensitive with their swelling ratio, transparency, surface water contact angle and mechanical properties changing with pH. In general, all of the mechanical and physical properties of PPEGMA-PAA DN hydrogels (regardless of the PEG size) passed through a transition point around pH 4, where a dramatic change occurred in the hydrogels'

properties. The swelling ratio of PPEGMA-PAA DN hydrogels increased almost 4 times when pH exceeded the transition point from acidic pHs (pH < 4) to more neutral pHs (pH 6), while surface contact angle and mechanical properties dropped dramatically around the same pH values. The appearance of hydrogels also changed with pH as well. As-prepared PPEGMA-PAA hydrogels were white/opaque, but their transparency increased significantly with increasing pH showing similar transition as swelling ratios. This pH sensitivity was attributed to the hydrogen bonding between PEG side chains of PPEGMA and carboxylic acid side groups of PAA. When pH is below the transition point (pH ~ 4) the carboxylic acid groups are protonated and can form very strong hydrogen bonding with ethylene glycol units of PEG chains. This interaction results into hydrophobic areas within the hydrogel which reflects its lower swelling ratio, higher water contact angle and white/opaque appearance with considerably enhanced mechanical performance. By increasing the pH above this transition value, the hydrogen bonds dissociate and the resulting hydrogel swells significantly more, with lower mechanical properties and lower water contact angle. Also, due to the disappearance of the hydrophobic hydrogen bonded zones the DN hydrogels become transparent at higher pHs.

Since the DN hydrogel system in Chapter 4 exhibited the desired mechanical performance and pH sensitivity, the same system was employed to develop tough and conductive hydrogels by incorporating a conducting polymer (CP) (Chapter 5) or carbon nanotubes (CNT) (Chapter 6) into the structure of DN hydrogels. Poly(3,4-ethylenedioxythiophene) (PEDOT) was used as the CP to introduce conductivity to the PPEGMA-PAA DN hydrogels. A simple but effective technique was employed to

increase the loading of PEDOT beyond the limiting parameter of 3,4-ethylenedioxythiophene (EDOT) solubility in water. Since EDOT is not very water soluble, the maximum amount of PEDOT which can be polymerized chemically within the DN hydrogel is limited by the EDOT solubility. However, multiple sequential PEDOT polymerizations were used to tackle this issue. The resulting PEDOT incorporated PPEGMA-PAA hydrogels showed 4-point probe conductivity of up to 4.3 S/cm (fully swollen) after three times polymerization of PEDOT. This value is very close to the electrical conductivity of commercial PEDOT-PSS films. Moreover, the hydrogels not only maintained their high mechanical properties of PPEGMA-PAA DN system, but also more improvement in both tensile and compression mechanical performance was observed. Compression strength of up to 11.5 MPa was obtained for a fully swollen hydrogel (70 % water) at pH 3 with electrical conductivity of around 3.5 S/cm after two PEDOT polymerizations. The same sample showed Young's modulus and tensile strength of about 110 and 600 kPa in its fully swollen state.

It is informative to compare the compression strengths of PPEGMA-PAA DN and PEDOT-PEDOT(PSS) hydrogels with other hydrogel systems. In Figure 7.1 the compression strength of hydrogels developed in previous chapters is plotted against their corresponding swelling ratio (mass ratio of fully swollen hydrogel to dry hydrogel). The dotted line in Figure 7.1 represents the 1 MPa compression strength, and the filled symbols are the hydrogels mentioned in previous chapters. DN1100 and DN475 indicate PPEGMA1100-PAA and PPEGMA475-PAA DN hydrogels. The change in the swelling ratio of these hydrogels is due to the changes in pH. As can be seen, the hydrogels developed here have lower swelling ratio than most of the systems in Figure 7.1, due to

the strong hydrogen bonding between the networks. However, the compression strength is considerably higher than conventional hydrogels with the same swelling ratio.

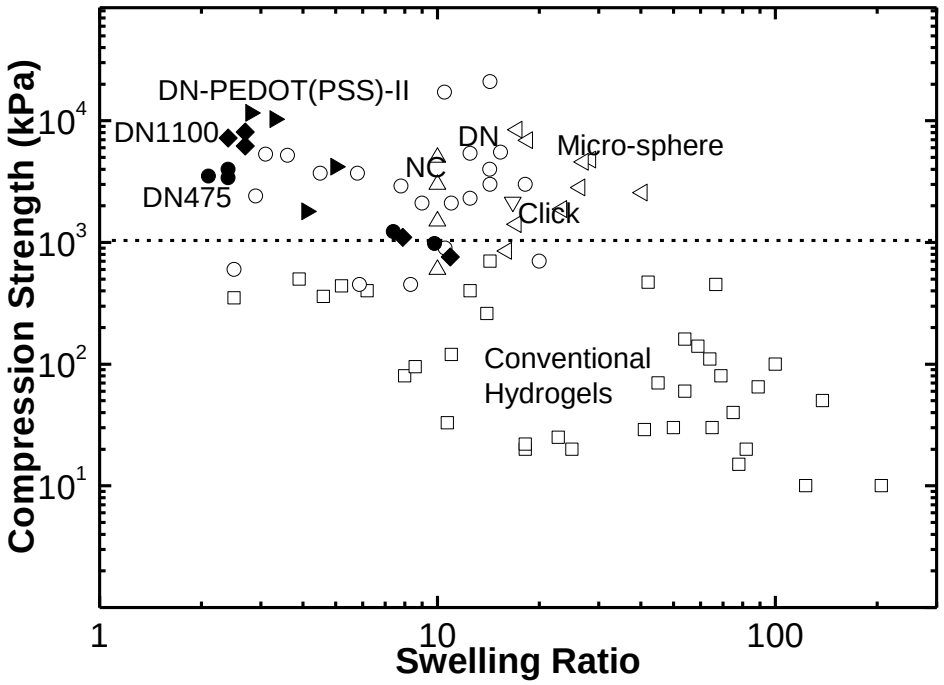

Figure 7.1. Compression strength of various hydrogels including (filled triangle) DN-PEDOT(PSS)-II, (filled diamond) PPEGMA1100-PAA DN, (filled circle) PPEGMA475-PAA DN hydrogels as a function of their equilibrium swelling ratio (except for NC hydrogels.)

Compared to other DN hydrogels, the PPEGMA1100-PAA DN (DN1100 in Figure 7.1) has swelling ratios similar to cellulose-based DN hydrogels [1] with higher compression strength. On the other hand, the swelling ratio of PPEGMA-PAA DN hydrogels is lower than most of the DN systems, while their compression strength is one

of the highest [2]. As swelling ratio increases with increasing pH, the compression strength decreases, reaching to the 1 MPa line which separates the conventional hydrogels from more enhanced systems.

The tensile strengths of hydrogels vs. their elongation at break of various hydrogels are plotted in Figure 7.2. Again, filled symbols represent the hydrogels developed here. Those data points with higher elongation at break display the hydrogels form previous chapters at lower pHs (pH < 4) with low swelling ratio. As the pH increases, the swelling ratio increases and both tensile strength and elongation at break of hydrogels dropped to conventional hydrogel area. On the other hand, at acidic pHs, hydrogels have elongation at breaks higher than previously reported PEG-PAA IPN system [3] and cellulose-based DN hydrogels [1], but lower than NC hydrogels [4] and PAMPS-PAAm DN hydrogels [5, 6]. Also, as can be seen, the PEG-PAA IPN system has higher strength than PPEGMA-PAA system, while the net of enhancement in mechanical properties was much higher for PPEGMA-PAA DN than PEG-PAA. Moreover, at higher pHs, when the hydrogen bonds are dissociated the PEG-PAA hydrogels hold higher tensile strength than PPEGMA-PAA at the same pHs. This indicates that our first network, PPEGMA, is significantly weaker than the end-crosslinked PEG network in reference [3]. One possible reason can be the bottlebrush structure of PPEGMA first network and the short-chain crosslinking agent which was used to crosslink this network. While the PEG side chains of PPEGMA1100 have 22 – 23 ethylene glycol units on every repeating units, the *N-N'*-methylenebisacrylamide crosslinking agent has a significantly shorter chain. The excluded volume imposed by PEG side chains is much larger than the length of crosslinking agent molecules and

considerable amount of defects is expected to be introduced to the first network during the crosslinking process, yielding a weak network.

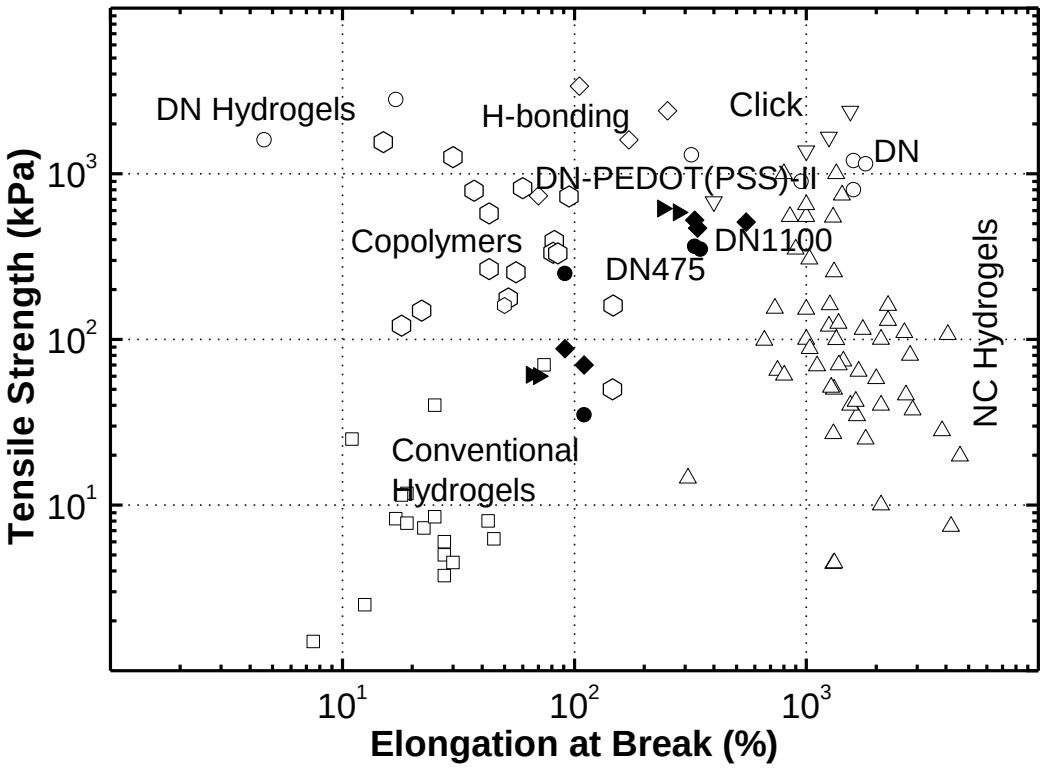

Figure 7.2. Tensile properties of various hydrogels including (filled triangle) DN-PEDOT(PSS)-II, (filled diamond) PPEGMA1100-PAA DN, (filled circle) PPEGMA475-PAA DN hydrogels.

The area under the tensile stress-strain curves of PPEGMA1100-PAA and PPEGMA475-PAA DN hydrogels along with DN-PEDOT(PSS)-II hydrogel was measured and then plotted against the corresponding swelling ratios in Figure 7.3. The area under the curve represents the work of extension and is a measure of the material's

toughness, as described in Chapter 1. In general, these systems fall mainly in the same area as copolymers and lenses, with work of extension considerably higher than conventional hydrogels but still lower than DN and NC hydrogels.

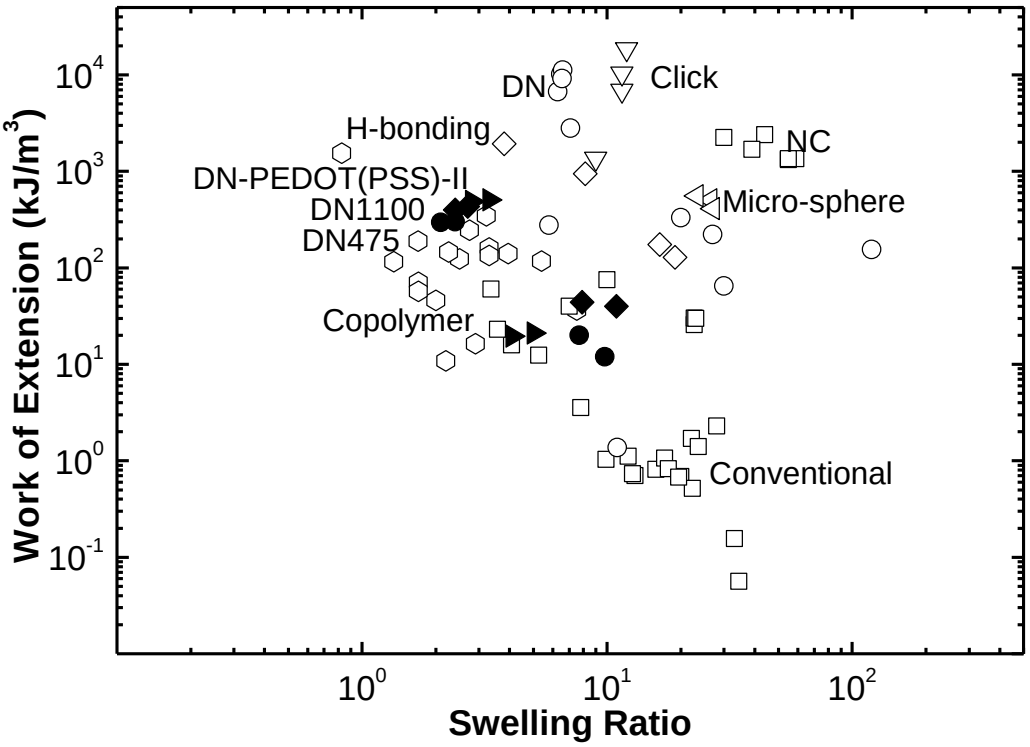

Figure 7.3. Work of extension of various hydrogels including (filled triangle) DN-PEDOT(PSS)-II, (filled diamond) PPEGMA1100-PAA DN, (filled circle) PPEGMA475-PAA DN hydrogels as a function of their swelling ratio.

Finally, in Chapter 6 the CNT-incorporated DN hydrogels were studied, where interesting phase segregation was observed. In the beginning, the CNT was only added to the first network monomer solution based on the same concept that was developed in

Chapter 2. Since the modulated release was successfully demonstrated in Chapter 2, the idea of developing a CNT-incorporated hydrogel with enhanced mechanical properties for drug release was one of the goals of this study. However, by addition of CNT to the first network and forming the second network within this CNT-incorporated first network, a CNT-rich sheath was always observed to be formed around the tougher DN core. This sheath formation was demonstrated to be independent of the mould surface. Investigation on this behaviour showed that the sheath does not form only when samples are polymerized within the second monomer solution in a monomer-immersion polymerization technique. Although the understanding of this phenomenon is not very clear yet, the structure formed may have useful applications in drug delivery applications. Since a CNT-rich phase forms around the inner core of pH sensitive DN hydrogels, a similar concept as in Chapter 2 might be useful to control the release of drugs from the inner core (Scheme 7.1). As illustrated in Scheme 7.1, a charged drug can be introduced to the hydrogel by immersing the hydrogel in the drug solution (Scheme 7.1a). The drug can diffuse into the surrounding media via a simple diffusion process (Scheme 7.1b) when there is no external voltage is applied. However, by applying the same charge as that of drug molecules to the CNT-rich sheath, the release of charged drug molecules may slow down similar to the study presented in Chapter 2 (Scheme 7.1c).

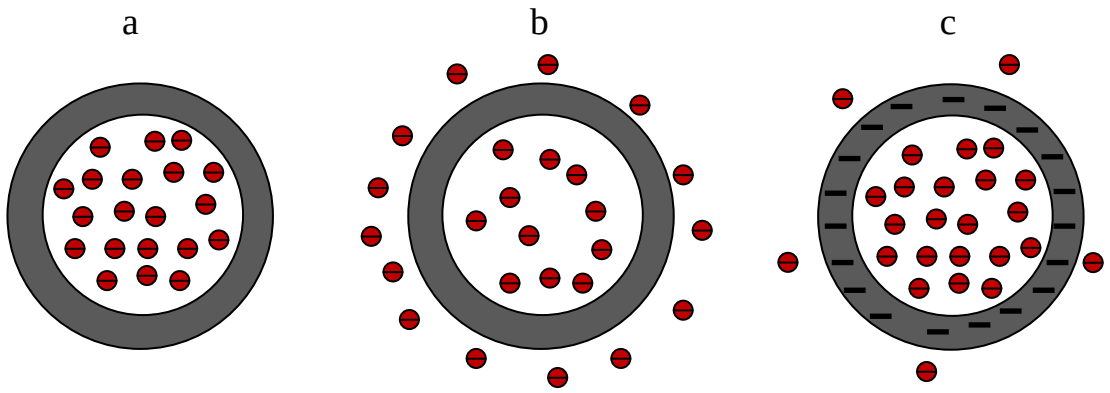

Scheme 7.1. Schematic illustration of controlled drug release, a) as-prepared hydrogels with CNT-rich sheath and DN core, where negatively charged drug is in the core, b) diffusion of negatively charged drug, c) a negative voltage applied to the CNT-rich sheath to slow down the diffusion.

7.2. Further Work

Unfortunately due to time restraints, the drug release studies on DN-PEDOT(PSS) and CNT-incorporated hydrogels were not completed. Also, attempts to produce more sophisticated structures (such as fibres) form these hydrogels were not particularly successful due to time issues. However, preliminary studies showed that it is certainly possible to produce spheres based on the PPEGMA-PAA DN hydrogel, by employing a biopolymer (chitosan, alginate, gellun gum) to form the spheres first. In this technique (Scheme 7.2) the PEGMA monomer along with initiator and crosslinking agent is mixed with the biopolymer, followed by forming the spheres by dropping the biopolymer mixture into a coagulation bath. Then, the PPEGMA network is formed in the spheres by thermal or UV polymerization. The biopolymer can be removed by dissolving the

physical crosslinked biopolymer chains or can remain until the end of process. The PAA network is formed by soaking the spheres in the AA monomer, followed by second polymerization. Using this technique, short fibres were also formed, by spinning the biopolymer mixture (Scheme 7.3). However, the whole process is considerably more difficult for fibres due to the size of fibres, and the subsequent polymerization process. Another possible method to fabricate fibres based on a DN system can be to spin the biopolymer with PEGMA as the inner core of a core shell fibre. The shell is to protect the inner core and first network monomer and other reagents and to slow down the diffusion process. The first network polymerization can take place inside the shell and then the shell can be removed for subsequent processes.

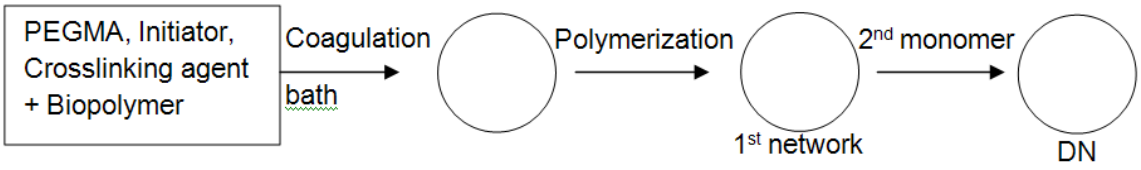

Scheme 7.2. Schematic diagram of forming DN hydrogel spheres.

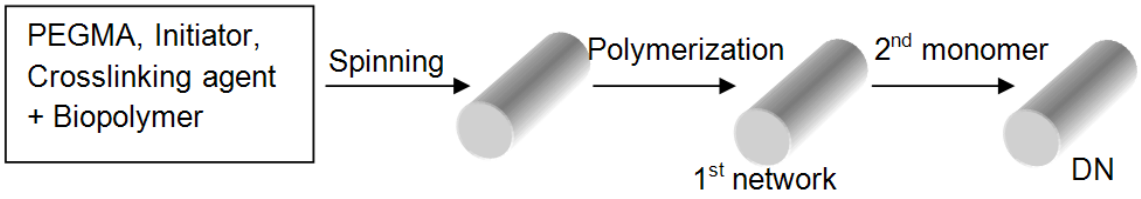

Scheme 7.3. Schematic diagram of forming fibrous DN hydrogels.

Apart from these proposed methods for fabricating useful forms of tough, conducting gels a further area of additional study was suggested by the work described in Chapter 6 on phase separated CNT containing gels. As described above, the mechanism of phase separation is not yet understood. The experimental evidence suggests that the second network forms from the inside out of the first network. In doing so, the CNTs are excluded to the outer surface. Further investigations are required to determine the reasons for 1) the formation of the concentration gradient of polymer from the core to the surface; and 2) the reasons for the phase separation when the polymer concentration increases above a given level.

7.3. References

1. Nakayama A, Kakugo A, Gong JP, Osada Y, Takai M, Erata T, and Kawano S. Advanced Functional Materials 2004;14(11):1124-1128.

2. Gong JP, Katsuyama Y, Kurokawa T, and Osada Y. Advanced Materials 2003;15(14):1155-1158.

3. Myung D, Koh W, Ko J, Hu Y, Carrasco M, Noolandi J, Ta CN, and Frank CW. Polymer 2007;48(18):5376-5387.

4. Zhu M, Liu Y, Sun B, Zhang W, Liu X, Yu H, Zhang Y, Kuckling D, and Adler H-JP. Macromolecular Rapid Communications 2006;27(13):1023-1028.

5. Na Y-H, Tanaka Y, Kawauchi Y, Furukawa H, Sumiyoshi T, Gong JP, and Osada Y. Macromolecules 2006;39(14):4641-4645.

6. Kawauchi Y, Tanaka Y, Furukawa H, Kurokawa T, Nakajima T, Osada Y, and Gong JP. Journal of Physics: Conference Series 2009;184(1):012016.